Superhydrophobic Engineered Cementitious Composites for Highway Applications: Phase I

CFIRE

CFIRE 04-09
May 2013

National Center for Freight & Infrastructure Research & Education
Department of Civil and Environmental Engineering
College of Engineering
University of Wisconsin–Madison

Authors:

Konstantin Sobolev, Habib Tabatabai, Jian Zhao, Ismael Flores-Vivian, Rossana Rivero, Scott Muzenski
University of Wisconsin-Milwaukee

Michael G. Oliva, Rehan Rauf
University of Wisconsin-Madison

Principal Investigator:

Konstantin Sobolev (PI), Habib Tabatabai (co-PI), Jian Zhao (co-PI)
University of Wisconsin-Milwaukee

Michael G. Oliva (co-PI)
University of Wisconsin-Madison

DISCLAIMER

This research was funded by the National Center for Freight and Infrastructure Research and Education. The contents of this report reflect the views of the authors, who are responsible for the facts and the accuracy of the information presented herein. This document is disseminated under the sponsorship of the Department of Transportation, University Transportation Centers Program, in the interest of information exchange. The U.S. Government assumes no liability for the contents or use thereof. The contents do not necessarily reflect the official views of the National Center for Freight and Infrastructure Research and Education, the University of Wisconsin, the Wisconsin Department of Transportation, or the USDOT's RITA at the time of publication.

Technical Report Documentation Page

1. Report No. CFIRE 04-09	2. Government Accession No.	3. Recipient's Catalog No. **CFDA 20.701**	
4. Title and Subtitle **Superhydrophobic Engineered Cementitious Composites for Highway Applications: Phase I**		5. Report Date **May 2013** 6. Performing Organization Code	
7. Author/s Konstantin Sobolev, Habib Tabatabai, Jian Zhao, Michael G. Oliva, Ismael Flores, Rosanna Rivero, Scott Muzenski, Rehan Rauf		8. Performing Organization Report No. **CFIRE 04-09**	
9. Performing Organization Name and Address National Center for Freight and Infrastructure Research and Education (CFIRE) University of Wisconsin-Madison 1415 Engineering Drive, 2205 EH Madison, WI 53706		10. Work Unit No. (TRAIS) 11. Contract or Grant No. **DTRT06-G-0020**	
12. Sponsoring Organization Name and Address Research and Innovative Technology Administration United States Department of Transportation 1200 New Jersey Ave, SE Washington, D.C. 20590		13. Type of Report and Period Covered **Final Report [10/1/2010 to 6/30/2012]** 14. Sponsoring Agency Code	
15. Supplementary Notes **Project completed for the USDOT's RITA by CFIRE.**			
16. Abstract **The strength and durability of highway bridges are two of the key components in maintaining a high level of freight transportation capacity on the nation's highways. This research focused on developing new hybrid superhydrophobic engineered cementitious composites (SECCs), engineered cement based concrete materials combined with polyvinyl alcohol fibers and hydrophobic compounds, to create a substitute concrete which can provide the strength and durability demanded in key regions of highway bridges.**			
17. Key Words superhdyrophobic, engineered cementitious composite, fiber reinforced composite, durability, ductile concrete, crack distribution, air void distribution	18. Distribution Statement **No restrictions. This report is available through the Transportation Research Information Services of the National Transportation Library.**		
19. Security Classification (of this report) **Unclassified**	20. Security Classification (of this page) **Unclassified**	21. No. Of Pages 70	22. Price **-0-**

Form DOT F 1700.7 (8-72) **Reproduction of form and completed page is authorized.**

Table of Contents

List of Figures

List of Tables

SUPERHYDROPHOBIC ENGINEERED CEMENTITIOUS COMPOSITES FOR HIGHWAY APPLICATIONS: PHASE I

EXECUTIVE SUMMARY

The United States infrastructure is in desperate need of repair, especially in regions exposed to harsh environments. Freezing and thawing cycles in northern regions lead to early need for repair or failure of bridges. Key elements that are especially prone to deterioration in these regions are bridge approach slabs. The main goal of approach slabs is to provide a smooth transition between the roadway and the bridge. A "bump" forms at the junction of the bridge and approach slab due to the differential settlement of the two structures, causing driver discomfort and excessive dynamic loading on these elements. Connecting the approach slab integrally to the bridge could eliminate the damage due to the bump to the bridge. In this system the approach slab would undergo increased bending. This bending should be accommodated without large cracks. Large cracks can cause water to infiltrate through the integral approach slab-bridge joint and cause maintenance issues.

A more durable material is required for these key portions of infrastructure in order to increase the service life of roadways and to minimize the need for repair. A material capable of lasting upwards of 100-120 years would drastically improve sustainability by reducing the amounts of raw materials required for the bridge and reducing the carbon emissions produced by vehicles that are delayed in traffic due to closures for maintenance of the bridge. Moreover, use of a material that incorporates up to 50% of supplementary cementitious materials or byproducts as portland cement replacement will reduce the carbon emissions resulting from the production of portland cement.

This goal is achieved by combining engineered cementitious composites with superhydrophobic admixtures to create an ultra-durable material. Engineered cementitious composites (ECC) provide drastically improved flexural behavior by allowing for several small cracks instead of single, large cracks by incorporating small randomly oriented synthetic (polyvinyl alcohol) fibers. This allows strain hardening behavior of the material to occur and thus the ability to withstand much higher loads after cracking which is essential for durable material. Recent research has indicated that combining ECC with superhydrophobic admixtures creates a material with water repellant air voids to even further improve durability. The use of these admixtures also allows a strong cementitious matrix to be used in ECC, whereas in the past the matrix was weakened to allow for high ductility in ECC. This is achieved by the admixtures creating numerous, small, well-spaced air voids throughout the system which act as artificial flaws to initiate cracking and allow for the desired multi-cracking and strain hardening behavior.

This research demonstrates improved flexural and durability behavior of ECC with superhydrophobic admixtures. The first step to achieve this was to create hydrophobic and superhydrophobic admixtures. These were tested for contact angle on plain mortar tiles as an indication of how their water repellant nature would perform on the surface of an air void. Next, these admixtures were tested in mortar samples without fiber reinforcement to determine the effect that the admixtures would have on strength and freeze-thaw resistance.

Several different parameters were considered in the creation of the ideal fiber reinforced concrete (ECC) as well. First, the proper mixing procedure was considered in order to achieve the best mix that distributes the fibers equally throughout material. Equally important in this step was to determine the point at which the superhydrophobic admixtures must be added to the material so that they could serve their intended cause without loss of air and without excessive air formation. Next, the kind and quantity of superhydrophobic admixtures were considered in ECC to determine their effect on compressive strength and flexural behavior. Finally, the use of different types and different quantities

of supplementary cementitious materials were considered to determine their effect on compressive strength and flexural behavior.

Large scale samples were also created to determine the characteristics of the material in a close to the field scenario as testing in laboratory condition with small size samples needed verification. A recent study at the University of Wisconsin-Madison determined that a bridge approach slab must be able to rotate 0.002 radians in order to adequately serve its purpose. Large scale samples were created to see if ECC would be capable of rotating to this extent. Additionally, mixing procedures for large quantities of ECC were explored.

Ultimately it was determined that the addition of superhydrophobic admixtures to ECC does indeed improve flexural behavior while still maintaining high compressive strengths. This was achieved by incorporating admixtures consisting of 4.4% polyvinyl alcohol surfactant along with 25% polymethyl hydrosiloxane and small quantities of sub-micro sized particles, which proved to be the most ideal admixture as small, well dispersed air voids were created within the cementitious matrix. The addition of supplementary cementitious materials also provided improved flexural behavior and in some cases improved compressive strengths as well. Additional work must be performed to even further improve the hydrophobicity of the admixtures and to study the durability properties of ECC with superhydrophobic admixtures.

1.0 INTRODUCTION

The strength and durability of highway bridges are the key components in maintaining a high level of freight transportation capacity on the nation's highways [1-5]. Highways, bridges, and other critical transportation infrastructure works are rapidly deteriorating due to loading and deformation, aging, de-icing, and other detrimental factors in addition to rebar corrosion [1-5]. The average service life of concrete infrastructure in Wisconsin is 40-50 years, with up to 10% of bridge decks reinforced by uncoated rebar needing replacement after 30 years [3, 6]. The direct costs for roadway improvements are escalating because the price of key materials needed for highway and bridge construction has increased rapidly (~46% from 2004) [2, 7]. Indirect costs of highway bridge construction, in the form of environmental damage, are being realized in relation to the production and recycling of basic concrete materials. The time is right for a paradigm change to address the urgent need for highly durable and more sustainable materials to meet the challenges that future freight transportation will demand.

The durability of concrete bridges is often limited by the performance of connection regions or joints between bridge components, especially in decks. A recent CFIRE project investigated the use of precast bridge approach slabs that could reduce early distress noted in service [8]. Critical bridge locations where durability problems are apparent and premature deterioration occurs include the connection between an approach slab and bridge deck, joints in the bridge deck and the portion of bridge deck bending in a negative curvature above mid-span bridge piers. This results in regular maintenance demands or early replacement. A high-performance material that does not exhibit early age shrinkage cracking, withstands the deformation demands from truck loading, and provides durability is necessary for these susceptible regions.

Engineered cementitious composite (ECC) materials exhibit high ductile performance under tension, like steel, as shown in Figure 1. The strain capacity of ECC may be increased by a factor of 200 when high-strength reinforcing fibers such as polyvinyl alcohol (PVA, Kuralon K-II) are three-dimensionally dispersed in the mortar [9-13]. The engineered fiber composite controls shrinkage cracking and provides extreme deformation and strain enhancement, as illustrated in our research team's previous results in Figure 1, left.

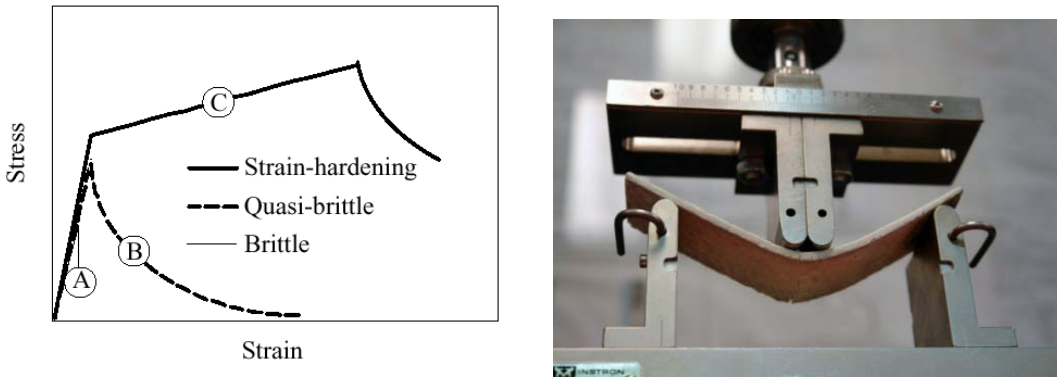

Figure 1. The Strain-Hardening Performance of ECC: Strain Hardening Performance of ECC (right [11]) and Tests at UW-Milwaukee Lab (rigtht)

The use of Polyvinyl Alcohol (PVA) fibers in engineered cementitious composite (ECC) proves to be an effective method to not only improve concrete ductility, but to also drastically improve its durability. Conventional reinforced concrete is a relatively brittle material that when loaded typically causes large cracks. These large cracks allow water to penetrate through the concrete, reaching the reinforcing steel resulting in steel corrosion, ultimately leading to failure of the reinforced concrete.

In conventional reinforced concrete, when a crack forms, the entire load is transferred directly to the reinforcing steel bridging the crack. This single crack is typically large enough to allow water to penetrate, but small enough to not allow for much ductility in the reinforcing steel. Since conventional reinforced concrete does not allow for large ductility it will not be able to survive large deformations caused by loading, impact, or freezing and thawing actions. Moreover, large cracks that allow water to penetrate can be extremely detrimental to its performance under freezing and thawing, and chemical attack due to penetration of chlorides. This in turn requires excessive maintenance on the concrete and a much shorter lifespan of the structure.

When PVA-ECC is loaded the initial crack is bridged by the PVA fibers with a high tensile strength. The bond between the PVA fibers and the cement matrix is also strong, unlike the bond in conventional reinforced concrete. These features allow for multi-cracking fracture. Instead of one crack forming and the entire load transferred to the material bridging this one crack, it is able to be distributed throughout several cracks. This facilitates much larger ductility, while at the same time maintaining cracks that are small enough to allow very little water, if any, to penetrate.

In addition to improved deformability and crack control provided by ECC, a new high-performance material with improved long-term durability can be realized by combining ECC with superhydrophobic hybridization [14,15]. The use of PVA fibers along with superhydrophobic emulsions not only generates multiple micro-cracking when loaded, but allows for the creation of air voids within the cement matrix to facilitate excellent resistance to freezing and thawing while maintaining its high strengths, unlike the typical air entraining approach. This enables structures that incorporate superhydrophobic emulsions along with PVA-ECC to have a lifespan of 120 plus years, with little to no maintenance required. This is an extremely cost effective practice, considering that any small price increase for materials would be drastically offset by labor and repair materials reduction costs for maintenance and early replacement over the entire life span of the bridge.

Superhydrophobic hybridization of concrete is a novel concept developed at UW-Milwaukee [14,15], which engages interdisciplinary work combining biomimetics (lotus effect) [16], chemistry (siloxane polymers) [14] and nanotechnology (nano-SiO_2 particles) [17] to resolve fundamental problems of concrete, such as insufficient durability and corrosion protection for internal reinforcing. The use of a superhydrophobic admixture helps to tailor the volume, size, and distribution of air voids in the concrete, and the bond with PVA fibers, to realize controlled pullout behavior. Furthermore, controlled air void structures can be used to produce the "preferred" fracture modes. These synergetic effects are verified by the research program.

The design of hybrid superhydrophobic ECC (SECC) is based on three principles:

1. Micromechanical design of ECC with 1 to 4 % (by volume) of polyvinyl alcohol fibers to realize ductile performance.

2. Application of small quantities (0.01 to 0.1% of cement weight) of siloxane-based hydrophobic admixtures (e.g., based onpolyethyl/polymethyl-hydrosiloxane, PEHSO/PMHS) modified by super-fine submicro- or nano-sized materials (such as nano-silica, nano-clay additives or SiO_2-rich reactive powders) and use of an effective superplasticizer to form a controlled air-void structure (Figure 2 and 3).
3. Inclusion of selected by-product or mineral additives (also known as supplementary cementitious materials, SCMs) to decrease cement content and improve the sustainability of the material.

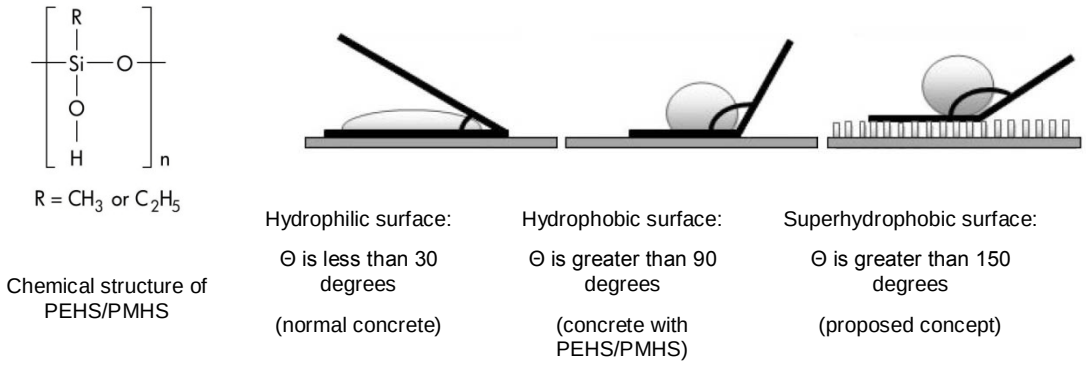

Figure 2. The Concept of Superhydrophobic Hybridization of Concrete Pore Surface

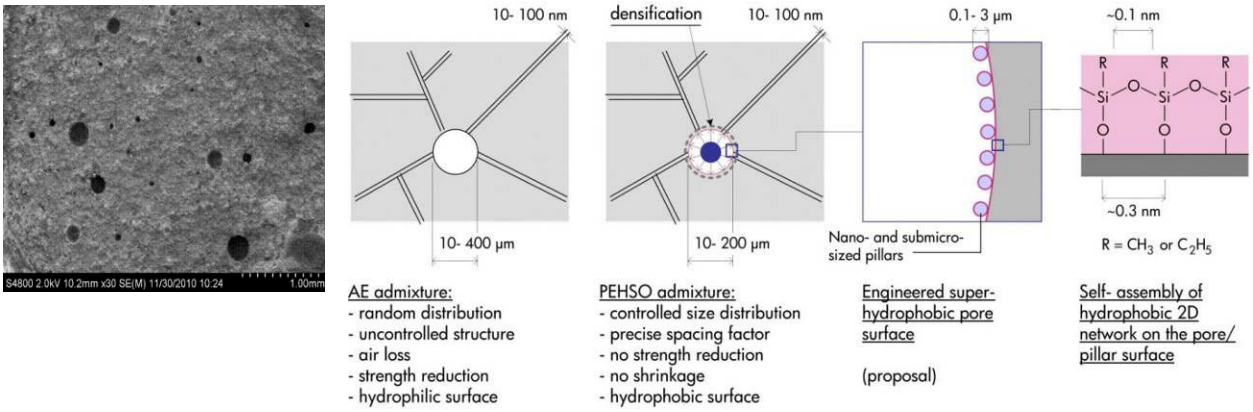

Figure 3. How the Superhydrophobic Hybridization of Concrete Works

Superhydrophobic surfaces, or surfaces that have a water contact angle Θ larger than 150° (Figure 3), have generated much interest due to their potential in industrial applications (mainly for self-cleaning), and have been tested for enhancing concrete durability. This nature-inspired approach improves the performance of hydrophobic materials that control wettability [15-17].

The superhydrophobic admixtures were manufactured by combination of the hydrogen containing siloxane admixture (e.g., PMHS) with small quantities of super-fine, submicro- or nano-sized particles such as nano-silica, nano-clay additives, or SiO_2-rich reactive powders (Figure 3).

A modified PEHSO/PMHS admixture (used at a dosage of 0.01…0.1% of cement weight) releases hydrogen and forms a small (10 - 100 μm), uniform air void evenly distributed within the cement paste (Figure 3, left). The volume, size, and distribution of the air void within the hardened cement

phase are precisely tailored by preparing the water-based emulsion of siloxane with a certain droplet size (Figure 4). For optimal performance, more than 70% of the PEHSO must be dispersed to the size of less than 10 μm [9]. As a result, the hydrophobic particles cover the surface of the voids, providing the superhydrophobic hybridization effect.

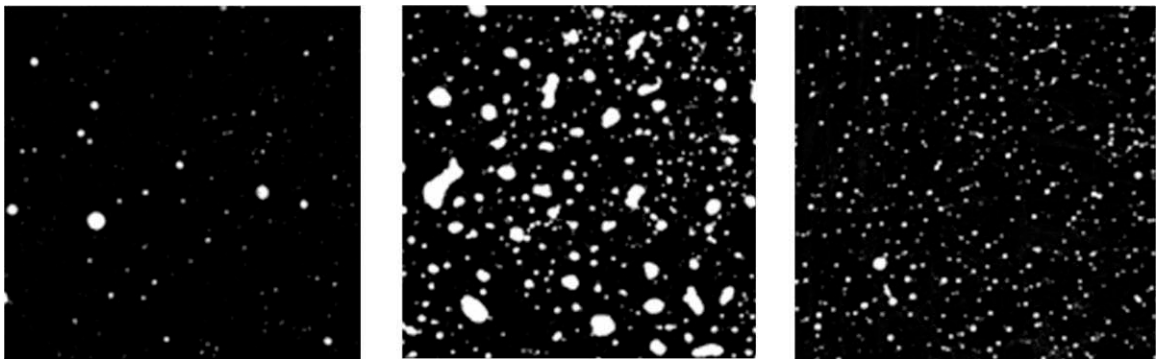

Figure 4. The Design of Preferred Microstructure Using PEHSO Admixture

1.1 Micro-mechanical modeling of PVA-ECC

Fiber reinforced cementitious composites (FRC) can be classified into three different groups based upon the volume of fibers in the matrix. Low volume fractions (VF) (<1%) FRC can greatly reduce the effects of shrinkage cracking [18]. Moderate VF (between 1 and 2%) FRC can improve mechanical properties such as modulus of rupture (MOR), fracture toughness, and impact resistance. FRC in this group can even be used in secondary reinforcement such as partial replacement of shear steel stirrups [19-21] or for crack width control [22, 23]. Within the past couple of decades, a class labeled as high performance FRC (HPFRC) was introduced. This class used high volume fractions (>2%) and typically exhibits tensile strain hardening behavior. Generally, this class of FRC requires the use of steel fibers [11].

More recently, the University of Michigan has developed and fine-tuned a new type of FRC called engineered cementitious composites (ECC). Rather than a strain softening behavior seen in most FRC and the brittle failure of plain concrete, the fiber bridging effect encourages a pseudo strain hardening behavior. Comprised of portland cement, fly ash, sand, water, small amounts of chemical admixtures, and synthetic microfibers, this material displays a high amount of tensile strain (3 and up to 7%) while utilizing fiber volumes in the moderate volume fractions FRC group [9,24]. A summary of the differences between an ECC, a typical FRC and a typical HPFRC are shown in Table 1.

Table1. Comparison between FRC, common HPFRC and ECC

	FRC	Common HPFRC	ECC
Composite Design Methodology	NA	Use high VF	Micromechanics based, minimize VF for cost and processability
Fiber	Any type, VF usually <2%; Diameter of fiber (df) (steel) ~500um	Mostly steel VF usually >5% df (steel) ~150um	Tailored, polymer fibers most suitable; VF usually <2%; df<50um
Matrix	Coarse aggregates used	Fine Aggregates used	Controlled for matrix toughness and initial flaw size; fine sand used
Interface	Not controlled	Not controlled	Chemical debonding energy and frictional bond controlled
Tensile behavior	Strain-softening	Strain-hardening	Strain-hardening
Tensile Strain capacity	0.1%	1.5%	3%; 8% demonstrated
Crack width	Unlimited	Typically several hundred μm unlimited for ε>1.5%	Typically < 100 μm during strain-hardening
Processing	Self-compaction demonstrated; Extrudability demonstrated	Self-compaction impossible due to high VF, often requires high frequency vibration; Extrudability demonstrated	Self-compaction demonstrated; Extrudability demonstrated

The extremely high ductility of ECC is attributed to micromechanical models. More specifically, in order to attain high ductility with lower fiber volumes, micromechanical calculations favor fibers with diameters less than 50 μm [9]. Steel fibers typically have diameters (df)ranging from 150 μm to 500 μm. In principle, smaller diameter steel fibers can be manufactured, but are very expensive to be feasible [11]. Therefore, cost effective polymeric fibers with diameters in the required range are preferred over steel fibers. Some examples of polymeric fibers that have been used for ECC applications are polypropylene (PP), polyethylene (PE), and polyvinyl alcohol (PVA). PVA fibers were selected in many applications due to their potential to balance cost and effectiveness.

1.2 ECC Material Design Basis

The theoretical framework that links the tensile strain-hardening with micromechanical properties of ECC was first established in the early 1990's [25]. For tensile strain hardening to occur, a steady-

state cracking criterion must be used [26] [27]. In order to satisfy this criterion, understanding the σ-δ relationship (which is controlled by tailoring of the fiber, matrix, and interface between the two) is critical [28]. This is the average tensile stress to be transmitted across a crack with a uniform opening experienced during a uniaxial tension test. This σ-δ relationship can be thought of and modeled as a non-linear, "inelastic spring" connecting the two surfaces of a crack. Therefore, the stretch in this "inelastic spring" represents the average force in the fibers bridging the crack [29]. Understanding this σ-δ relationship provides a link between the matrix and the composite ductility (Figure 5).

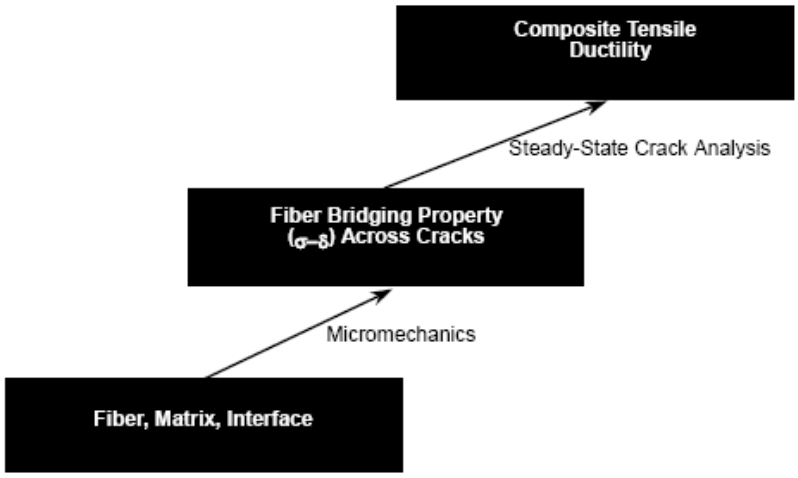

Figure 5. The Link between Material Interactions, Crack Bridging Properties, and ECC Ductility [29]

1.3 Steady-state cracking: flat crack mode (from defect site)

When steady-state crack propagation is achieved, a flat crack with uniform width at the crack tip region is formed under constant ambient tensile stress (σ_{ss}). When this does not occur, the width behind the crack tip will open up to an infinite width and eventually will exceed the bridging stress capacity of the fiber, resulting in either fiber rupture or pullout. Once this capacity is exceeded, no additional multiple cracks can form [25]. This process is known as modified Griffith cracking and this particular cracking scenario is the main failure mode of conventional FRC [25].

Rather than failing under modified Griffith cracking, ECC tends to be governed by steady-state cracking [28]. Marshall and Cox demonstrated that this phenomenon will prevail when the following equation is satisfied [26].

$$J_{tip} = \sigma_{ss}\delta_{ss} - \int_0^{\delta_{ss}} \sigma(\delta)\, d\delta$$

In the above equation, J_{tip} (energy at the crack tip) is approximately equal to the matrix toughness (K_m^2/E_m) at low fiber volumes (appropriate because a typical ECC contains fiber at less than 3%). The matrix fracture toughness (K_m) and matrix modulus of elasticity (E_m) are both dependent on concrete mix design parameters such as water/cementitious material ratio and sand/cementitious material ratio. The right hand side of this equation relates to the energy being supplied by external work minus the energy dissipated by an "inelastic spring" [13]. This inelastic spring analogy is a valid way to conveniently capture the energy dissipated by fiber deformation/rupture and fiber interface debonding/slippage on fibers bridging cracks [13]. Therefore, the equation represents the energy balance of steady-state cracking.

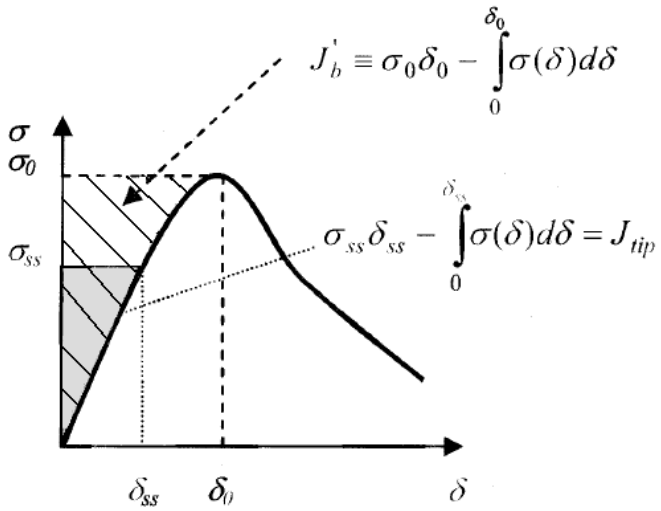

Figure 6. Qualitative Schematic Representation of the Energy Balance Concept on a Fiber Bridging Stress vs. Crack Opening, σ-δ Curve [13]

The concept of energy balance between the fiber bridging stress-crack opening, σ-δ relationship is illustrated in Figure 6. The right-hand side of the previous equation is represented by the area shaded in grey. Furthermore, the maximum energy of the system (located at peak stress (σ_o) and crack opening (δ_o)) is known as complimentary energy (J_b') and is represented by the hatched area. It is the highest possible energy level where steady-state cracking will prevail over modified Griffith cracking. Hence, an upper limit on the matrix toughness (J_{tip}) for the strain-hardening is implied [13].

$$J_{tip} \leq \sigma_0\delta_0 - \int_0^{\delta_0}\sigma(\delta)\,d\delta \equiv J_b'$$

In the above equation, the matrix toughness is limited by the complimentary energy of the system. Therefore, in order to properly design an ECC, the effect of the fiber, matrix, and interface properties must be understood. Specifically, modifying factors such as fiber and interface properties that most directly affect shape of the σ-δ curve are the most important. Maximizing J_b' while keeping J_{tip} at moderate levels is the main idea behind the design of any ECC [13].

When the fiber/matrix interface bond is too weak, the fibers will pull out, resulting in a small σ_o. When the fiber/matrix interface is too strong, the spring cannot stretch hence the fibers will not slip and will prematurely rupture, resulting in a small δ_o. In either case, the result is the same; both ECCs will have a small complimentary energy and will fail under modified Griffith cracking [28]. Figure 7 shows a schematic of the theoretical "inelastic" spring.

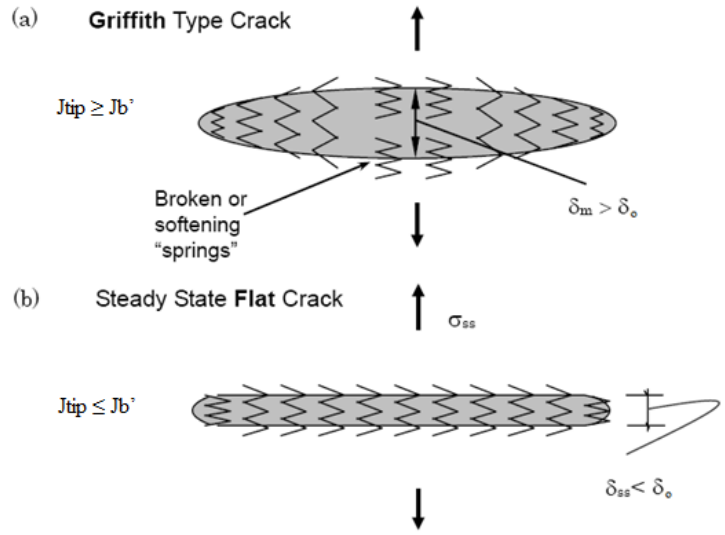

Figure 7. Qualitative Schematic of the Two Different Cracking Scenarios [29]

1.4 Tailoring the Fiber Bridging Stress vs. Crack Opening Curve, σ-δ Curve

The shape or more importantly, the slope of the σ-δ curve shown in Figure 6 is governed by many fiber/matrix interaction mechanisms. In the simplest case where the fiber/matrix bond is only controlled by friction, the curve begins at the origin and the slope of this curve (fiber bridge stiffness) is mainly regulated by the fiber content (V_f), length (L_f), modulus (E_f), and interface frictional bond (τ_o) [13].

When a chemical bond is present, the curve no longer starts at the origin, rather it shifts upwards. This vertical shift represents the initial energy required to break the bond between the fiber and the matrix. Without this debonding, the fiber will not be allowed to stretch and deform the width of the crack opening. Therefore, with the presence of this chemical bond, the J_b' can decrease to a point where the $J_{tip} \geq J_b'$. This implies that the fiber will rupture before any crack forms and will not carry any tensile stresses [13].

Ideally, because of uncertainties in pre-existing crack flaws and fiber distribution of a typical ECC, maximizing the ratio between J_b' and J_{tip} is recommended. ECC with larger ratios have a much better chance to steady-state crack [30]. It is important to note that the models for determining FRC behavior do not apply to one type of fiber, but it applies to different fiber types. Each fiber has unique fiber properties and will not interact with the matrix in the same way. Substituting a different fiber type into a successful ECC mix design may produce a concrete that does not display steady-state cracking.

1.5 PVA Fiber Behavior

The selection of a synthetic fiber for an ECC is based upon several parameters such as tensile strength, modulus of elasticity, chemical bond interaction between the fiber and the concrete matrix, and cost [31]. With PVA fiber's high strength, high modulus of elasticity, and low cost, it is a fiber that is considered to have excellent potential [24]. Its cost is about 1/8 that of the high-modulus PE fiber and is even lower than steel fibers on an equal volume basis [24].

Table 2. Properties of PVA Fiber (RECS15 x 8 mm) [32]

Diameter (mm)	0.04
Thickness (dtex)	15
Cut length (mm)	8
Tensile Strength	1600 N/mm^2 (232.1 ksi)
Elongation (%)	7
Young's Modulus	40 kN/mm^2 (5801 ksi)
Specific Gravity	1.3

Since PVA fibers have a hydroxyl group in its molecular chain and are hydrophilic by nature, the fibers tend to strongly bond with the cement [31]. Li *et al*. (2001) determined that the bond properties of PVA fibers are greater than optimal [33]. Therefore, this strong bond encourages premature rupture of the fiber, thus decreasing the tensile strain capacity of the composite [31]. Furthermore, during fiber pullout tests, Reden *et al*. concluded that this high chemical bond also promotes a strong slip-hardening behavior that can lead to shear-delamination failure of the fiber. With respect to micromechanical theory mentioned above, this strong bond will severely reduce the complimentary energy (J_b') of the composite [34].

Even with all the problems associated with its strong bond, PVA fibers can still be considered a promising alternative because interface bond properties can be modified. The application of an oiling agent to the fibers is one potential solution to this bond problem. When this oiling agent is applied to the fibers, the cement-fiber bond strength will decrease, thus the complimentary energy of the matrix will increase [31]. It was determined that applying oil at 1.2% by volume of fiber to an ECC with fiber content at 2% by volume of concrete, the PVA-cement bond strength can reach an optimum level [33]. The ECC will have an increased tensile strain capacity and decreased crack spacing because it will fail under the steady-state cracking instead of the modified Griffith cracking [33].

2.0 EXPERIMENTAL PROGRAM

The focus of this research project was to develop a new hybrid superhydrophobic engineered cementitious composite (SECC) [9-15], using polyvinyl alcohol fibers and hydrophobic compounds, to create a substitute concrete which can provide the strength and durability demanded in key regions of highway bridges. Normal cement based concrete is a brittle material and inevitably develops cracking, often due to shrinkage during curing which are extended after loading. A new generation of superhydrophobic fiber reinforced concrete material, SECC with enhanced durability and large ductility, will result in up to a 120 year service life as required for critical parts of highway bridges, as well as other concrete infrastructure components.

The superhydrophobic hybridization approach [14-17] is a highly effective method for controlling concrete durability with large volumes of mineral additives, or byproducts used as cement replacements. The developed superhydrophobic ECC meets top sustainability benchmarks and

serves as the next technological level for sustainable concrete infrastructure with improved performance and longer service life.

The first task of the project was to identify the composition and technological approach to produce the ECC with improved ductility and strain-hardening response. The next task is to produce different types of superhydrophobic admixtures and investigate the performance of SECCs with PVA fibers and different dosages of superhydrophobic admixture (0.01 - 0.1% of cement weight).

Initially, the research work focused on the proportioning and dispersion of hydrophobic/ super-hydrophobic (PEHSO/PMHS/PEHS-based) admixtures needed to achieve optimal volume, size, and distribution of air voids within the hardened paste and to provide long-term durability for the concrete/ECC. Different types of PMHS additive were produced (at different emulsification speeds and concentrations of emulsifying agent and nano-particle dosage), characterized and tested in mortars.

Mortar tests with PMHS admixtures were conducted in order to understand the effect of superhydrophobic hybridication on performance (strength and durability) of cement based systems.

It was demonstrated that the application of the developed PMHS admixture in ECC helps to control the bond of PVA fibers and realize controlled pullout behavior rather than fiber rupture. Furthermore, the controlled air void structure can be used to design "preferred" fracture modes (Figure 8). These synergetic effects were further investigated.

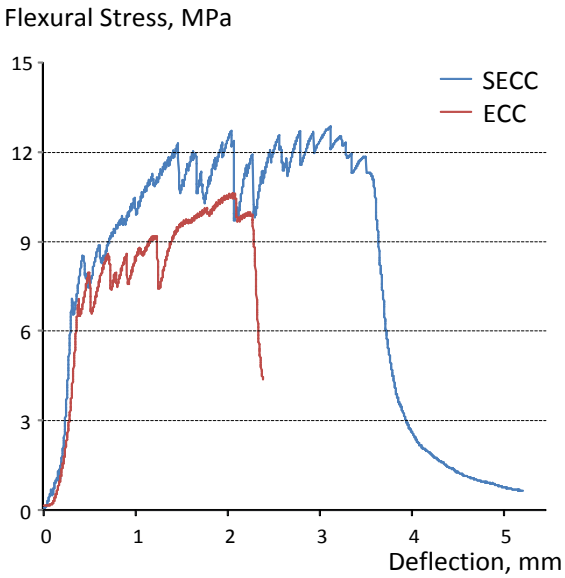

Figure 8. The Strain-Hardening and Improved Ductility Performance of SECC

To determine the proper way to use PVA fibers within the ECC matrix, several steps had to be considered. A preliminary study was performed in order to determine the correct water to cement ratio (W/C). The W/C is one of the key parameters correlating to the workability and strength of the ECC. A lower water to cement ratio facilitates higher strengths, while at the same time greatly reduces the workability. Finding the proper tradeoff and balance between these two while also determining the correct dosage of superplasticizer is extremely critical.

The superplasticizer enables a lower W/C to be used, while a maintaining good workability. Excessive quantities of superplasticizer lead to bleeding of water and also segregation between the matrix and sand and these effects are especially evident when PVA fibers are used. Another parameter determined during this study was the correct amount of PVA fibers to use. Since fibers are added at dosages of around 2-4% by volume, they comprise a good portion of the ECC matrix. However, when larger volumes of fibers are used they can greatly reduce the workability of the concrete and can be detrimental to the performance of the ECC due to voids created and the difficulty of compaction.

Sand content was determined in order to maintain a good performance of the ECC while allowing for an economical mix of cementitious material and sand for the ECC. The final parameter considered for the preliminary study was the mixing procedure used for the ECC. This is a key parameter as the fibers need to be mixed in the proper way to ensure even distribution throughout the matrix and with no "clumps" which would reduce concrete strength by creating a less uniform matrix.

The four different hydrophobic emulsions were then compared. These four emulsions were applied to the PVA-ECC matrix at a single and double dose and then compared to a reference sample and a sample with air entraining admixture.

A study considering several different supplementary cementitious materials (SCM) was also performed. The use of SCM in ECC is useful for several different reasons. First, by using materials in place of portland cement, the material becomes "greener" by utilizing by-products and reducing raw materials usage. It will also lower the burden on cement production, one of the largest contributors of CO_2 emissions into the atmosphere. The use of selected SCM can also lead to ultra-high strength concrete as well as ultra-durable concrete. This is possible as the particle size of the byproduct material can be smaller than that of portland cement, allowing for a better contact zone and making a much stronger matrix. Commonly, the use of SCMs such as fly ash or ground granulated blast furnace slag weakens the matrix and reduces the bond between the cementitious matrix and the PVA fibers. Since the cement-PVA bond is very strong, the failure modes for the composite specimens are typically fiber ruptures. Ideally the fibers should be able to slightly slip out of the cementitious matrix allowing for maximum ductility while still maintaining enough bond for maximum strength. One approach to implement this is by oiling the fibers [12]. Another approach is to use SCM such as a high volume of fly ash to weaken the overall cementitious matrix and the bond between the cementitious material and the PVA fibers [13]

However, high volumes of fly ash reduce the strengths of the PVA-ECC especially at early ages. This approach is not desirable for most cementitious materials. An ideal mixture of SCM and portland cement allows the matrix to be weak enough to enable the fibers to slip out instead of rupturing, while at the same time maintaining high strength. This study demonstrates the appropriate combination of SCM and portland cement to allow for both maximum strength and ductility. A reference ECC specimen was produced with 100% portland cement and compared to specimens with 10% fly ash, 20% fly ash, 10% metakaolin, 10% silica fume, 10% blast furnace slag, and 50% blast furnace slag as supplementary materials for portland cement. Each specimen was tested both with and without a single dosage of emulsion in order to determine the compatibility of emulsions and SCMs.

Superhydrophobic emulsions were studied and consisted of a reference specimen compared to superhydrophobic emulsions with particles. Superhydrophobic emulsions created by incorporating portland cement, metakaolin, and silica fume were then compared against the reference specimen for fresh and mechanical properties of the PVA-ECC. Each type of emulsion was applied at a single and double dose.

The flow of fresh ECC mortars, 1-, 7-, and 28-day flexural strength and ductility, cracking patterns, as well as 1-, 7-, and 28-day compressive strengths were tested and recorded. Larger PVA-ECC specimen testing was performed in order to confirm the main investigation based on smaller specimens.

2.1 Materials

Commercial type I ordinary portland cement (OPC) from Lafarge and supplementary cementitious materials (SCM) such as: fly ash Class F (FA-F) from We Energies, metakaolin (MK) from Burgess Optipozz, silica fume (SF) from Elkem, lime (L) from Western Lime and blast furnace slag (BFS) from Lafarge were used in this research project. The chemical and physical properties of OPC and FA-F are shown in Tables 4 and 5, respectively. X-ray diffraction for OPC, FA F, SF and BFS are presented in Figures 9 and 10.

ASTM-graded quartz sand and tap water were used to produce mortar specimens.

The mechanical and geometrical properties of the Kuralon K-II PVA Fibers from Kuraray Japan used in this study are shown in Table 3. Commercially available polyacrilate/polycarboxylate superplasticizer (PAE/SP, 31% concentration, supplied by Handy Chemicals) was used as modifying admixtures. The air-entraining admixture was MB AE-90 from BASF and it was used at a dosage of 50 ml per 100 kg of cementitious materials as recommended by the company.

Table 3. Properties of PVA Fibers

PVA Fiber	Density (dtex)	Length (mm)	Tenacity (cN/dtex)	Elongation (%)	Modulus (cN/dtex)
RECS 7x6mm	7	6	12	7	300

Note: 1 dtex= 1 x 10^{-7} kg/m =0.9 denier

Table 4. Properties of Portland Cement Type I as per as ASTM C-150 Requirements

CHEMICAL

Item	Spec. Limit	Test Result
SiO_2, %	--------	20.6
Al_2O_3, %	--------	4.7
Fe_2O_3, %	--------	2.7
CaO, %	--------	63.9
MgO, %	6.0 max	2.3
SO_3, %	3.0 max	2.4
Ignition loss, %	3.0 max	2.1
Insoluble residue, %	0.75 max	0.36
Free lime, %	--------	1.1
CO_2, %	--------	1.3
Limestone, %	--------	3.4
$CaCO_3$ in limestone, %	--------	93.0
Potential, %		
C_3S	--------	55.0
C_2S	--------	17.6
C_3A	--------	8.0
C_4AF	--------	8.2
$C_4AF+2(C_3A)$	--------	24.2
$C_3S+4.75(C_3A)$	--------	93.0
Na_2O_{equi}	0.6 max	0.55

PHYSICAL

Item	Spec. Limit	Test Result
Air content, % (C-185)	12 max	7.5
Blaine fineness, m^2/kg (C-204)	260 min	380
Autoclave expansion, % (C-151)	0.8 max	0.02
Compressive strength, MPa		
1 day	--------	12.4
3 days	12.0 min	21.7
7days	19.0 min	27.6
28 days	28.0 min	37.9
Time of setting, minutes		
Initial	45 min	110
Final	375 max	225
Heat of hydration at 7 days, kJ/kg	--------	411
Percent Passing 325 Mesh (C-430)	--------	95.4

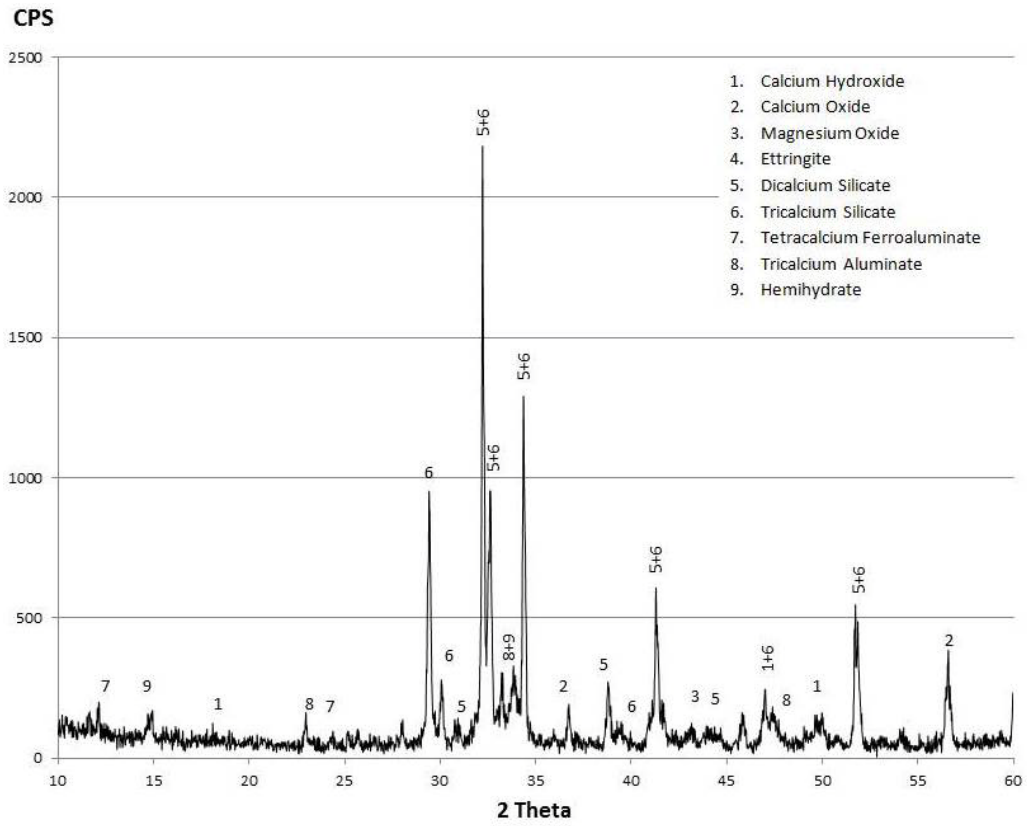

Figure 9. X-ray Diffraction of Ordinary Portland Cement

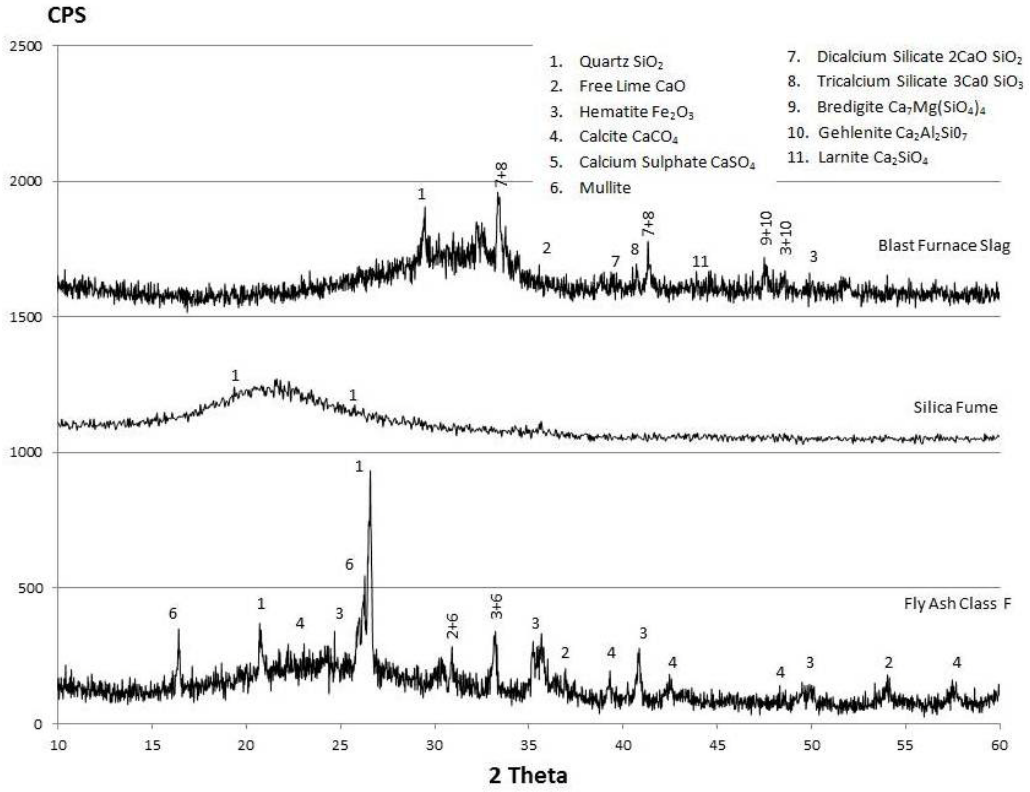

Figure 10. X-ray Diffraction of Fly Ash Class F, Silica Fume and Blast Furnace Slag

Table 5. Chemical Composition of Fly Ash Class F

Chemical composition, %	Class F	ASTM C618 limits
Silicon Oxide, SiO_2	49.9	-----
Aluminum Oxide, Al_2O_3	24.0	-----
Iron Oxide, Fe_2O_3	14.4	-----
Total, $SiO_2+Al_2O_3+Fe_2O_3$	88.0	70 min
Sulfur Trioxide, SO_3	0.88	5.0 max
Calcium Oxide, CaO	3.23	-----
Magnesium Oxide, MgO	0.98	-----
Potassium Oxide, K_2O	2.46	-----
Moisture Content	0.11	3.0 max
Loss on Ignition	3.50	6.0 max

Physical Tests	Class F	ASTM C618 limits
Fineness, % Retained on #325 Sieve	25.7	34 max
Pozzolanic Activity Index with Portland Cement, 28 days, %	93	75 min
Water Requirement, % of Control	103	105 max
Soundness, Autoclave Expansion, %	0.08	0.8 max
Specific Gravity	2.30	-----

The morphology of OPC, MK, SF, L, FAF, and BFS were analyzed using SEM (Figure 11). Angular particles with sizes from 0.2 to 35 μm were found in ordinary portland cement. Rough and flaky particles with sizes from 0.8 to 12 μm with a certain degree of agglomeration were found in metakaolin. Spherical particles with sizes from 0.2 to 1 μm with a certain degree of agglomeration were found in silica fume. Angular particles with sizes from 0.3 to 3 μm with a certain degree of agglomeration were found in lime. Spherical particles with sizes from 0.3 to 15 μm were found in fly ash Class F. Angular particles with sizes from 0.5 to 17 μm were found in blast furnace slag.

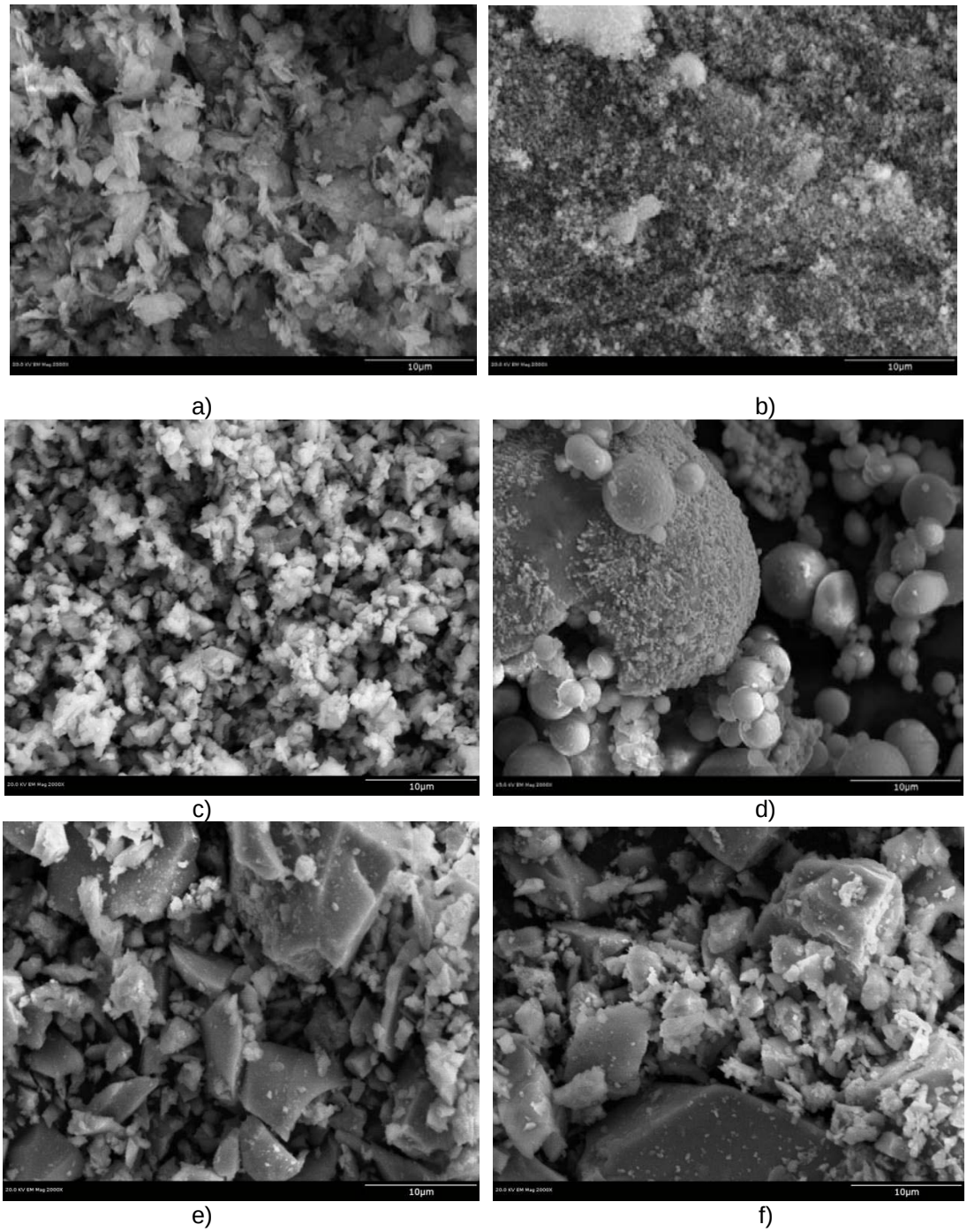

Figure 11. SEM Images at 2000x Magnification for Particles of: a) Metakaolin; b) Silica Fume; c) Lime; and b) Fly Ash Class F; e) Blast Furnace Slag (Slag Cement); and f) Portland Cement

2.2 Standard Procedures and Testing Protocols

Microstructural Characterization

X-ray diffraction (XRD), SEM and optical microscopy were used to investigate the internal structure, morphology and size distribution of the materials used.

Preparation and Testing of Emulsions

The concentration of siloxane was kept constant at 25% by weight of the emulsion, while the concentration of the PVA surfactant was 2.2% or 4.4% by weight of the water, as a lower and upper limit. The PVA was gradually added to de-ionized water and stirred for 10 minutes at 23±3°C temperature, on a hot plate using a magnetic stirrer. The temperature was then increased to 90°C, and kept constant for 40 minutes while continually stirring the solution. Then, siloxane was added and mixed for 10 minutes using a high speed mixer (Silverson model L5M-A) at 1,000 or 10,000 rpm, at lower and upper levels. A summary of the emulsions produced and used is presented in Table 6.

2.3 Superhydrophobic emulsions and coatings

The concentration of siloxane and surfactant was kept constant at 25 and 4.4% by weight of the emulsion. The PVA was gradually added to de-ionized water and stirred for 10 minutes at 23±3°C temperature, on a hot plate using a magnetic stirrer. The temperature was then increased to 90°C, and kept constant for 40 minutes while stirring the solution. The solution was allowed to remain in a water bath until 23±3°C was achieved. A sketch of this procedure and additions of siloxane and 0.5% of metakaolin by weight of the emulsion are seen in Figure 12. High speed mixer (HSM, from Silverson model L5M-A) was used to mix siloxane and metakaolin (or other powder component such as portland cement or SF) in PVA and water solution. The emulsions were characterized by an optical microscope (Olympus BH-2) at 100x and 1000x magnification.

Table 6. Specifications of Cement Mortars with Different Siloxane Emulsions

Mix	Name	W/C	C/S	PVA %	Emulsion Preparation and Use		
					Siloxane %	Speed of mixing (rpm)	Admixture Quantity (g/l)
1	slow1	0.35	1	4.4	25	1000	0.25
2	slow2	0.35	1	4.4	25	1000	0.50
3	fast1	0.35	1	4.4	25	10000	0.25
4	fast2	0.35	1	4.4	25	10000	0.50
5	pslow1	0.35	1	2.2	25	1000	0.25
6	pslow2	0.35	1	2.2	25	1000	0.50
7	pfast1	0.35	1	2.2	25	10000	0.25
8	pfast2	0.35	1	2.2	25	10000	0.50
9	reference	0.35	1	-	-	-	-
10	AE50	0.35	1	-	-	-	0.25

Fabrication of specimens for testing of super-hydrophobic admixtures

Small mortar tiles were prepared for tests on hydrophobicity and contact angle. The water to cement ratio (W/C) of 0.5 and sand to OPC ratio (S/C) of 2.75 were used. Tiles of 10 x 10 x 5 mm were cast and compacted using a shaking table. After 24 hours, tiles were de-molded and cured in saturated lime water for 28-days.

After curing, the tile surfaces were slightly polished with a silicon carbide grinding paper with a grit of 320, in order to expose the fresh surface. High porosity and scratches were revealed on the specimens after the polishing procedure. The porosity of non-covered specimens is shown in Figure 13, at a different magnification.

Wire glued on one border of the tile was used to dip it into the emulsion for 20 seconds. The excess of emulsion in the tile was removed using a soft-plastic spatula. Specimens were dried at a room temperature for 48 hr. This procedure was repeated when two layers of coating were required. Contact angle of the treated surfaces was measured for a single- and double- coat procedure.

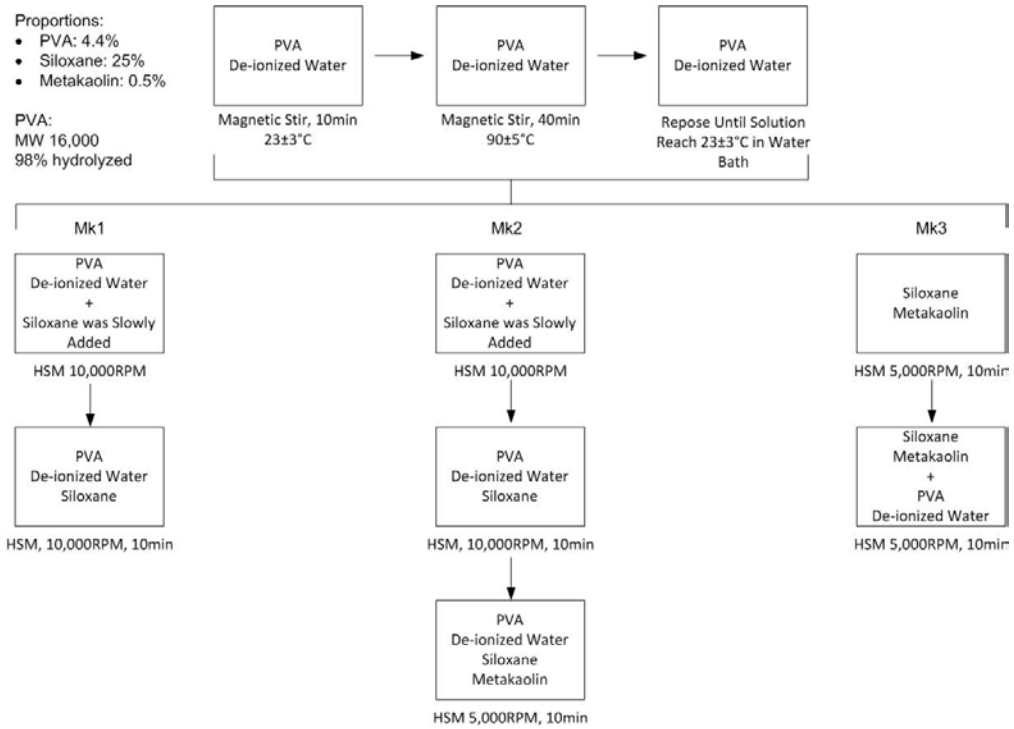

Figure 12. Sketch of the Procedure for Preparation of Superhydrophobic Emulsions

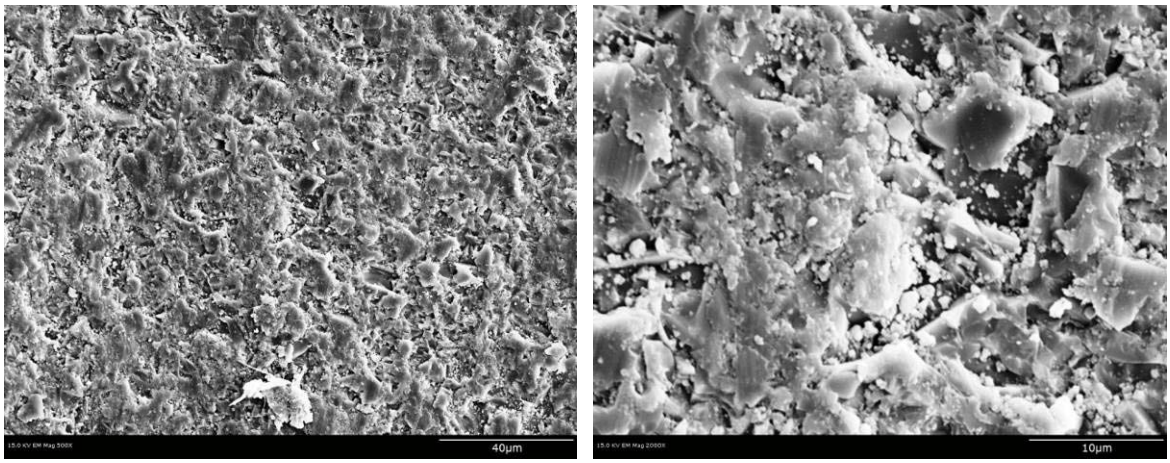

a) b)

Figure 13. The Surface of Mortar Tiles after Polishing as observed by SEM at Magnification of: a) 500x and b) 2000x

Contact Angle Testing

Distilled water was used to analyze the hydrophobic coating properties of emulsions. To measure the contact angle, 15 µl of water was placed on different parts of the specimen surface and photographed using state-of-the-art testing equipment.

Evaluation of Siloxane Emulsions in Mortars

Ten portland cement mortar mixes were prepared for this study. The reference mix and the air-entrained mix (AE50) were used to compare the behavior of samples with emulsions. A summary of the characteristics of each mix is shown in Table 6 with two sets of mortar samples produced, per each emulsion prepared. Thus, the rest of the samples had a siloxane-based admixture at 0.25 and 0.50 g/l of siloxane content by the total volume of the batch for a single- and double dose , respectively.

The water-to-cementitious material ratio (W/C) was 0.35 and sand-to-cementitious material ratio (S/C) was 1.

The fresh properties of the mixtures such as flow and air content were investigated. For all mortars the flow was measured following ASTM C230 [35], while the air content was evaluated following ASTM C185 [36]. Air content was measured over 2 hours for the mixes containing emulsions to measure the increase of air content over time. In order to obtain the measurements, 2/3 of a standard type B measuring bowl was filled with concrete which was enabled to harden, leaving a total volume of 2.4 liters for the mortar samples. After the initial reading, the sample was kept in the bowl and subsequent readings were taken every 30 minutes for 2 hours from the time of the mixing. Air content was measured in two reference samples in order to find a correlation between the standard and modified procedure using a bowl with reduced volume. As a result, a correlation factor was determined and used for analysis and comparison.

The hydrophobicity of the mixes can be evaluated by contact angle and by water absorption test. In contact angle tests, surface hydrophobicity is assessed by placing a water drop on the hydrophobic surface and measuring the angle between the surface of the mortar and the edge of the droplet. In

the latter, water absorption is tested by drying and immersing the 28-day cube specimen in water. The weight of the cube is recorded, when dry and after 24-hours immersion in water. The change in weight is the amount of water the sample has absorbed, providing a value of internal open porosity. Here, the kinetics of absorption can be used as an estimate of hydrophobicity.

The materials for mortar specimens were mixed according to ASTM C305 [37]. The following specimens were produced for this study: 9 cube specimens of 50.8 mm x 50.8 mm x 50.8 mm, 5 beam specimens of 40 x 40 x 160 mm, 2 beam specimens of 40 x 40 x 160 mm with steel inserts, 2 cylinders of Ø 75 x 150 mm and Ø 100 x 200 mm.

Cube specimens were produced, cured and tested for compressive strength testing according to ASTM C109 [38] at 7, 14 and 28 days. Beam specimens were molded and cured according to ASTM C348 [39] and tested for flexural and compressive strength, dynamic Young's modulus of elasticity according to ASTM C349 [40] and ASTM C666 [41], respectively. Specimens of 40 x 40 x 160 mm with steel inserts were molded and cured according to ASTM C348 [39] and tested for length variations according to ASTM C666 [41], respectively. Because these beams are shorter than the commonly used 11-inch beams, the deformation device was adjusted to shorter beams, having an L_g factor of 5 in. Cylindrical specimens of Ø75x150 mm were molded and cured according to ASTM C348 [39] and used for the analysis of air void system according to Zalocha's method [42]. Lastly, cylindrical specimens of Ø100x200 mm were molded and cured according to ASTM C-348 [39] for subsequent tests for rapid chloride permeability according to ASTM C1202 [43].

After 14 days of standard curing, the specimens were removed from the water tank and exposed to frost action. The freezing and thawing cycle was set in the environmental chamber in order to test mortar specimens at 20 °C with 95% of relative humidity for 2 hours; and later the temperature switched to -50 °C with 0% of relative humidity for 2 hours [14]. This procedure was considered to simulate an accelerated freezing and thawing cycle.

Compressive strength, transverse frequency and weight loss of the mortars were established in order to assess damage to specimens undergoing freeze-thaw testing at different cycles.

2.4 Preparation of PVA-ECC

The mixing procedure for PVA-ECC was determined in the preliminary phase of research. Since there are no standards for mixing materials with PVA fibers and superhydrophobic emulsions, several different methods were tested. The main goal of the mixing procedure was to determine how to evenly disperse the fibers and create uniformity throughout the mixture. One problem that arose with some of the mixing procedures was that the PVA fibers formed "clumps" thus creating portions of the specimen with an absence of fibers leading to lower strengths and ductility when tested. Another approach in the mixing methods was to determine when would be the best time to add the emulsion. One suggestion was that by wetting PVA fibers in the emulsion prior to mixing of cementitious materials and sand, the PVA fibers would have lesser bond to the cementitious matrix and, therefore, be able to pull out of the matrix, instead of having the fibers rupture. This method was thought to act in a similar way to the proposed use of oiling agents to allow for more ductility [12]. Finally, the best results for mixing all of the materials in the PVA-ECC, was determined by adding the superplasticizer along with ¾ of the water, followed by the addition of ASTM standard silica sand. Next, the PVA fibers would be added in two increments followed by the portland cement also in two increments. Finally, the emulsion would be added. Other methods did not

provide adequate distribution of the fibers and created “clumps”, leaving some areas without reinforcing fibers, so the fibers are unable to act as designed. Typically when water and cementitious materials were added to the mixture prior to the sand and PVA fibers, there were areas of segregation between the cement matrix and the PVA fibers. By mixing the sand and PVA fibers during the early stages of mixing, the abrasion of the sand allowed for good distribution of the fibers. Table 7 demonstrates the different methods attempted and the results. Procedure 3G was chosen as the best procedure because it was able to distribute the fibers in an ideal manner throughout the mixture.

For each mixture the ECC cube and beam specimens were produced. The beams were 160 mm long x 14 mm tall x 40 mm wide. The cubes were 50.8 mm x 50.8 mm x 50.8 mm as per ASTM C-109 [38] standards for testing hydraulic cement mortars for compression. The molds were coated with a release agent (WD-40) prior to placing the PVA-ECC mix so that the specimens could be easily removed after 24 hours. The fresh PVA-ECC mix was placed in the molds in two layers. Each layer was compacted using a standard hard rubber tamper (13 x 25 x 152 mm) for mortars. Finally the molds were compacted by 20 drops using a jolting table (Figure 14c) and leveled to produce a smooth surface.

Table 7. Mixing Procedures used for ECC

	Procedure	Maximum Flexural Stress (MPa)	Flexural Strain at Max. Stress (mm/mm)
1A	Sand+ PC→ water+super+Si→Sand→PVA	20.22	0.0069
1B	water+Si+50% fiber→cement+super→sand→50% PVA	18.24	0.0037
1C	H2O+Si→cement+super→PVA→sand	15.17	0.0049
1D	cement→50%PVA+water+Si→sand→50%PVA	16.92	0.0037
2A	water+Si→100%PVA→cement→super→sand	12.88	0.0026
2B	water+Si→50% PVA→cement→super→50%fiber→sand	13.13	0.0049
2C	water+Si→cement→super→100%fiber→sand	16.86	0.0051
3A	90% water+Si→cement→super + 10% water→PVA→sand	17.74	0.0054
3B	33% water+Si+super→sand→PVA in two increments→50% cement + 66% water→50% cement	19.80	0.0073
3C	90% water+Si→cement→super + 10% water→PVA+sand mixed separately then combined with remaining mixture	20.12	0.0057
3D	90% water+Si+ PVA →sand →cement in two increments→super + 10% water	18.05	0.0055
3E	33% water +Si→sand→PVA in two increments→50% cement + 66% water + super→50% cement	15.00	0.0081
3F	90% water+Si+ PVA →sand →50 % cement + super + 10% water→50% cement	14.29	0.0069
3G	75% water+super→sand→PVA in two increments→50% cement + 25% water + Si→50% cement	16.72	0.0051

Notation: super=superplasticizer; Si=siloxane emulsion; cement=any cementitious material; PVA=PVA fibers

After placing the ECC in the molds they were covered with glass plates and placed in a curing room at room temperature (20 ± 3°C) and a relative humidity of no less than 90% as per ASTM C-192 standards. Specimens were removed from the molds after 24 hours. One-day tests were then performed on the appropriate specimens and the remaining specimens were placed in a lime water bath until they reached their testing age. To test the flow of the fresh ECC, a 10-in flow table was used as per ASTM C230 standards [35] (Figure 14b). The ECC was then placed in a flow mold in two layers. Each layer was compacted with a standard hard rubber tamper 20 times and then leveled to create a smooth top surface. The flow mold was in a form of a conical shape with the

bottom base being 100 mm wide and a top surface of 70 mm in diameter [35]. The height of the mold was 50.8 mm tall. After the top surface of the ECC was leveled the flow mold was removed and the flow table dropped 25 times. The diameter of the flow was then recorded in order to compare the flow to other mixtures.

Compression tests were performed on the 50.8 x 50.8 x 50.8 mm cubes. The specimens were placed in the compression machine and loaded at a rate of 0.9 kN/sec as per as ASTM C 109 standard. The maximum load (kN) as well as the maximum compressive stress (MPa) were then recorded. Flexural tests were then performed on the 160 mm long x 14 mm tall x 40 mm wide beams using the 4-point bending test. The end supports were 120 mm apart with the middle loading supports 40 mm apart (Figure 14d). The beams were then loaded at a rate of 1.2 mm/min to observe the stress-strain behavior after initial cracking. After the beams were tested under flexure they were examined under a magnifying glass to view the cracking patterns. Typically, only the failure crack could be observed by the naked eye, therefore magnification must be used in order to observe small cracks that are consistent with ECC flexural behavior. These cracks were then highlighted with black marker and compared against one another for their cracking behavior.

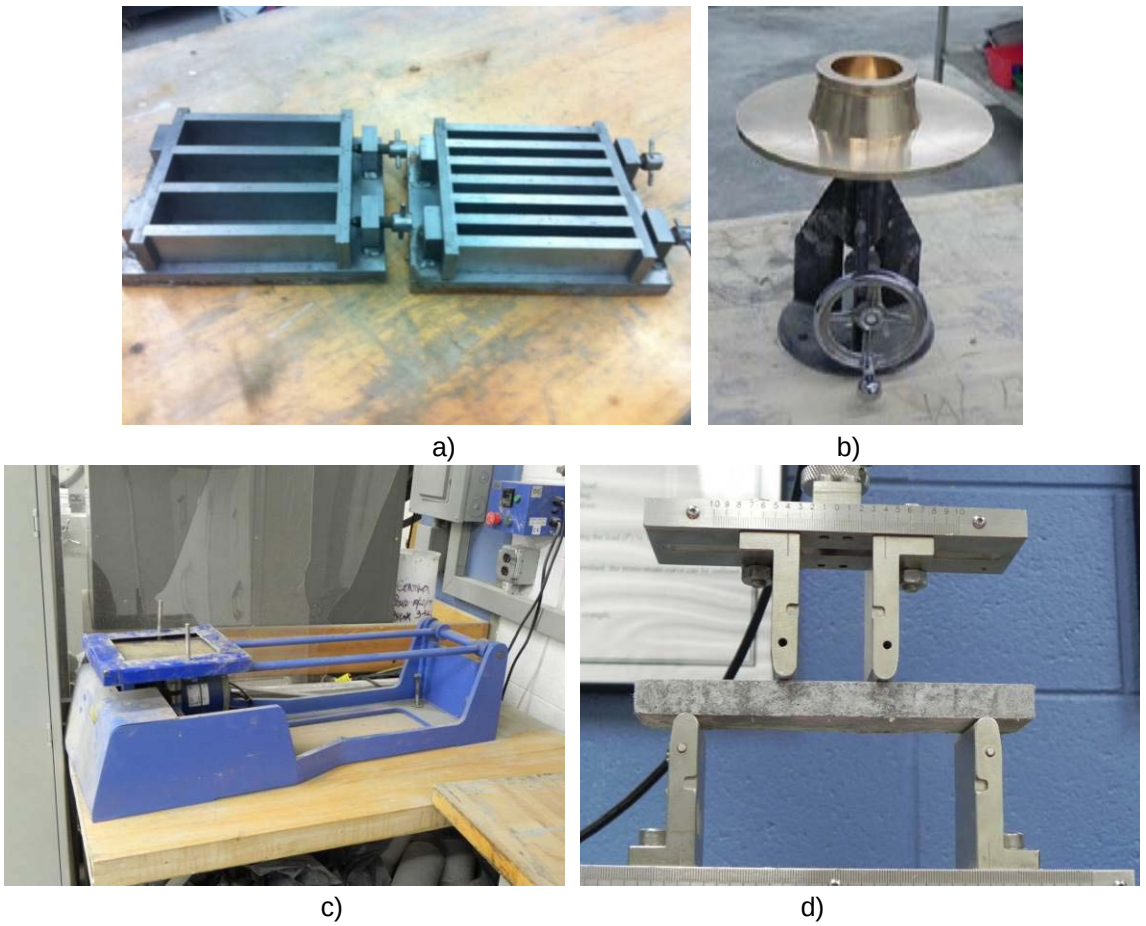

Figure 14. The Equipment Setup Used in ECC/SECC Study: a) Six-Gang Mold used for ECC Specimens; b) Flow Table; c) Jolting Table; d) The Setup of 4-Point Bending Test

2.5 SECC: Hydrophobic Emulsion Study

In cold weather climates with freezing and thawing cycles, it is important to create the air voids within the cementitious matrix to allow for better resistance to these detrimental effects. This allows water to expand into the manufactured voids within the concrete instead of creating excessive pressure within the smaller voids which under freezing causes early cracking. To do this, air entraining admixtures are commonly added to concrete mixtures to allow these manufactured air voids to be present within the concrete. However, these air entraining admixtures typically create a reduction in strength for the concrete. The use of hydrophobic emulsions allows these air voids to be created within the concrete, but maintaining the same strengths seen in the plain reference specimens. Moreover, the hydrophobicity of the emulsions helps to reduce the amount of water entering the voids within the concrete, which when frozen causes local stresses within the concrete leading to cracking and concrete failure.

The flexural behavior and compressive strength of SECCs with four different hydrophobic emulsions were compared against a reference specimen and a specimen with an air entraining agent. Each of the hydrophobic emulsion consisted of 25% siloxane and varying amounts of emulsifier (water-soluble PVA). Each emulsions was also mixed at different speeds to determine if a faster mixing speed (10,000 rpm compared to 1,000 rpm) affects the stability of the emulsion. The experimental matrix for this study can be seen in Table 8. For reference purposes, specimen ID displays the emulsion being used. The first two characters represent either 4.4% or 2.2% PVA emulsifier for P4 and P2, respectively. The next character represents mixing speed S and F, for a slow (1,000 rpm) or fast speed (10,000 rpm) respectively. The last character represents the emulsion dosage being used, which is either 1 for a single- or 2 for a double-dosage. Here, the reference specimen did not include any admixture while the air entraining specimen incorporated MB AE-90 at a dosage of 100 ml of admixture per 100 kg of portland cement (as recommended by the manufacturer).

Each of the mixtures incorporated a W/C ratio of 0.3 and superplasticizer content of 0.125% by weight of the cement as determined in the preliminary study. The sand to cement (S/C) ratio used for the following specimens was 0.5 while ASTM standard silica sand was used. Finally, the fiber content for all specimens was 3% by total volume using Kuraray II RECS 7 x 6 mm fibers.

To determine the compressive strength of the above specimens, 50.8 x 50.8 x 50.8 mm cubes were cast. These cubes were tested for compressive strength at 1, 7, 14, and 28 days. Two cubes were tested for 1, 7, and 14 days and the maximum compressive stress of the two cubes was averaged and displayed in the figure below. The 28 day compressive strength results were determined by averaging three cubes.

The flexural behavior of the specimens was observed at 28 days. Three beams were tested for each specimen and the stress vs. strain curve of each was used when compared against other specimens. Since both flexural stress and flexural strain was of concern in these results, determining the median curve was not always as straight forward as the reference. However, since the 28 day flexural results showed little variation between beams of the same specimen, the curve that was chosen as the median curve accurately represents the behavior of the specimen.

Table 8. The Experimental Matrix for Studying the Effect of Hydrophobic Emulsions

Specimen ID	Siloxane Content	PVA Content	Mixing Speed	Dosage	Corresponding Cement Mortar Mix (Table 2)
E1_REF	Reference (no emulsion or air entraining admixture used)				9 (Reference)
E2_AE	100ml of air entraining admixture (MB AE-90)/100kg of portland cement				10 (AE 50)
E3_P4S1	25%	4.4%	1,000 rpm	1	1 (Slow 1)
E4_P4S2	25%	4.4%	1,000 rpm	2	2 (Slow 2)
E5_P4F1	25%	4.4%	10,000 rpm	1	3 (Fast 1)
E6_P4F2	25%	4.4%	10,000 rpm	2	4 (Fast 2)
E7_P2S1	25%	2.2%	1,000 rpm	1	5 (P Slow 1)
E8_P2S2	25%	2.2%	1,000 rpm	2	6 (P Slow 2)
E9_P2F1	25%	2.2%	10,000 rpm	1	7 (P Fast 1)
E10_P2F2	25%	2.2%	10,000 rpm	2	8 (P Fast 2)

2.6 Supplementary Cementitious Materials (SCM) Study

Several supplementary cementitious materials were considered for use in the composition of ECC/SECC. These materials not only lessen the burden on cement production by incorporating by-products as cementitious material, but also, if used correctly, can actually improve performance of the ECC. Fly ash, metakaolin, silica fume, and blast furnace slag were considered in this study. First, each SCM replaced 10% of the portland cement and was tested both with and siloxane emulsion. The emulsion chosen in this study was one incorporating the larger amount of PVA mixed at a faster speed (E5_P4F1) and was regarded as the best emulsion based on emulsion study results. Mixtures with 20% fly ash and 50% blast furnace slag were also considered. The experimental matrix is shown in Table 9. It should be noted that the water to cementitious material ratio, superplasticizer amount, sand to cemententitious material ratio, and PVA fiber volume remained the same for all samples except for the two incorporating metakaolin. For these specimens the superplasticizer amount had to be slightly increased to 0.2% of the cementitious material weight, in order to maintain similar workability as compared to other specimens. Extra water that may be present in the emulsion and the superplasticizer was taken into account when determining the proper amount of water to use, therefore the water to cementitious ratio remained exactly the same for all specimens.

For each specimen, 1 day, 7 day, and 28 day flexural behavior was observed along with the cracking patterns of each beam tested. Compressive strengths corresponding to the same ages were also observed. Since the introduction of SCM into the cementitious matrix can significantly change the

chemistry and behavior, the differences in results varied between the specimens. That being said, 2 beams were tested for flexure at 1 and 7 days, while 3 beams were tested for flexure at 28 days and the results of the beams of the same specimen did not show much deviation, thus selecting a single beam's flexural behavior in order to compare to another, can confidently be considered an accurate representation.

Table 9. Experimental Matrix of Supplementary Cementitious Materials

Specimen ID	SCM	Hydrophobic Emulsion
SCM1_REF_0	None (100% PC)	None
SCM2_REF_1	None (100% PC)	Single Dosage (4.4%PVA, 10,000rpm)
SCM3_10FA_0	10% Fly Ash	None
SCM4_10FA_1	10% Fly Ash	Single Dosage (4.4%PVA, 10,000rpm)
SCM5_20FA_0	20% Fly Ash	None
SCM6_20FA_1	20% Fly Ash	Single Dosage (4.4%PVA, 10,000rpm)
SCM7_10MK_0	10% Metakaolin	None
SCM8_10MK_1	10% Metakaolin	Single Dosage (4.4%PVA, 10,000rpm)
SCM9_10SF_0	10% Silica Fume	None
SCM10_10SF_1	10% Silica Fume	Single Dosage (4.4%PVA, 10,000rpm)
SCM11_10Slag_0	10% Blast Furnace Slag	None
SCM12_10Slag_1	10% Blast Furnace Slag	Single Dosage (4.4%PVA, 10,000rpm)
SCM13_50Slag_0	50% Blast Furnace Slag	None
SCM14_50Slag_1	50% Blast Furnace Slag	Single Dosage (4.4%PVA, 10,000rpm)

2.7 SECC: Superhydrophobic Emulsion Study

Several superhydrophobic emulsions were tested for their effect on mechanical properties and compared against the reference hydrophobic emulsions. A standard mix with water to cementitious ratio of 0.3 and sand to cementitious ratio of 0.5 along with a 3% volume of PVA fibers were used for all mixes. First, a single- and double-dosage of reference hydrophobic emulsion (consisting of 4.4% PVA, 25% siloxane, mixed at 10,000 rpm) was used. Next, three different superhydrophobic emulsions were considered, each at a single- and double- dosage. Three superhydrophobic emulsions were produced using MK2 approach (Figure 12). In addition to MK, portland cement and silica fume were used for manufacturing of superhydrophobic emulsions.

Table 10 shows the experimental matrix for the different superhydrophobic emulsions tested in this study.

Table 10. Experimental Matrix of Superhydrophobic Emulsions

Specimen ID	Superhydrophobic Emulsion	Dosage
SH1_REF_1	E5_P4F1 (reference hydrophobic emulsion)	1
SH2_REF_2	E6_P4F2 (reference hydrophobic emulsion)	2
SH3_PC_1	PC2	1
SH4_PC_2	PC2	2
SH5_MK_1	MK2	1
SH6_MK_2	MK2	2
SH7_SF_1	SF2	1
SH8_SF_2	SF2	2

3.0 RESULTS AND DISCUSSION

3.1 Hydrophobic Emulsion Study

The investigated emulsions were prepared at different concentrations of the surfactant and various speeds of mixing. It can be observed from the graph that the diameter of the siloxane droplets decrease with larger quantities of surfactant and mixing at higher speeds. The change in droplet size is even more significant when using lower quantities of surfactant.
Figure 15 shows that emulsions with lower content of PVAS have larger droplet sizes, while the use of higher PVAS amounts results in the formation of uniform small droplets. Also mixes labeled as “Fast” contain larger number of smaller droplets, since the amount of the siloxane is the same in all of the emulsions. This is because the faster the emulsion is mixed, or the higher the mechanical input, the smaller the droplets because the siloxane phase is further divided.

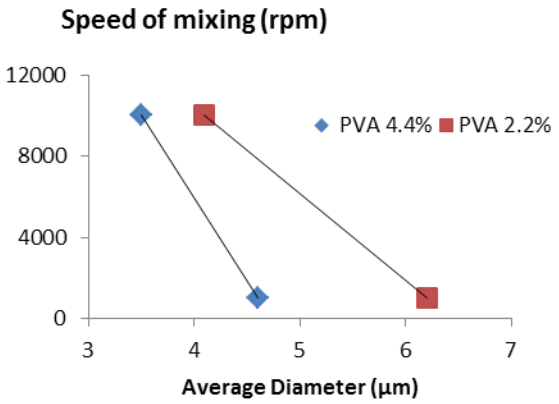

Figure 15. Average Diameter of Emulsion Droplet as a Function of PVAS Concentration and Speed of Mixing

3.2 Superhydrophobic Emulsion Study

The droplet size and the dispersion of metakaolin in the emulsions were determined by optical microscope (Figure 18). Emulsion Mk1 (Figures 18a and 18b) is presented by uniform droplets of approximately 2 µm with some inclusions of larger droplets from 2 to 20 µm. Emulsion Mk2 is presented by well-distributed droplets with sizes from 3 to 30 µm. Particles of metakaolin were found on droplet boundaries. Emulsion Mk3 is presented by well-distributed droplets with sizes from 2 to 40 µm. In this emulsion, the particles of metakaolin were found to be embedded within the droplets.

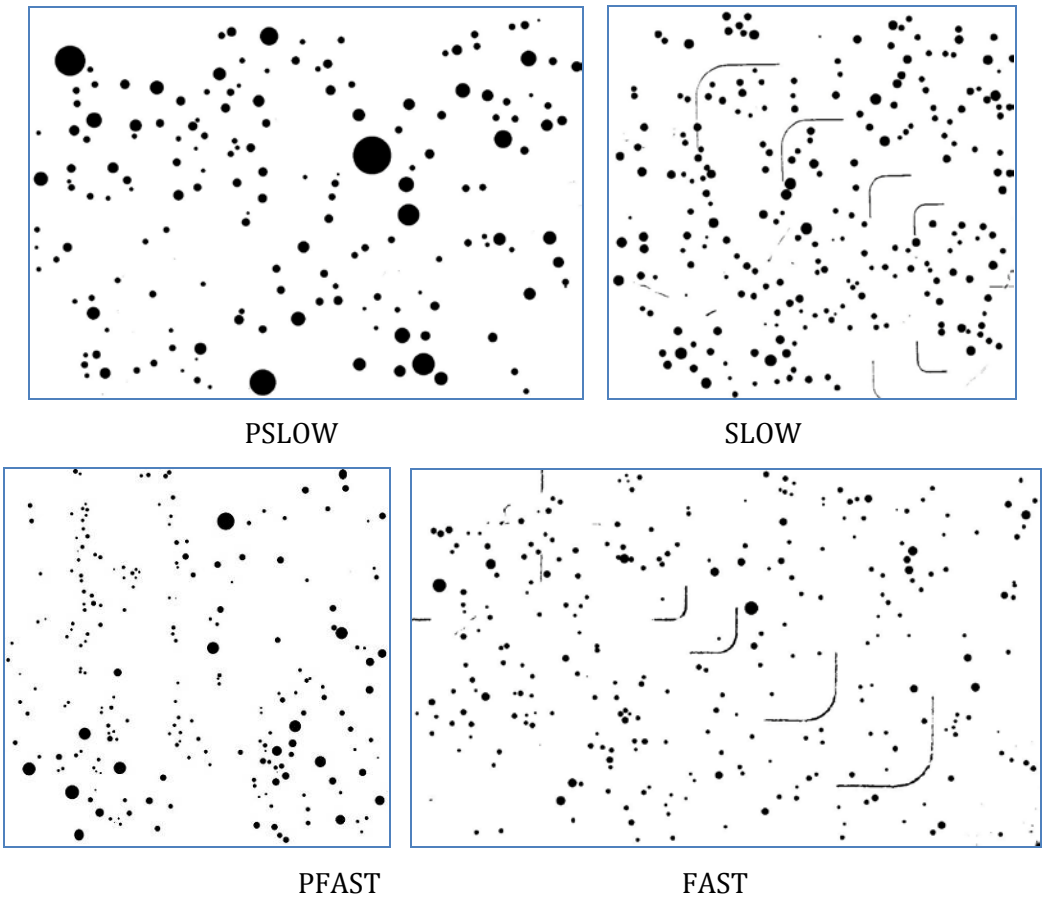

Figure 16. Micrographs of Investigated Emulsions with Dark Dots representing Siloxane Phase

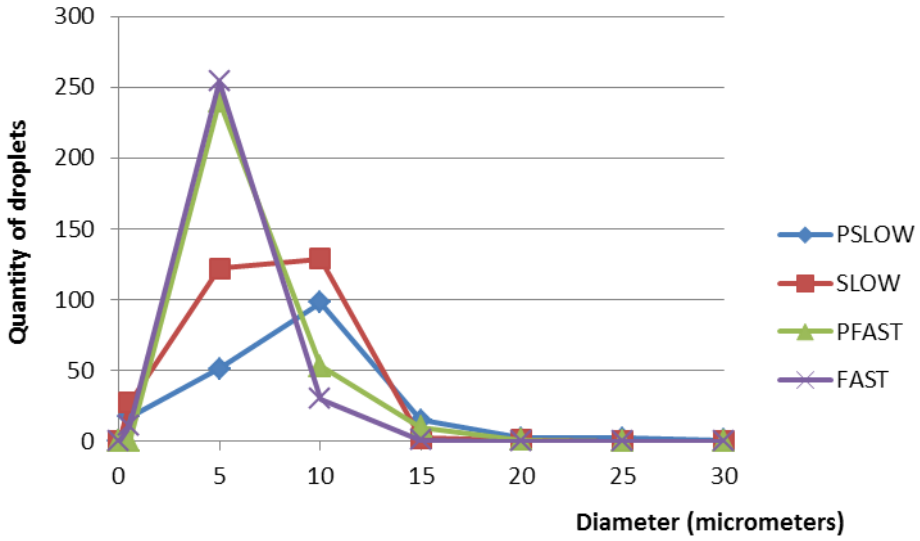

Figure 17. Droplet Size Distribution of Investigated Emulsions

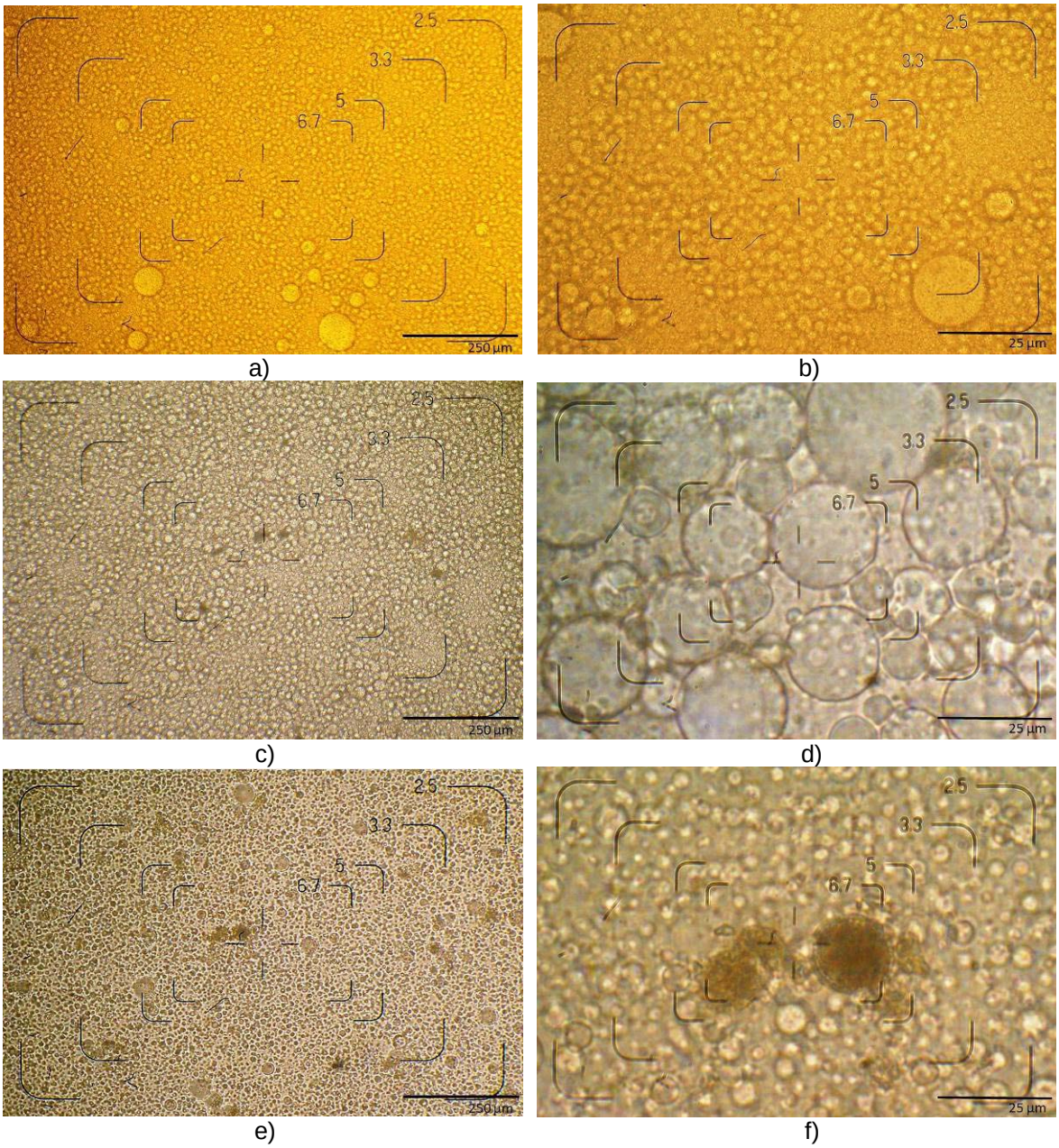

Figure 18. Emulsion Images taken by Optical Microscope at 100x (left) and 1000x (right) Magnification for: a,b) Mk1; c,d) Mk2; and e,d) Mk3

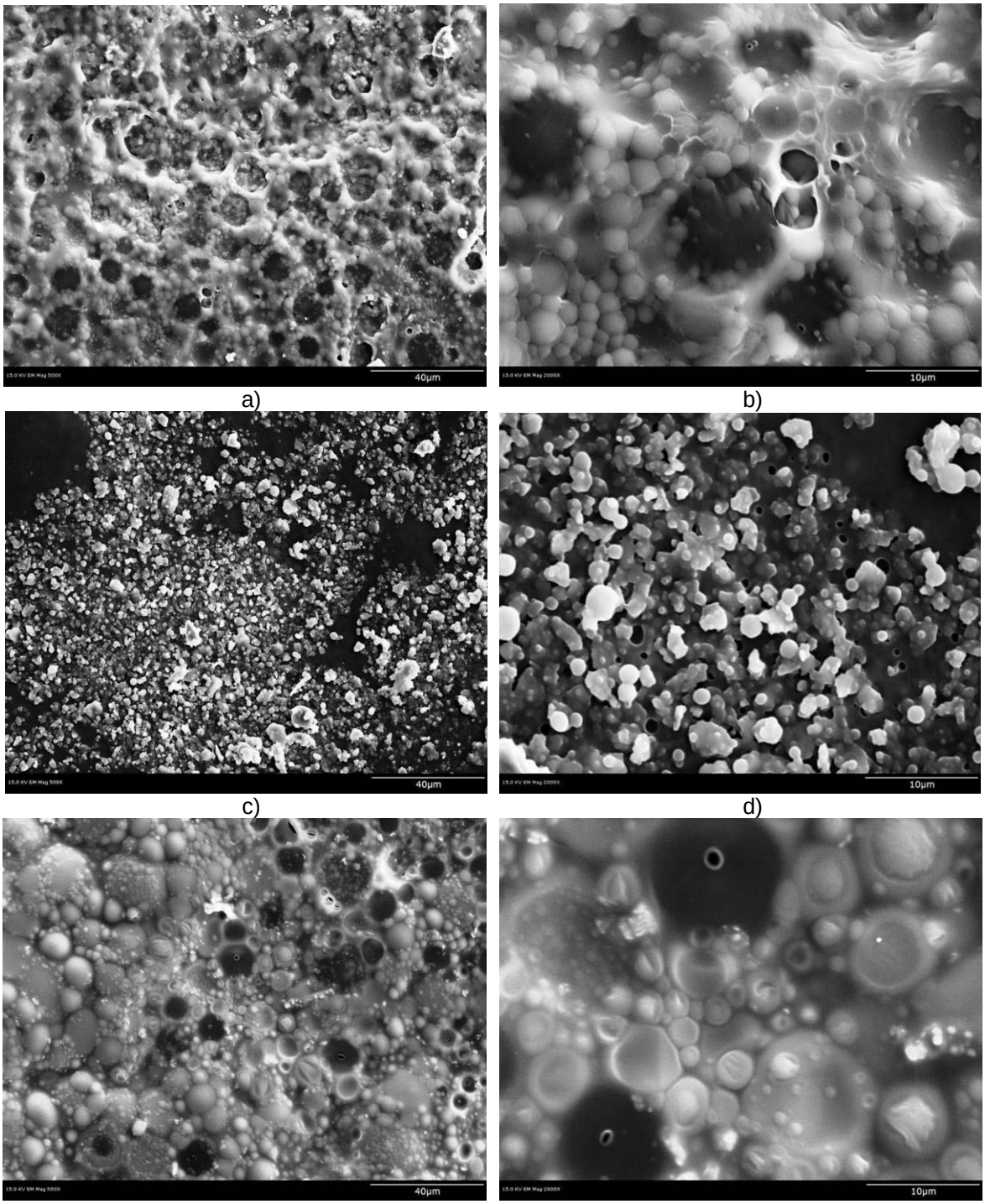

Figure 19. SEM Images of Superhydrophobic Coatings at 500x and 2000x Magnification for: a,b) Mk1; c,d) Mk2; and e,d) Mk3

Two-layer superhydrophobic coatings were analyzed by SEM technique (Figure 19). An irregular "moon crater"-like surface structure is produced by collapsed bubbles with size of 8 to 15µm and smaller bubbles of 0.5 to 3µm were observed for Mk1 coating (Figures 19a and 19b). Mk2 coating appears to fill all the voids leaving a smooth surface in large areas of the coating. Bubbles of 0.5 to

3μm remained on the specimen surface. Some collapsed bubbles of 1 to 30 μm can be seen on Mk3 coatings.

The contact angle of single and double coatings was measured (and verified by duplicate measurements) on mortar tiles and the average values of the contact angle are shown in Figure 20. It was determined that the contact angles of all coated specimens increased by more than 120% vs. the reference. Application of a second layer of the hydrophobic coating did not improve the performance of Mk1 and Mk3. A remarkable performance of Mk2 was observed not only on single-coated specimens (with contact angle of 3 times better vs. the reference), but also for double-coated specimens where the contact angle was actually 4 times that of the reference. Contact angle images of the different hydrophobic coatings are shown in Figures 21 and 22 (with a), b), c), d) corresponding to the reference, Mk1, Mk2, Mk3 coatings, respectively).

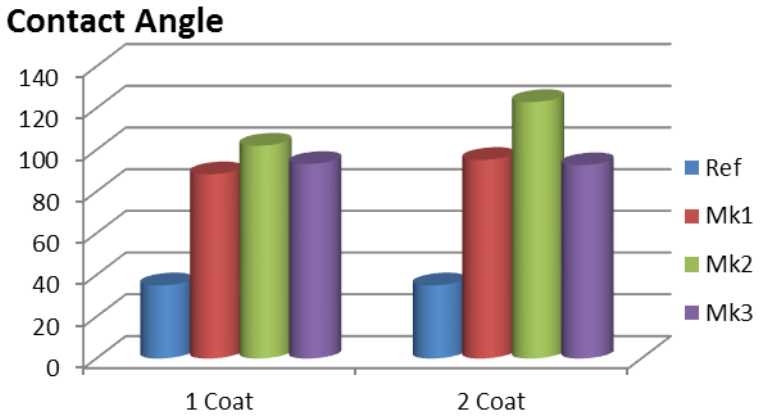

Figure 20. The Contact Angle of Specimens with Single- and Double- Superhydrophobic coatings

a) b) c) d)

Figure 21. The Contact Angle of Mortar with a Single Coat

a) b) c) d)

Figure 22. The Contact Angle of Mortar with a Double Coat

3.3 Mortars with Hydrophobic/Superhydrophobic Emulsions

Flow and air content properties of fresh mortars were investigated. The flow of all mortars was varied within the relatively narrow band of 95-115%, as shown in Figure 23. In general, the use of emulsions improves the flow of the mortars compared to air-entraining admixtures. Mixes with single dose emulsions prepared at 10,000 rpm (Fast) appear to improve the flow, compared to mixes containing slowly mixed (Slow) emulsions. On the other hand, a double dosage emulsion appears to increase the flow when mixed at 1,000 rpm vs. 10,000 rpm. In addition, the effect of PVAS surfactant concentration on flow has a similar pattern. In addition, it is important to observe that the lowest flow was obtained using Fast2 emulsion, while the highest flow was obtained using Fast1 emulsion. These two cement mortar mixes differ only in the quantity of emulsion used.

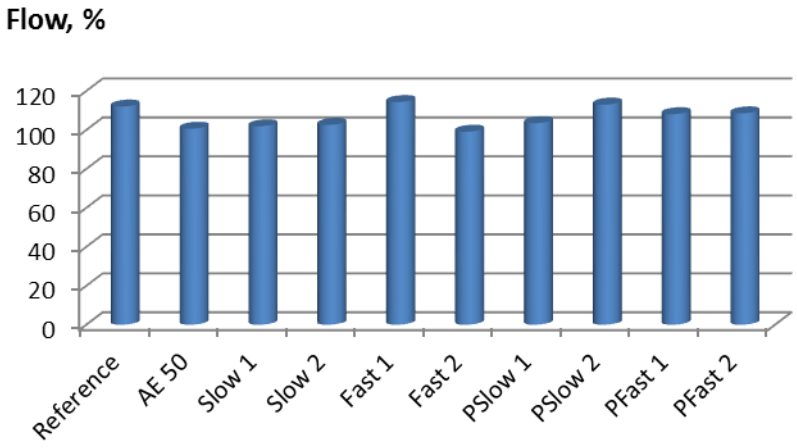

Figure 23. The Flow of Investigated Mortars

The air content was measured immediately after the flow readings were recorded. In general, mixes with air entraining admixtures yield larger air content than any mixes prepared using emulsions, regardless of the characteristics of the emulsion or the time. Initial readings (Figure 24a) show that mixes with double emulsion dosage gave higher values than their respective single dosage samples, except where the PVA surfactant was low and the emulsion was prepared at low speed (Slow). With regards to the latter case, Pslow1 and Pslow2, the single dosage had a higher air content percentage, than their counterparts with higher concentrations of PVAS.

The air content in mixes prepared with siloxane emulsions increased over time, as seen in Figure 24b. The samples that show higher air content were Fast, Slow and Pfast with double dosages of emulsion. Pfast1 had higher reactivity than any other sample. Also, the mix with the lowest air content was Pslow2.

From the series of images (Figure 24c), it can be observed that generally, samples with emulsions have larger quantities of air voids (white areas) than the reference or air-entrained samples. Also, samples containing double dosage (Slow2, Pslow2, Fast2 and Pfast2) appear to have larger numbers of voids than those containing a single dosage (Slow1, Pslow1, Fast1, Pfast1). Comparisons between samples that contain the same dosage, demonstrates that a higher PVA content (Slow1, Slow2, Fast1, Fast2) may increase the quantity of air voids.

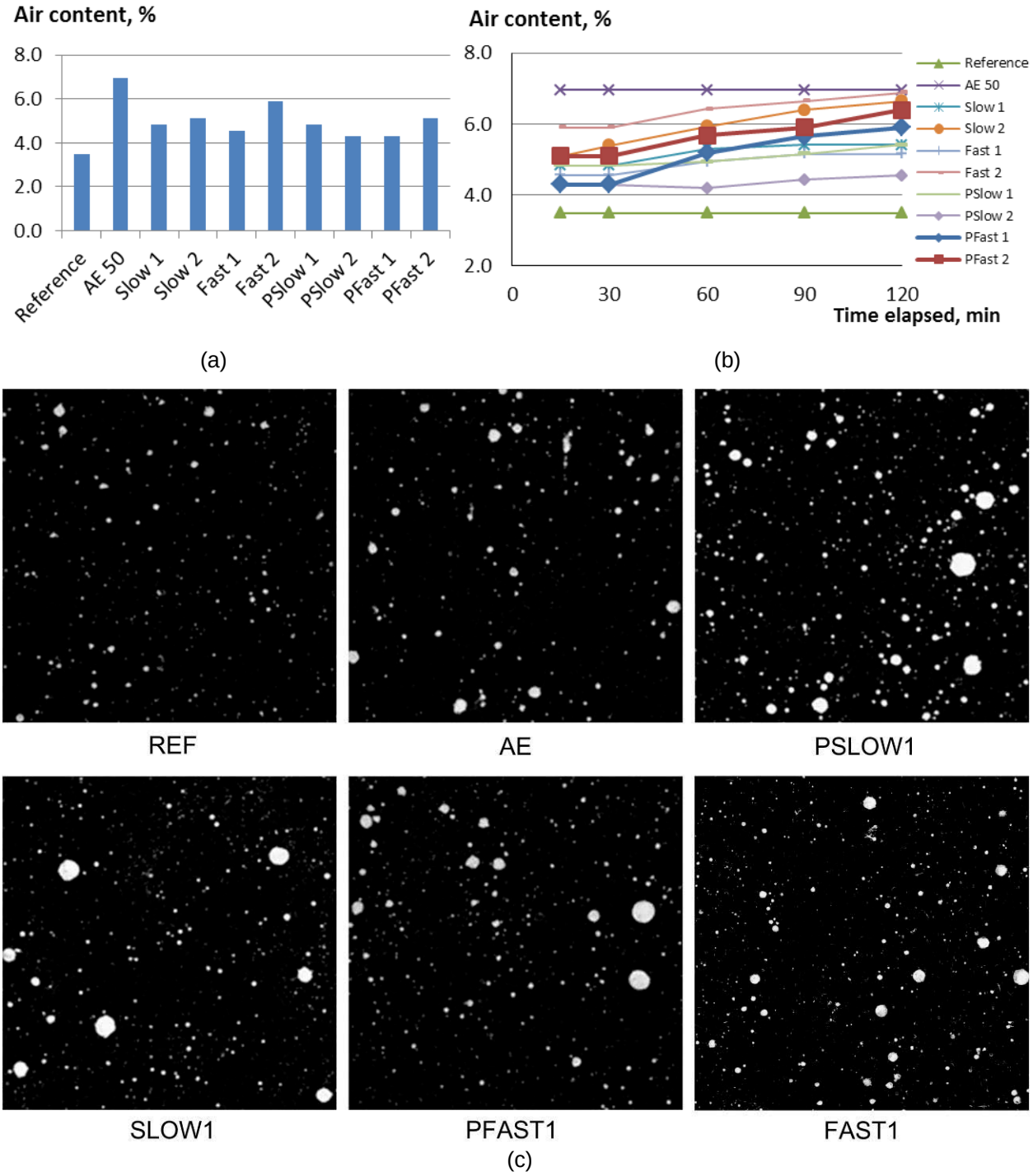

Figure 24. The Initial Air Content (a), The Kinetics of Air Content Over Time (b), and Air-Void Structure of Investigated Mortars (c)

With respect to air void size, samples with emulsions mixed at higher speeds show smaller sizes of voids that are more uniform and almost circular, as compared to counterpart mortars with slowly mixed emulsions. Samples without emulsion (reference and with air entrainment) seem to have a wide distribution of void sizes instead of a uniform size, and somehow irregular shapes instead of circular. In addition to the sizes and shapes, voids in these samples seem to be further apart than

voids in samples containing emulsions. In conclusion, samples with optimal emulsions present ideal characteristics of an air void system: closely spaced and with small air voids.

The development of compressive strength of investigated mortars is presented in Figure 25.

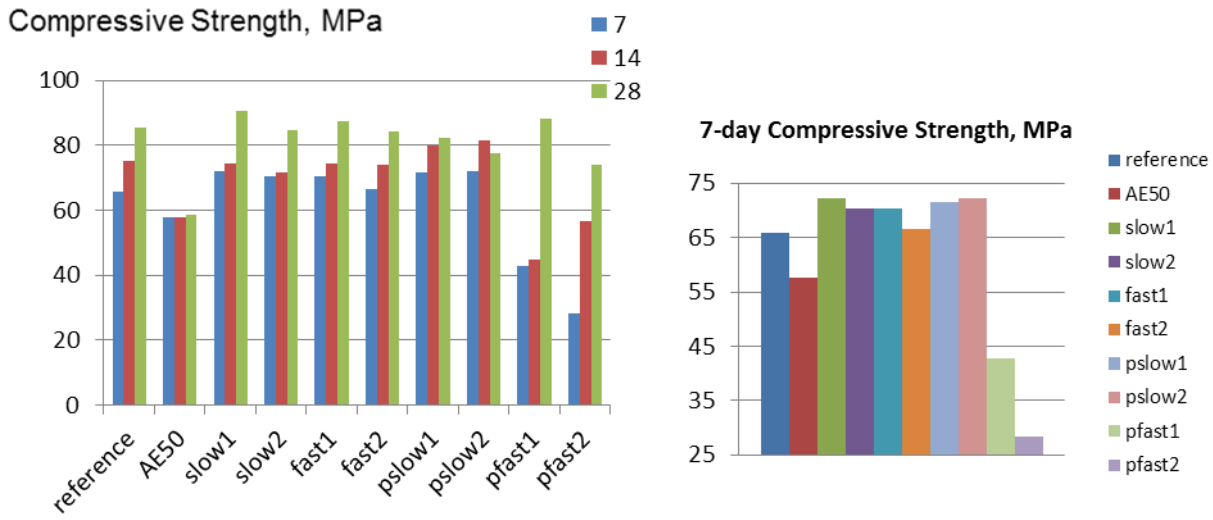

Figure 25. The Compressive Strength of Investigated Mortars

Air-entrained mortars demonstrated a lower compressive strength than reference samples. In general, samples labeled as Pfast1 and Pfast2 show lower compressive strength than the reference. The rest of the samples had higher compressive strength.

Samples with emulsions Slow1, Slow2, Fast1 and Fast2 demonstrate an increment of compressive strength over time which was not observed in samples with air entraining. In other words, the use of air entraining does affect the compressive strength of mortars, not only by having a lower 7-day strength, but also by hindering strength development over time. On the other hand, all of the samples prepared with siloxane based emulsions presented excellent strength development with many specimens exceeding 28-day strength of the reference.

Figure 26 shows the percentage of water absorbed in one hour and in one day for each sample. The reference sample, absorbed more water than any other sample. Other samples (Fast2, Pfast1 and Pfast2) have a similar behavior compared to air-entrained (AE) mortar. This means that despite these samples having more porosity, they absorbed less or equal amounts of water than the reference or air-entrained samples. Other samples have excessive voids to allow the emulsion to fully cover void surfaces with hydrophobic material and consequently the amount of water absorbed. These samples contained more voids due to the slow mixing of the emulsions and thus larger droplets of siloxane. Slow2 containing a higher dosage of emulsion and larger droplets, logically produced more voids with uneven hydrophobicity and thus absorbed more water. Also PVAS concentrations result in variation of water absorption. This graph showed that higher concentrations of PVA resulted in more water absorption.

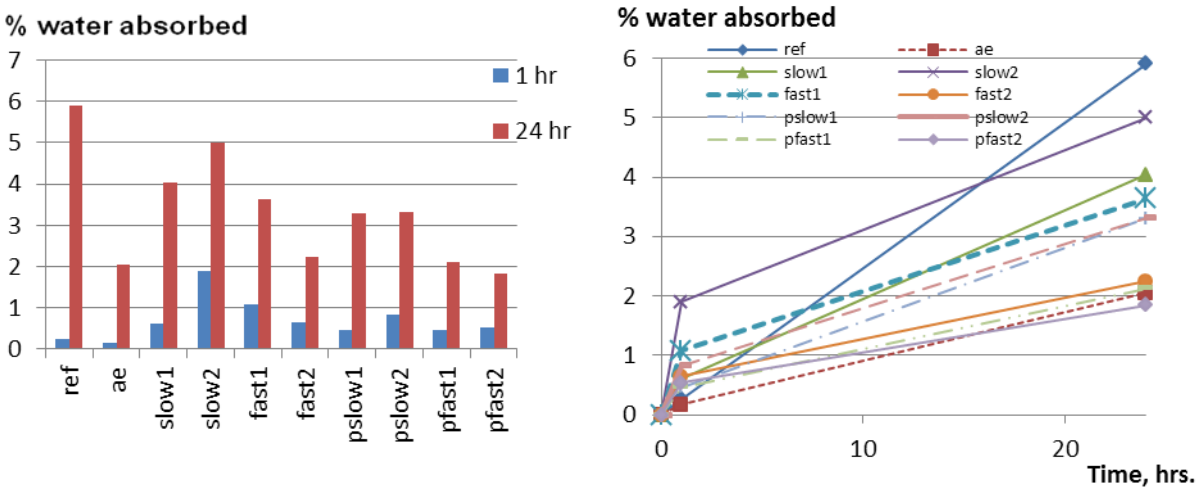

Figure 26. Water Absorption of Investigated Mortars

From the results shown in Figure 27, it can be concluded that good quality pastes can still hydrate and develop strength under severe freeze thaw cycling with a minimum temperature of -50°C. This may be due to a dense structure developed especially in the presence of a hydrophobic agent, Reference samples, however, presented a drop in compressive strength after 300 cycles of freeze-thaw, as well as Slow1 and Slow2 specimens. The rest of the samples developed an increase in strength after 300 cycles. After 500 cycles, air-entrained, Pslow1 and Pslow2 showed a decrease in compressive strength. Pslow1 lost 14% of the compressive strength during the last 200 cycles of freezing and thawing.

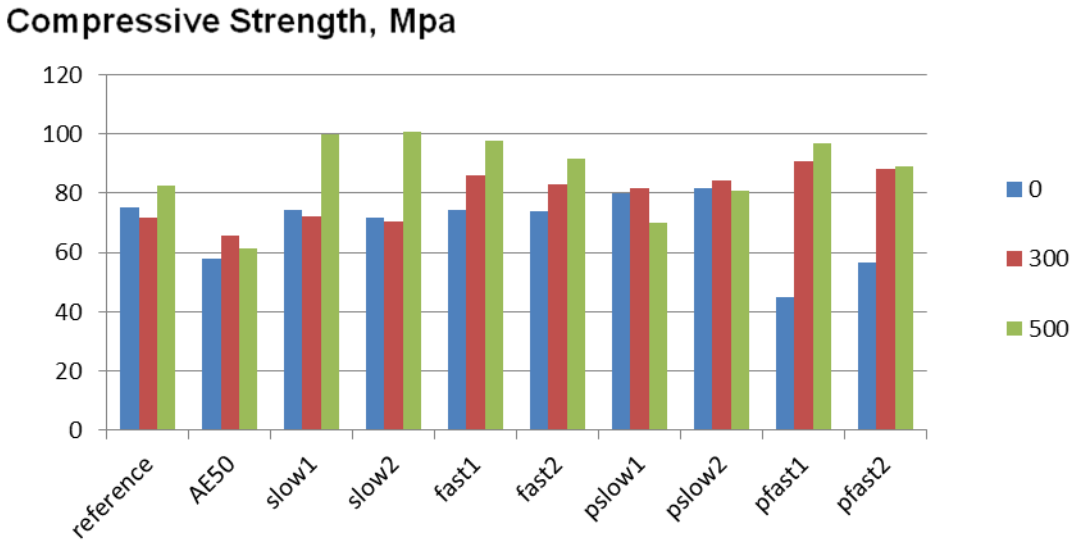

Figure 27. The Effect of Freeze-Thaw on Compressive Strength of Investigated Mortars

3.4 SECC: The Effect of Emulsion Type

The flow of investigated ECC was within a relatively narrow band of 28.5 – 33.7% as shown in Figure 28. The flow of the specimens with hydrophobic emulsions was slightly lower as compared

to reference specimens. The mixture containing an air entraining admixture displayed the lowest flow. This is unusual since the addition of air would create less friction between the particles in the mixture and therefore allow for a greater flow. The can be explained by the formation of a lighter but more cohesive mix which provides smaller driving force for flow to extend. Figure 28 displays the flow as a percentage for all the mixtures created in this study.

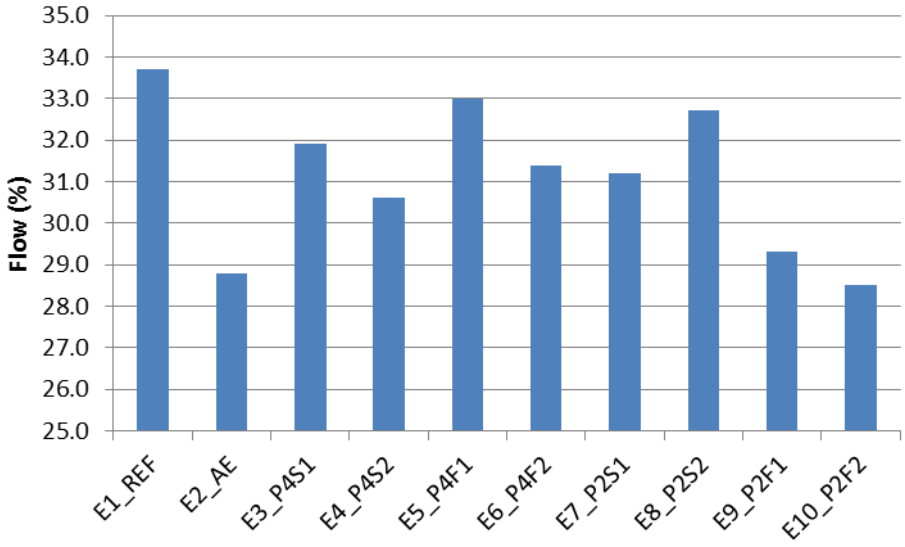

Figure 28. Flow for ECC Specimens with Hydrophobic Emulsion

The reference specimen has the highest 28 day compressive strength of 99.3 MPa (Figure 29). All of the specimens with air entraining admixtures or siloxane emulsions experienced some reduction in strength however; the most significant reduction was that of the specimen incorporating an air entraining admixture. As anticipated, the air entraining admixture resulted in the most significant strength reduction, while hydrophobic emulsions maintained strength close to that of the reference mortar.

The mixtures that incorporated emulsions with 2.2% PVAS emulsifier had slightly lower strengths. Mixing speed did not appear to have much of an effect on the compressive strength, but the stability of the emulsion may have decreased at lower speeds. There also appeared to be little difference in 28-day compressive strength when comparing specimens with single or double dosages of emulsion. This was not the case, however, at early test ages. The 1-day compressive strength of the specimens incorporating a double dosage of emulsion typically tended to be lower than those with a single dosage. This could possibly be due to the fact that a double dosage of emulsion creates excessive retardation and some expansion within the fresh/green samples during early stages of curing. This phenomenon was observed in all specimens with higher dosages of emulsion. Excessive amount of expansion was observed due to the gas generation released from the emulsion during the curing process. However, preliminary tests on freeze-thaw resistance of mortars (non-reinforced, without PVA fibers) proved that emulsions mixed at a higher rate, with larger amounts of PVAS emulsifier, and a double dosage of emulsion (similar to E6_P4F2) had the best durability. For example, E6_P4F2 specimen had good compressive strengths at 28 days, but it also demonstrated the lowest early age strengths.

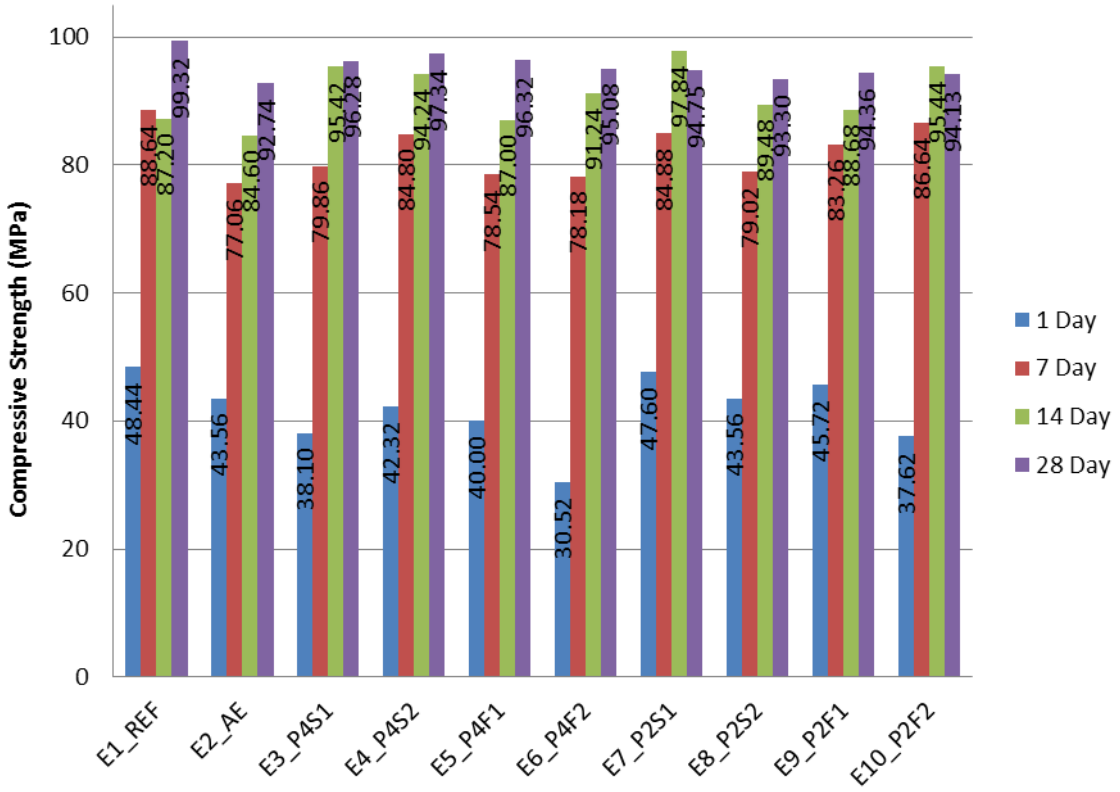

Figure 29. Compressive Strengths of Mortars with Hydrophobic Emulsions

As seen in Figure 30, all of the specimens displayed similar flexural strengths; however specimens that incorporated emulsions containing larger amounts of PVAS emulsifier mixed at higher speeds showed the best ductility. This, combined with the compressive stress results, illustrates that a double dosage of emulsion is not beneficial from a mechanical standpoint. The two best performing specimens each used 4.4% PVA emulsifier mixed at a higher speed; however the specimen with a single emulsion dosage actually provided slightly higher flexural stresses and maintained these higher stresses at a larger strain, as compared to the same emulsion with a double dosage (Figure 30).

Figure 31 displays the flexural behavior of the reference specimen, the air entrained specimen and SEEC specimen that was considered to have the best emulsion (E5_P4F1). All of the above specimens demonstrated similar ultimate flexural stress; however the one incorporating the hydrophobic emulsion was able to withstand much larger deformations before a failure crack was observed. The modulus of elasticity appeared to be significantly lower as compared with the reference and air entrained specimens. The first initial crack in the hydrophobic emulsion specimen also appeared at a much higher load then that of the reference and air entrained specimens. Figure 32 displays all of the specimens with a single dosage of emulsion and all the specimens with a double dosage of emulsion separately. The difference in flexural behavior between a single dosage and a double dosage of emulsion is negligible, with the exception of the emulsion with a smaller quantity of PVA mixed at a slower speed (E7_P2S1 and E8_P2S2). At a single dosage this emulsion performed very well, however when a double dosage was introduced, the flexural behavior of the specimen was poor.

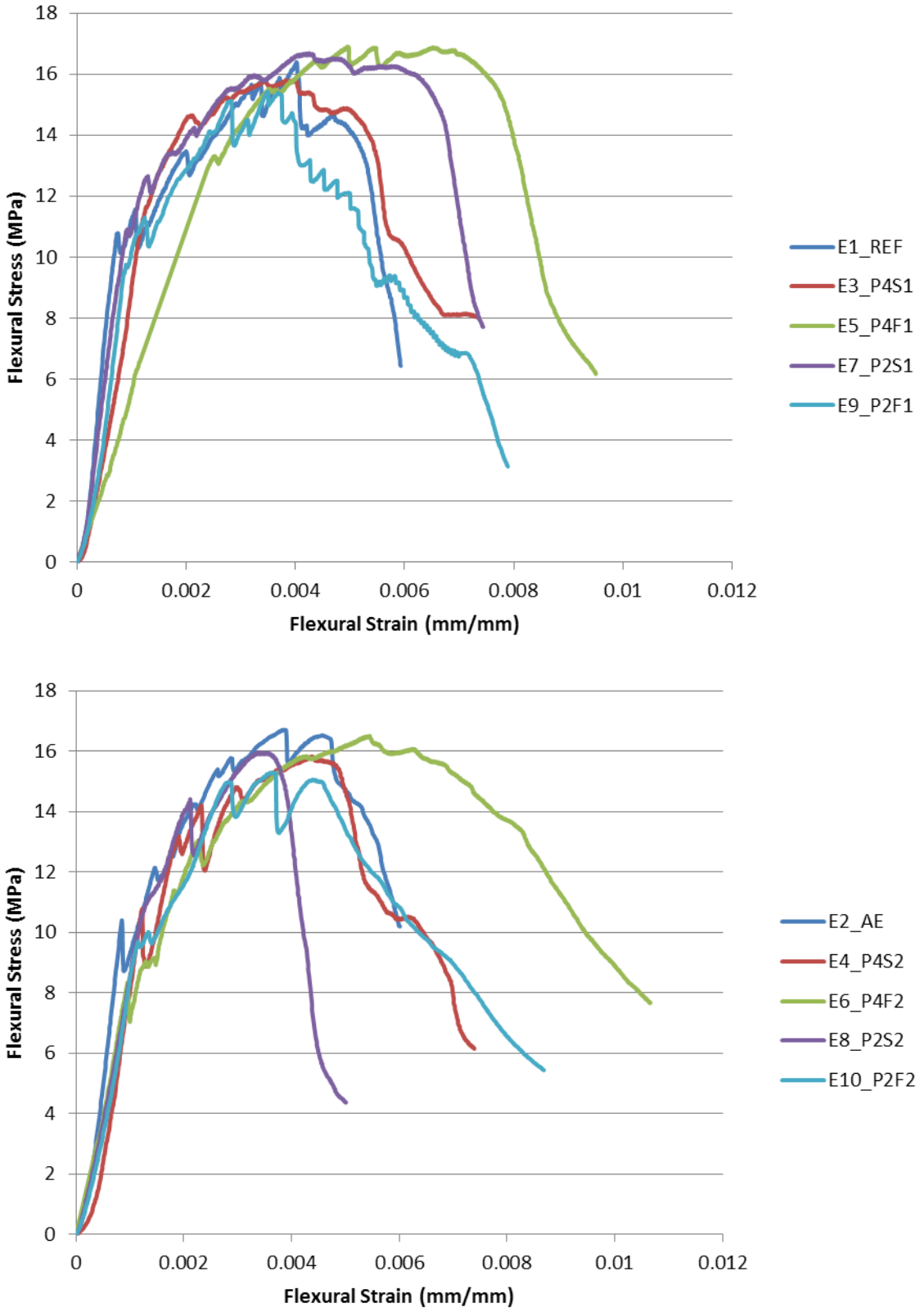

Figure 30. 28-Day Flexural Behavior of Specimens with Hydrophobic Emulsions

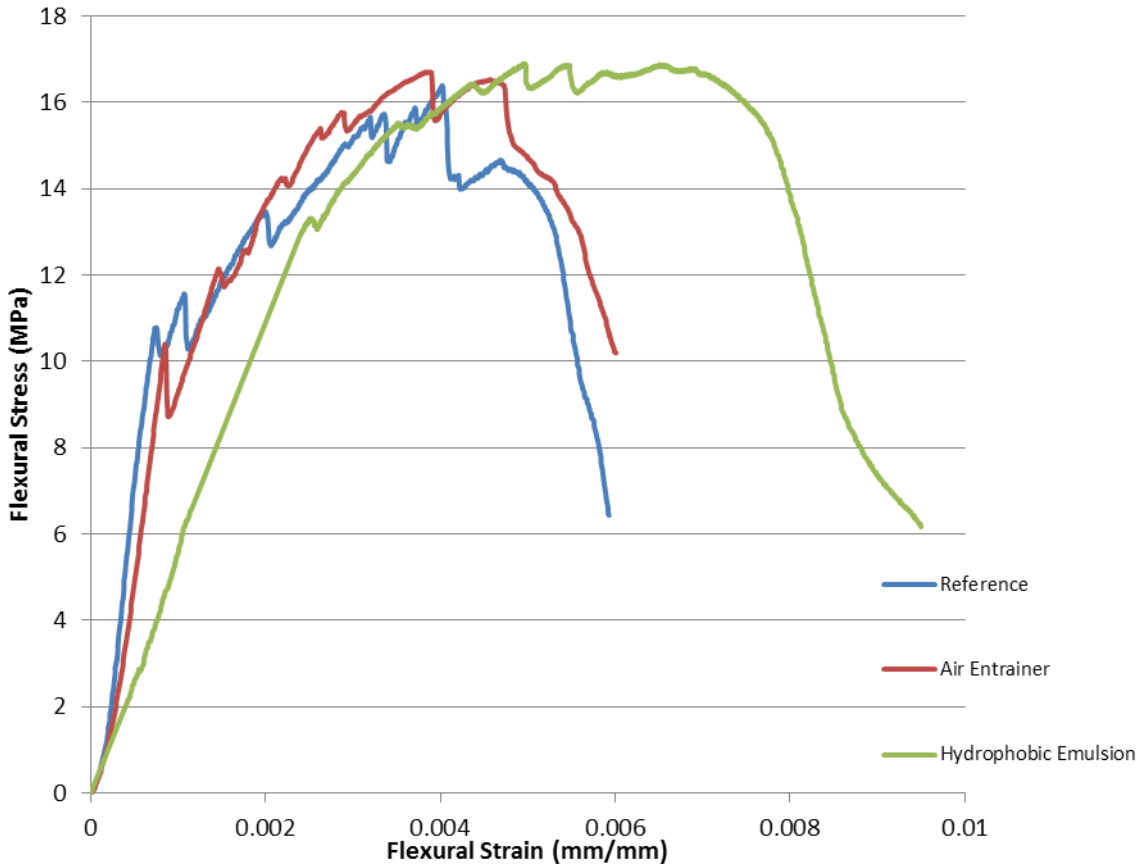

Figure 31. The Comparison of Flexural Behavior of a Reference Specimen, Air Entrained Specimen and Specimen with a Hydrophobic Emulsion

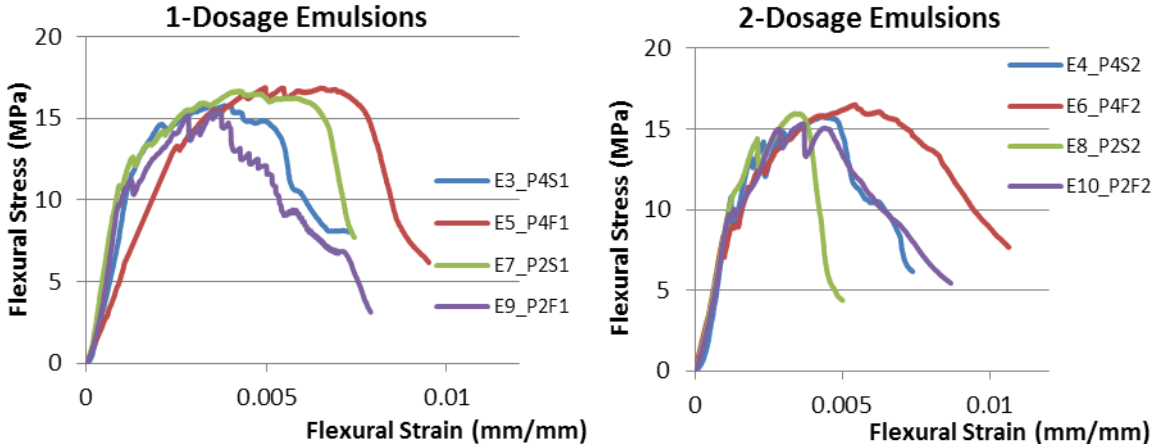

Figure 32. The Flexural Behavior of SECC with Single- and Double-Dosage of Emulsion

Potentially, this data could assigned to the fact that slow emulsion mixing results in the formation of larger siloxane droplets; therefore, when introduced within the cement matrix at higher dosages, it created some excessive local expansion. This being considered, and the observation of the minimal difference in flexural behavior between a single and a double dosage of emulsion, it can be concluded that a single dosage of hydrophobic emulsion is sufficient to maintain the desired flexural performance.

3.5 SECC: Supplementary Cementitious Materials (SCM) Study

The flow for all SECC mixtures with SCMs remained within a relatively narrow band of 32 - 46%, as shown in Figure 33. Specimens with fly ash and blast furnace slag tended to have a higher flow. It can be noted that with the addition of a single dosage of emulsion, the flow increased.

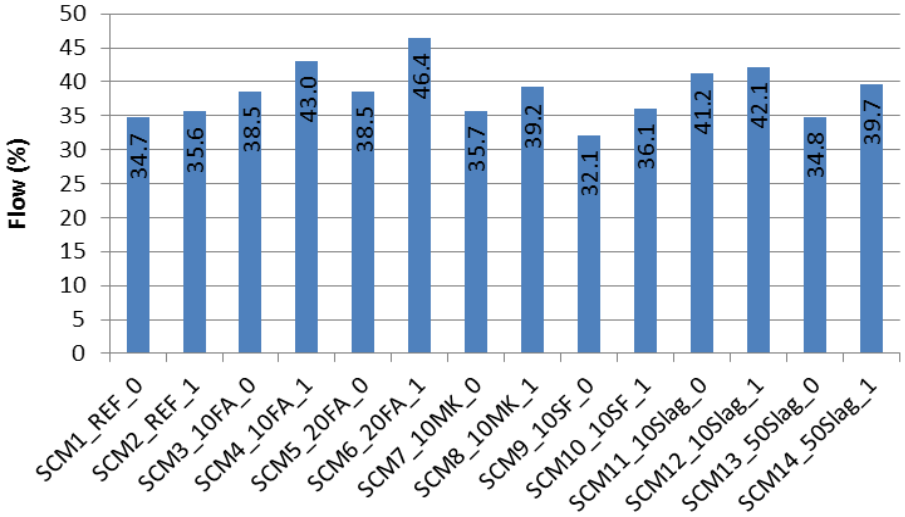

Figure 33. Flow of ECC/SECC with Supplementary Cementitious Materials

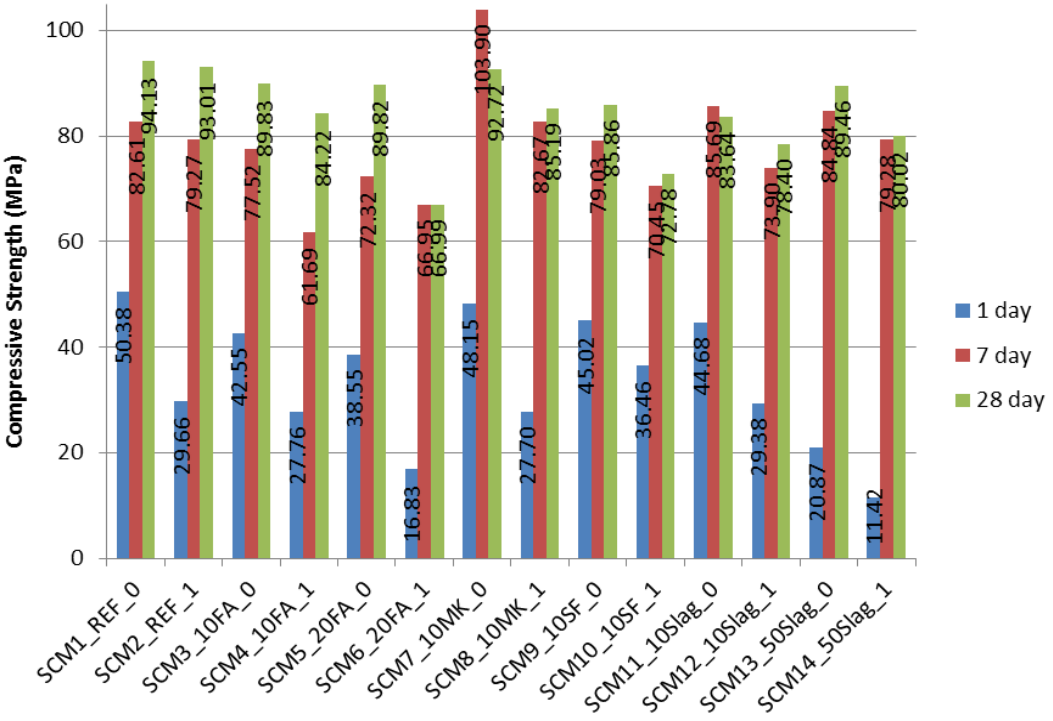

Figure 34. Compressive Strength of ECC/SECC with Supplementary Cementitious Materials

Figure 34 demonstrates 1-, 7-, and 28-day compressive strengths of ECC with different SCMs tested. There is a much larger deviation in compressive strengths as compared to the emulsions study as different SCMs have different effects on strength. Very small particles such as metakaolin and silica

fume have the ability to create a uniform particle size distribution and increase the density of the contact zone between the cementitious matrix and fibers/aggregates. This allows for an improved, stronger interfacial transition zone and therefore a much stronger and more durable concrete. Supplementary cementitious materials such as fly ash and blast furnace slag result in lower early strengths, but have comparable strengths at 28 days. On examination of the two reference specimens, it can be noted that the addition of hydrophobic emulsions did not create a very large reduction in strength as compared to specimens with SCM. It can be seen that the addition of siloxane emulsion caused a significant reduction of strength at 1-day of age; however, it is important to find the proper SCM that will not cause a significant reduction of strength when the hydrophobic emulsion is introduced. In consideration of the research data, several interesting results emerge. First, the 7-day strength of ECC with metakaolin without emulsions was extremely high (>100 MPa), but the 28-day strength is then reduced. Possibly a negative reaction may have occurred while the specimens were curing in water for 28 days. Also, compressive strengths of the specimens incorporating silica fume were not as high as originally expected, especially since these specimens were the ones that allowed the largest flexural strengths. Although the 28-day compressive strengths of the ECC specimen incorporating silica fume was among the largest, when the emulsion was added SECC strength was significantly reduced. The addition of an emulsion to the specimen with 20% fly ash demonstrated a significant drop in early strength and it did not gain any additional strength after 7 days. Of all the specimens that incorporated a single dosage of emulsion the specimen with metakaolin provided the best performance.

Since the addition of different supplementary cementitious materials can drastically affect the early strengths of SECC it is important to display 1, 7, and 28 day flexural behaviors. The 28-day flexural behavior of all the specimens was relatively similar; however the flexural stress was considerably different when comparing early age specimens.

As seen in Figure 35, the ECC specimen incorporating silica fume, not only provided the best ultimate flexural stress, but also provided the best flexural strain. The SECC specimen with silica fume and emulsion has a relatively mediocre flexural stress and flexural strain performance. The best 1-day flexural performance was demonstrated by ECC with metakaolin. The ECC specimen that does not incorporate an emulsion has a very good 1-day flexural stress of a little over 15 MPa, but only demonstrates a flexural strain of around 0.013 mm/mm. When compared to other SCMs, there is a significant drop in performance for ECC with emulsions. However, this is not the case for metakaolin as its flexural strength was around 13 MPa, only slightly lower than the strength of ECC without the emulsion. The flexural strain of SECC incorporating metakaolin and an emulsion was around 0.02 mm/mm.

The 7-day flexural behavior as seen in Figure 36 shows that the specimen with silica fume provides the best flexural stress. Unlike 1-day testing, the 7-day flexural stress and strain of the SECC specimen with silica fume and an emulsion has only a slight decrease vs. the reference.

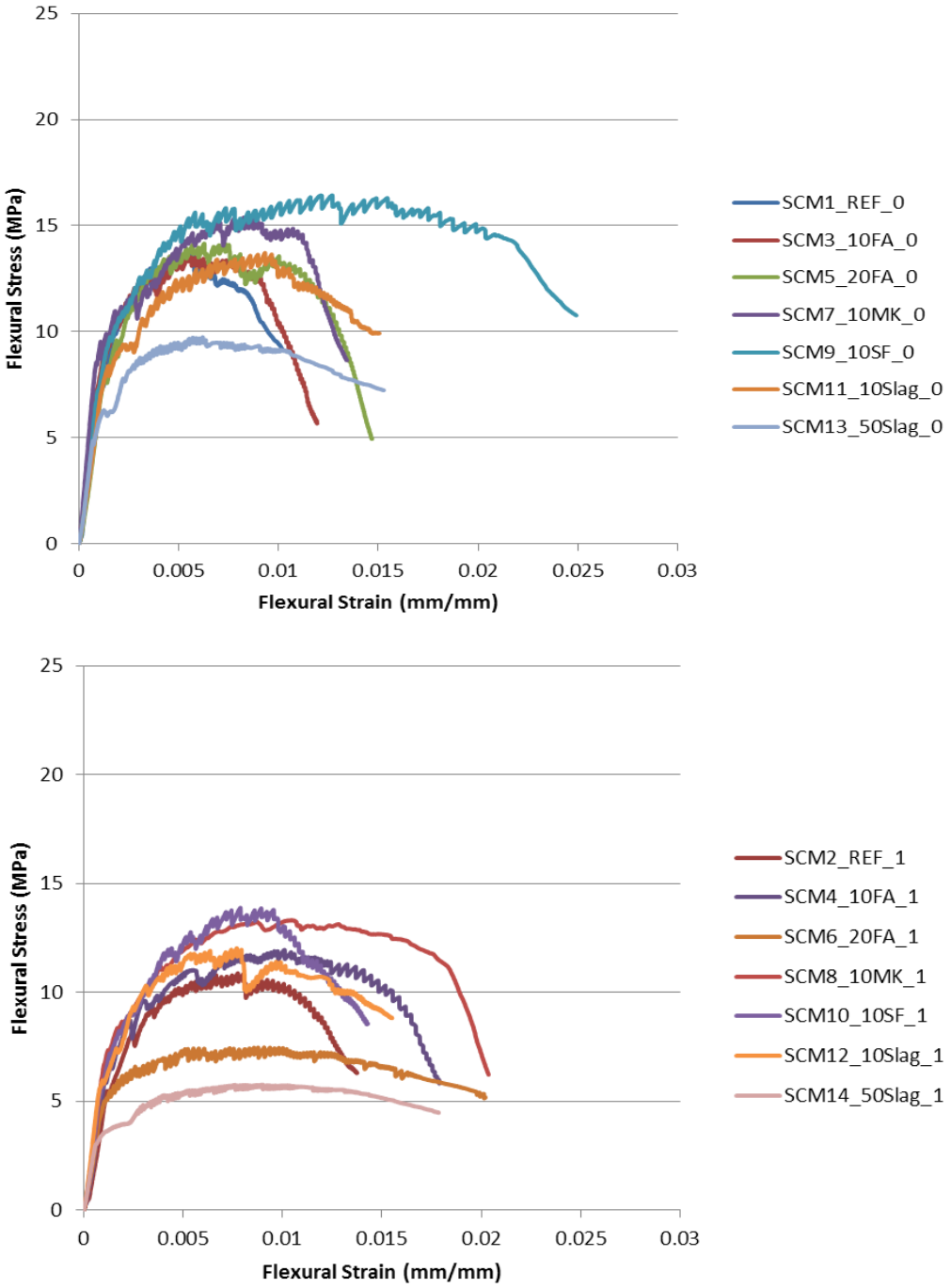

Figure 35. 1-Day Flexural Behavior of SECCs with Different SCMs

Both the ECC/SECC 7-day specimens with metakaolin, with and without emulsion, also performed very well. The specimen with 10% fly ash and a single dosage of emulsion provided a good ductility. This SECC provided very similar ductility as it did at the age of one day, but was able to significantly increase its flexural stress from 1 day to 7 days. This was not typical with most of the specimens. As flexural stress increases, there is usually a decrease in flexural strain, but this did not occur when 10% of fly ash was used to replace the portland cement.

Flexural behavior at 28 days again shows that the specimen with silica fume provides a very high flexural stress (Figure 37). The specimen with silica fume and an emulsion also performed very well with a flexural stress of over 20 MPa and a flexural strain larger than the same specimen without an emulsion. The two specimens with 10% of blast furnace slag and 50% of blast furnace slag displayed very good flexural strains while still maintaining a relatively good flexural stress. However, these same specimens demonstrated a dramatic loss in performance on introduction of an emulsion. The best results were shown in both the metakaolin and silica fume specimens, with and without emulsions. At an early age the silica fume displayed large losses of performance when a single dosage of emulsion was added, however at 28 days the specimens with silica fume showed no reduction in performance.

Specimens with metakaolin displayed opposing results. At an early age metakaolin showed little loss in performance, but larger losses occurred at later ages when an emulsion was added. Figure 38 compares 1-day and 28-day flexural behavior of metakaolin and silica fume specimens.

3.6 SECC: Superhydrophobic Emulsion Study

The flow for specimens with superhydrophobic emulsions remained within a relatively close band of between 38.7-45.0% as seen in Figure 39. There appears to be no correlation between emulsion type and dosage when observing the flow data.

Compressive stresses for 1 day and 7 days were also observed (Figure 40). There was a drop in strength when the emulsion dosage was doubled, similar to compressive strengths in hydrophobic emulsions. This observation is even more evident the age of one day. The superhydrophobic emulsion incorporating metakaolin provided the best compressive strength vs. the reference hydrophobic emulsions. Moreover, this emulsion also showed the smallest decrease in strength when a double dosage was used. Observing the 1 day flexural behavior of specimens with superhydrophobic emulsions (Figure 41), it can be seen that the emulsion incorporating metakaolin performs very well. It is the most ductile and among the specimens with the highest flexural stress. However, there is a large drop in flexural stress when a double dosage of emulsion is added to the specimen incorporating metakaolin. A single dosage of the emulsion with silica fume also performed very well. This is consistent with compressive stress results (Figure 40) of this specimen having the highest compressive strength at 1-day age.

The results of the 7-day flexural behavior of the specimens (Figure 42) show some inconsistencies with 1 day results. The emulsion incorporating portland cement demonstrated one of the best flexural behaviors.

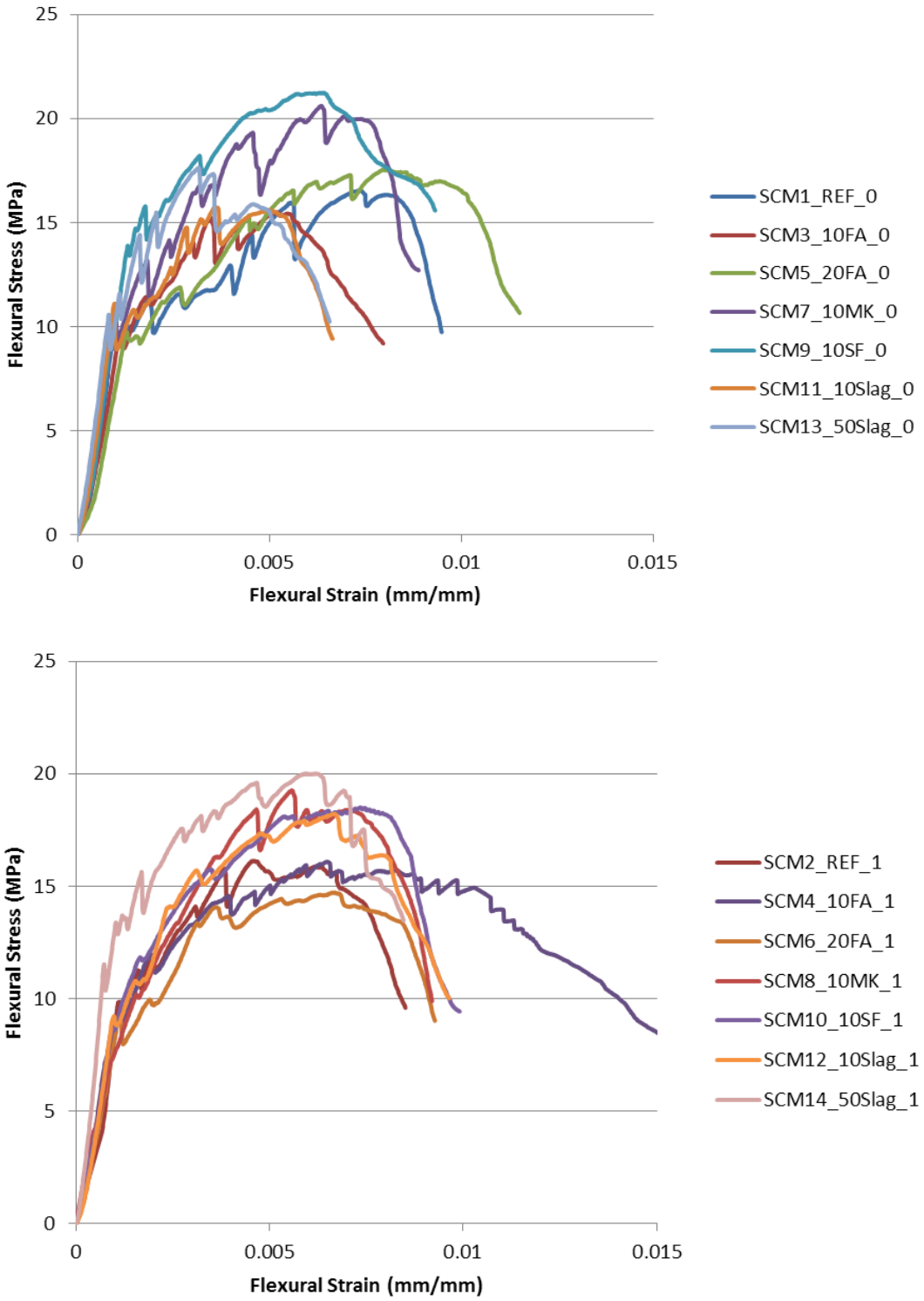

Figure 36. 7-Day Flexural Behavior of SCM Specimens

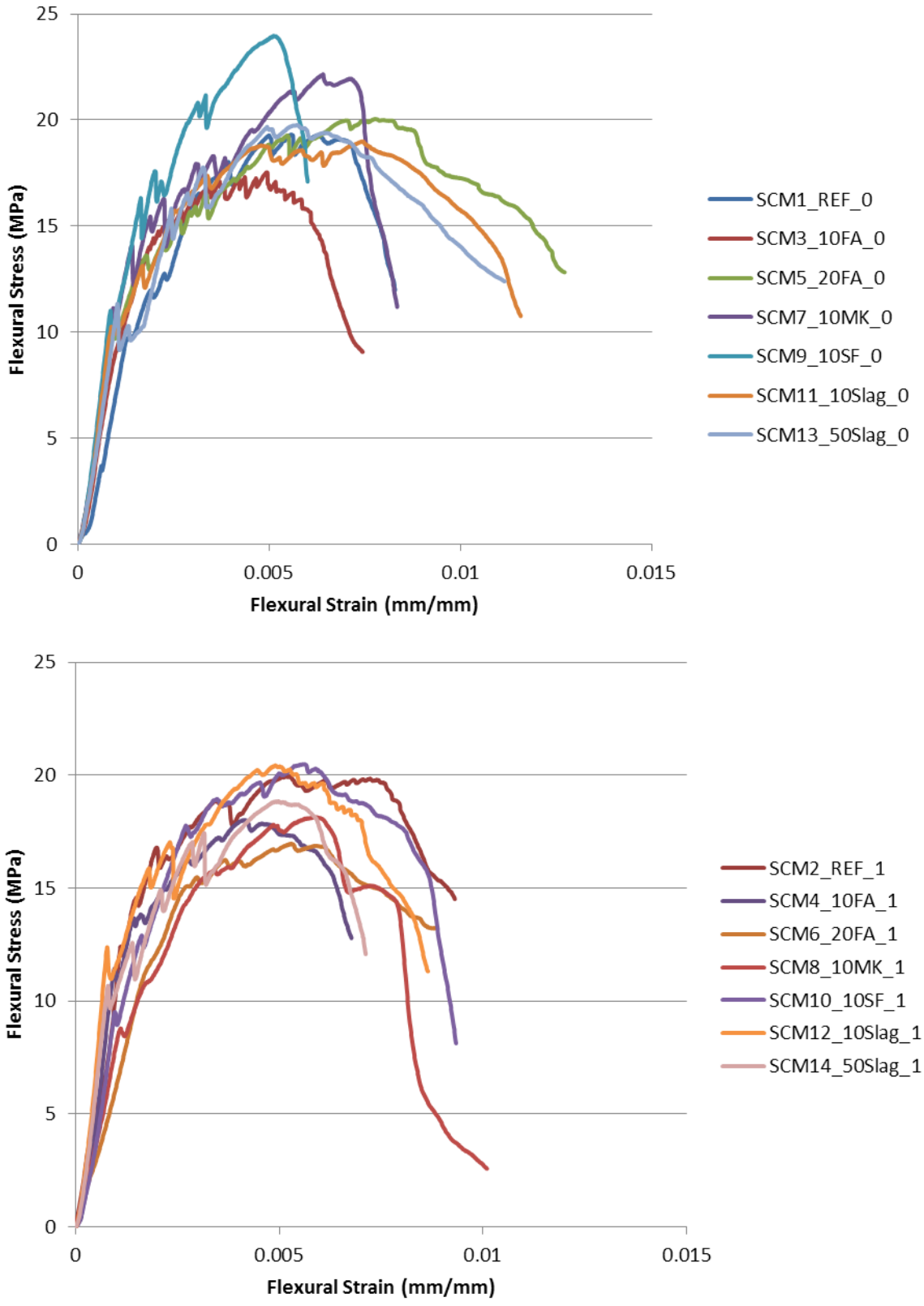

Figure 37. 28-day Flexural Behavior of SCM Specimens

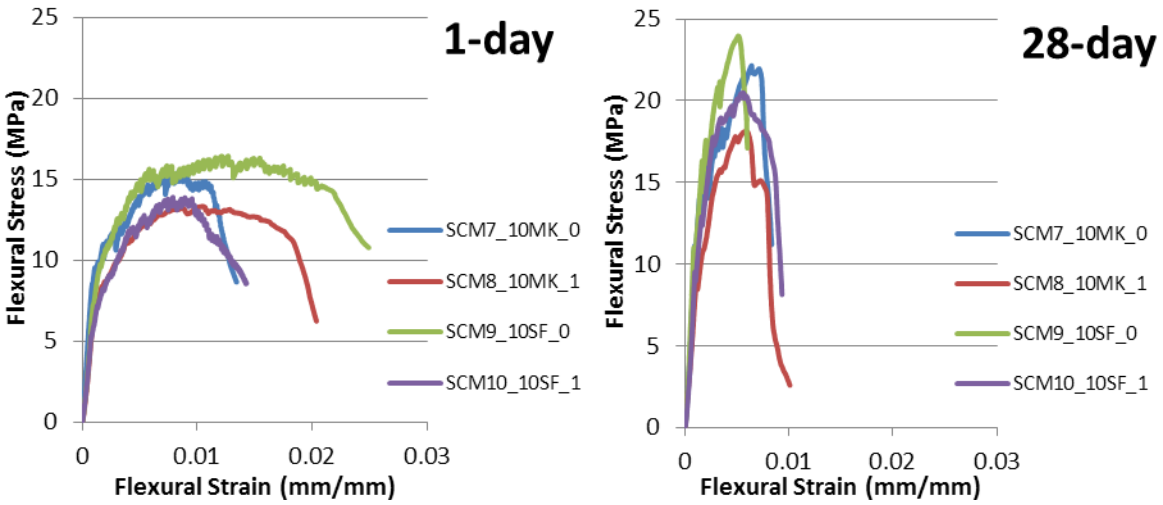

Figure 38. 1- and 28-Day Flexural Behavior of Metakaolin and Silica Fume Based ECC with and without Emulsions

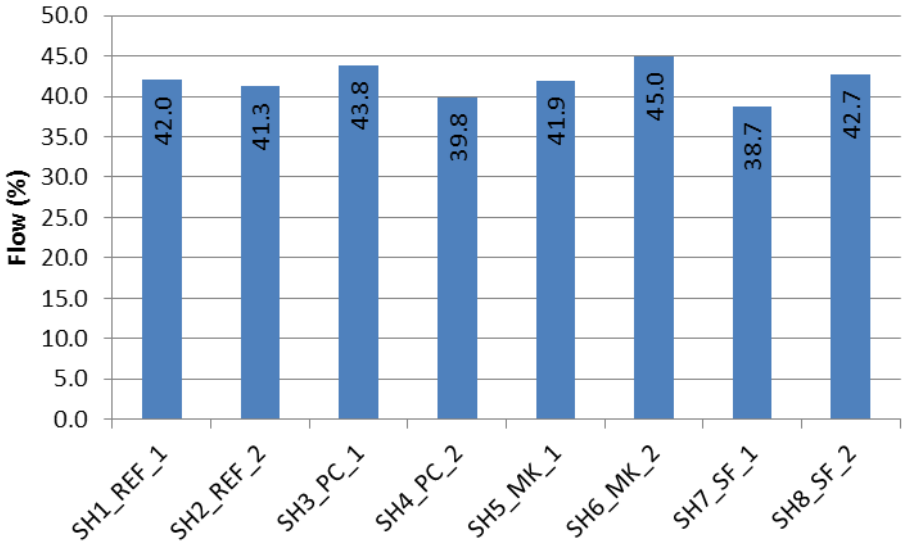

Figure 39. The Flow of Specimens with Superhydrophobic Emulsions

Interestingly, a double dosage of emulsion with metakaolin performed dramatically better than that with a single dose. A double dosage of emulsion with metakaolin displayed a very good compressive strength, which can be correlated to its good flexural behavior.

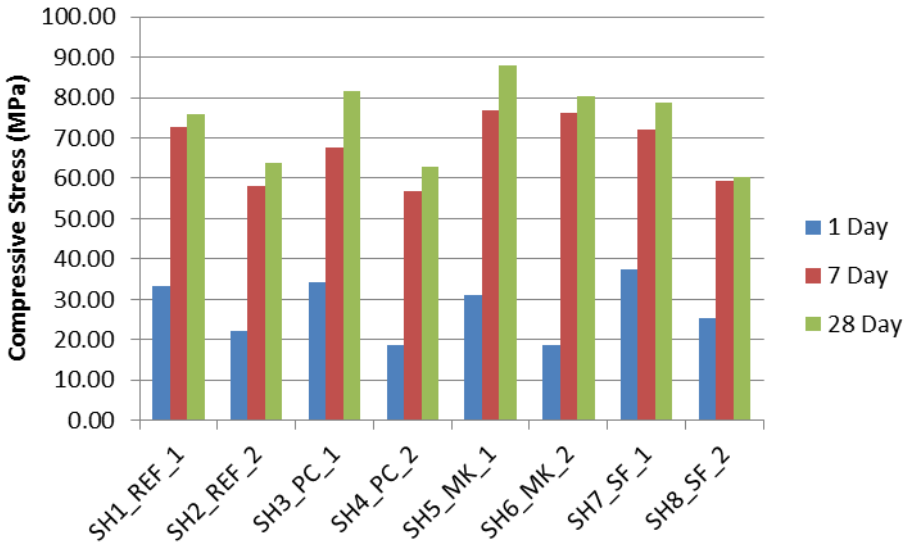

Figure 40. The compressive strength of ECC with superhydrophobic emulsions

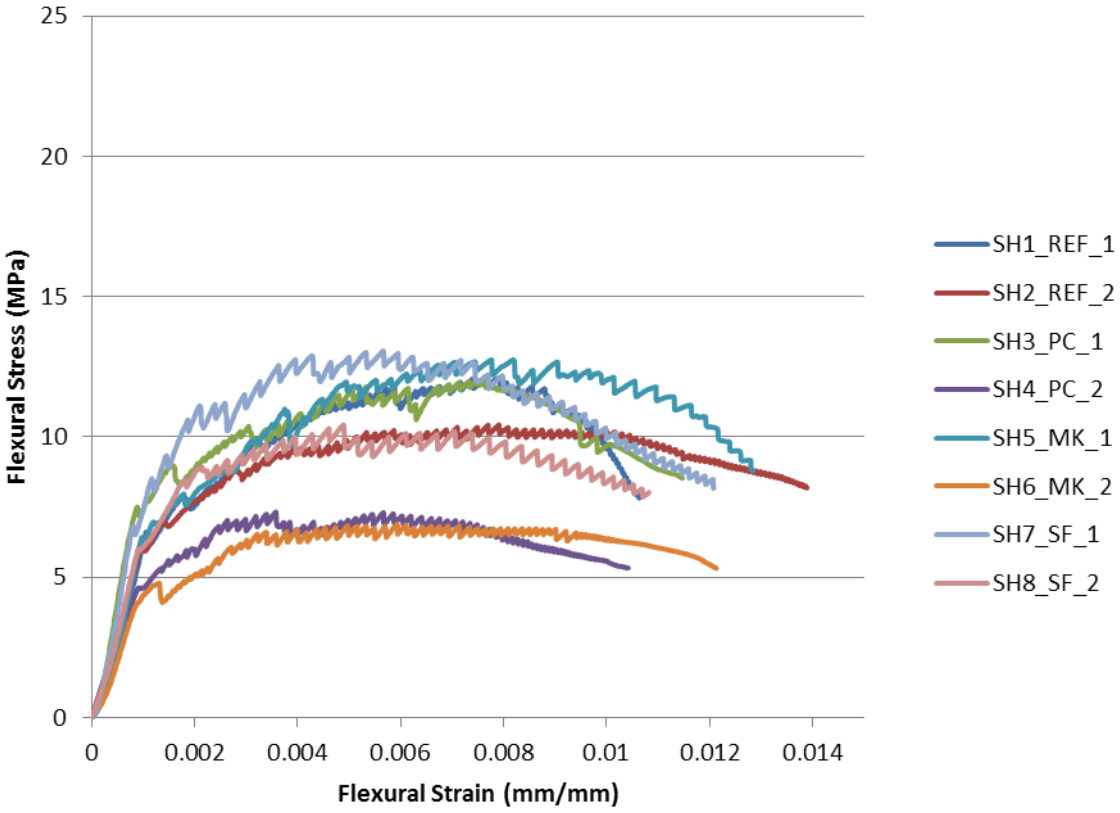

Figure 41. 1-Day Flexural Behavior of ECC with Superhydrophobic Emulsions

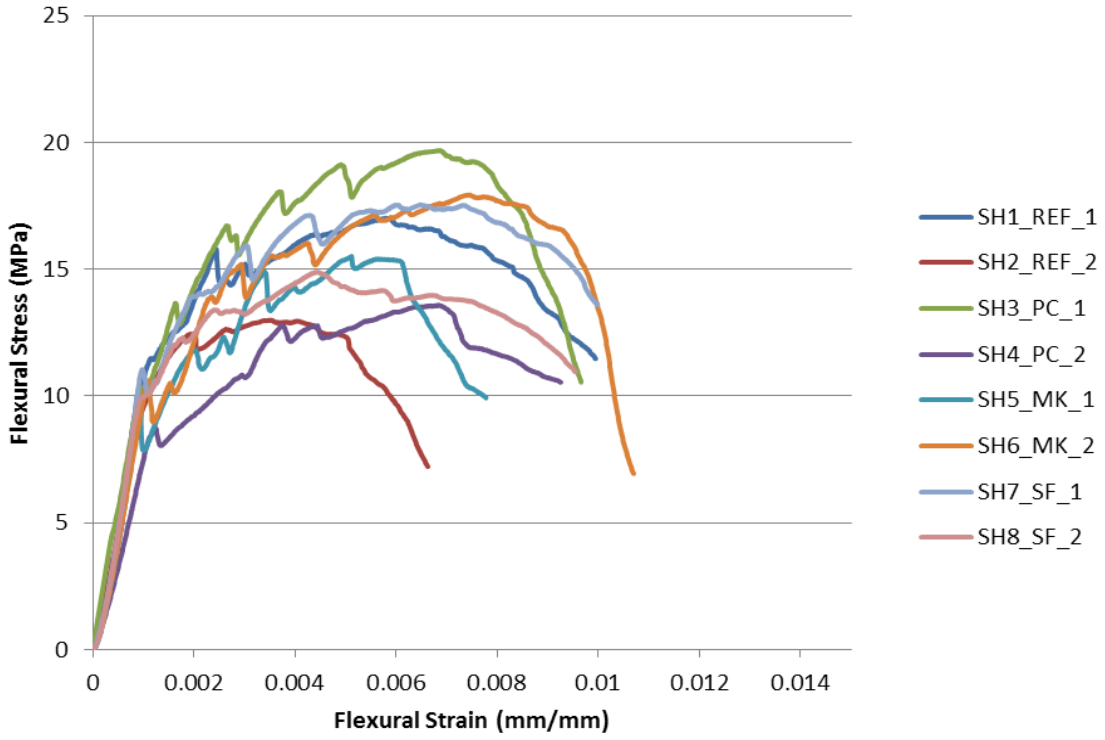

Figure 42. 7-Day Flexural Behavior of ECC with Superhydrophobic Emulsions

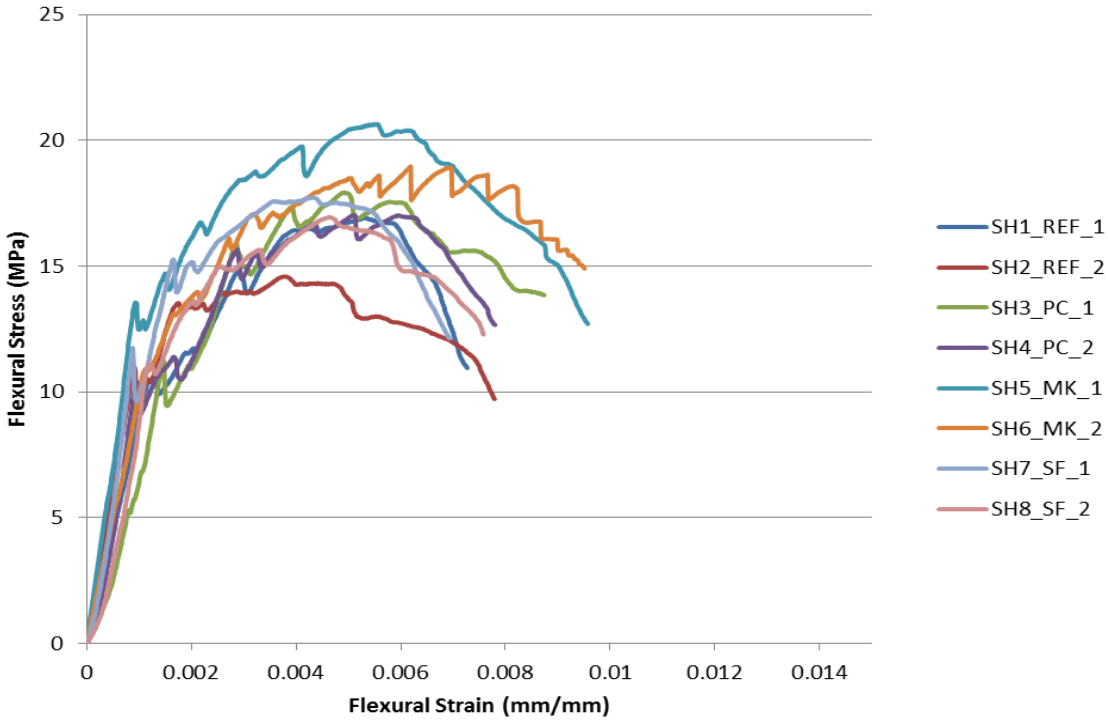

Figure 43. 28-Day Flexural Behavior of ECC with Superhydrophobic Emulsions

4.0 CONCLUSIONS

The use of PVA fibers in ECC/SECC structural materials proved to be an effective innovative solution, resulting in exceptional ductility and durability, which are important for maintaining high levels of freight transportation capacity on the nation's highways. Experimental programs have successfully demonstrated that the use of 3% by volume of PVA fibers displays good ductility and provides greater strain hardening behavior, as compared to ECC with fewer fibers.

Superhydrophobic hybridization of concrete is a novel concept engaging interdisciplinary work combining biomimetics (lotus effect), chemistry (siloxane polymers) and nanotechnology (nano-SiO_2 particles) to resolve the fundamental problems of concrete such as insufficient durability and corrosion resistance for internal reinforcing. It was demonstrated that the use of a hydrophobic/ superhydrophobic admixtures helps to tailor the volume, size, and distribution of air voids in the concrete, and the bond between the cementitious matrix and PVA fibers realizing controlled pullout behavior. The controlled air void structure was used to perfect "preferred" fracture modes.

It was determined that a siloxane based emulsions manufactured with higher quantities of PVAS emulsifiers (4.4% PVA) mixed at high speed (10.000 rpm) when used at a very small dosage of 0.25 g/l (0.4 lb/yd^3) and in addition to hydrophobic hybridization of concrete, provided the best flexural behavior. Superhydrophobic emulsions based on metakaolin over-performed those with silica fume or portland cement demonstrating the increase in contact angle and resistance to water penetration in addition to impressive compressive strength and flexural behavior. However, it was observed that the use of excessive quantities of hydrophobic/superhydrophobic admixtures (up to 0.5 g/l or 0.8 lb/yd^3) sometimes contribute to excessive gas generation, and expansion of unrestrained specimens during the initial stages of curing.

The addition of selected SCMs to the SECC matrix also results in an improved flexural behavior. Not only does this make the ECC material more environmentally friendly, but it can also improve durability. Experiments determined that the use of either metakaolin or silica fume can improve the flexural behavior and compressive strength of the PVA-ECC. Moreover, when siloxane based emulsions are added, metakaolin and silica fume samples displayed very little loss in strength and flexural behavior as compared to specimens with other SCMs.

Experimental research demonstrated that the use of superhydrophobic emulsions can be very beneficial for the mechanical behavior of SECC and it is expected that these materials will provide drastic improvements in freeze-thaw resistance as opposed to conventional mortars. Freeze-thaw studies are currently being performed on selected PVA-ECC with hydrophobic siloxane based emulsions and are displaying excellent performance through 200 cycles. Further research must be performed on PVA-SECC to determine performance under freeze-thaw cycling and chloride permeability.

It was successfully demonstrated that the obtained ECC demonstrated strain-hardening performance and multi-cracking patterns. The deflection behavior of larger ECC beams is controlled by interfacial bond and fiber pullout and a very consistent performance was noted for ECC manufactured at low W/C; however, significant scattering of experimental data was observed at higher water-to-cement ratios.

REFERENCES

1. Poor Infrastructure Fails America, Civil Engineers Report http://www.cnn.com/2009/US/01/28/infrastructure.report.card/index.html
2. Deteriorating Urban Pavement Conditions Cost the Average Driver More Than $400 Annually http://www.reuters.com/article/pressRelease/idUS101228+12-Mar-2008+PRN20080312
3. Tabatabai, H., Ghorbanpoor, A., and Turnquist-Nass, A., Rehabilitation Techniques for Concrete Bridges, WHRP Report 05-01, Wisconsin Highway Research Program, 2005, 310 pp.
4. Klaiber, F.W., Dunker, K.F., Wipf, T.J., Sanders, W.W., Methods of Strengthening Existing Highway Bridges. Transportation Research Record 1180, NRC, National Academy Press, 1988.
5. Hooks, J.A., Holding it together: FHWA Bridge Plan Part I, Roads & Bridges Magazine, 41(6), 2003.
6. Tabatabai, H., Tabatabai, M., and Lee, C., Reliability of Bridge Decks in Wisconsin, ASCE Journal of Bridge Engineering, 2010, (in press.)
7. Trends in Highway Material Costs http://www.wsdot.wa.gov/biz/construction/constructioncosts.cfm
8. Oliva, M., Schneider, J., "An Innovative Focus on Highway Bridge Approach Slabs," proposal funded by the FHWA CFIRE National Transportation Center, July 2009.
9. Li, V.C., "Engineered Cementitious Composites – Tailored Composites Through Micromechanical Modeling," in *Fiber Reinforced Concrete: Present and the Futur*e. Eds. N. Banthia *et al*, CSCE, Montreal, 64-97, 1998.
10. Zhang, J., H. Stang and V.C. Li., "Experimental Study On Crack Bridging In FRC Under Uniaxial Fatigue Tension," ASCE J. of Materials in Civil Engineering, Vol. 12, No. 1, pp. 66-73, 2000.
11. Li, V. C., "Advances in ECC Research," ACI Special Publication on Concrete: Material Science to Applications, SP 206-23, pp. 373-400, 2002.
12. Li, V.C., Wu, C., Wang, S. Ogawa, A., & Saito, T. (2002). Interface Tailoring for Strain-Hardening Polyvinyl Alcohol-Engineered Cementitious Composite (PVA-ECC). ACI Materials Journal, 463.472.
13. Wang, S., & Li, V.C. (2007). Engineered Cementitious Composites with High-Volume Fly Ash. ACI Materials Journal, 233-241.
14. Sobolev K. and Batrakov V., The Effect of a PEHSO on the Durability of Concrete with Supplementary Cementitious Materials. ASCE Journal of Materials in Civil Engineering, 19(10), 2007, 809-819.
15. Sobolev K., Batrakov V.G. The Development of High-Performance Concrete with Polyethylhydrosiloxane-Based Admixture. ConcreteLife'09: 2nd International RILEM Workshop on Concrete Durability and Service Life Planning, Haifa, Israel, 2009
16. Kerstin Koch, Bharat Bhushan and Wilhelm Barthlott. Diversity of structure, morphology and wetting of plant surfaces, Soft Matter, 2008, 4, 1943 – 1963.
17. Becky Poole, Biomimetics: Borrowing from Biology http://www.thenakedscientists.com/HTML/articles/article/biomimeticsborrowingfrombiology/

18. Sobolev K. and Ferrada-Gutiérrez M., How Nanotechnology Can Change the Concrete World: Part 2. American Ceramic Society Bulletin, 11, 2005, 16-19.

19. Batson, G., Jenkins, E. Spatney, R., "Steel fibers as shear reinforcement in beams", *ACI Journal*, 69, 10, 640-644, 1972.

20. Sharma, A. K., "Shear strength of steel fiber reinforced concrete beams", *ACI proceedings*, 83, 4, 624-628, 1986.

21. Swamy, R.N., Bahia, H.M., "The effectiveness of steel fibers as shear reinforcement", *Concrete International*, 35-40, 1985.

22. Stang, H., Aarre, T. "Evaluation of crack width in FRC with conventional reinforcement", Cement & Concrete Composite, 14, 2, 143-154, 1992.

23. Stang, H., Li, V.C., Krenchel, H. "Design and structural applications of stress-crack width relations in FRC", *RILEM J. Materials and Structures*, 1993

24. Li, V.C., Wang, S. and Wu, C. (2001). Tensile strain-hardening behavior or polyvinyl alcohol engineered cementitious composite (PVA-ECC), ACI Materials Journal: 98(6): 483-492.

25. Wang, S., "Micromechanics based matrix design for engineered cementitious composites," Ph.D. thesis, University of Michigan, 2005

26. Marshall, D. and Cox, B.N. "A J-integral Method for Calculating Steady-State Matrix Cracking Stress in Composites," Mechanics of Materials 7, 127-133, 1988.

27. Balaguru, P., and S. Shah, Fiber Reinforced Cement Composites, McGraw Hill, 1992

28. Li, V.C. and Leung, C.K.Y., Steady State And Multiple Cracking Of Short Random Fiber Composites, ASCE J. Engineering Mech., 118[11] 1992, 2246-2264.

29. Li, V.C. On Engineered Cementitious Composites (ECC) A Review of the Material and Its Applications

30. Kanda, T. and Li, V. C., "Practical Design Criteria for Saturated Pseudo Strain Hardening Behavior in ECC", Journal of Advanced Concrete Technology, Vol. 4, No. 1, pp59-72, 2006.

31. Li, V.C., Wu, C., Wang, S., Ogawa, A. and Saito, T. (2002). Interface tailoring for strain-hardening polyvinyl alcohol-engineered cementitious composite (PVA-ECC), ACI Materials Journal: 99[5]: 463-472.

32. Kuralon K-II Fibers, Kurary, Japan. http://www.kuraray.co.jp/kii/english/

33. Kim, Y.Y., Kong, H.-J. and Li, V.C. (2003). Design of Engineered Cementitious Composite Suitable for Wet-Mixture Shotcreting, ACI Materials Journal: 100[6]: 511-518.

34. Redon, C., Li, V. C., Wu, C., Hoshiro, H., Saito, T., & Ogawa, A. (2001). Measuring and modifying interface properties of PVA fibers in ECC matrix. Journal of Materials in Civil Engineering, 13(6), 399-406.

35. ASTM C230 / C230M - 08 Standard Specification for Flow Table for Use in Tests of Hydraulic Cement

36. ASTM C185 - 08 Standard Test Method for Air Content of Hydraulic Cement Mortar

37. ASTM C305 - 06 Standard Practice for Mechanical Mixing of Hydraulic Cement Pastes and Mortars of Plastic Consistency

38. ASTM WK31276 - Revision of C109 / C109M - 08 Standard Test Method for Compressive Strength of Hydraulic Cement Mortars (Using 2-in. or [50-mm] Cube Specimens)

39. ASTM C348-97 Standard Test Method for Flexural Strength of Hydraulic-Cement Mortar
40. ASTM C349 - 08 Standard Test Method for Compressive Strength of Hydraulic-Cement Mortars (Using Portions of Prisms Broken in Flexure)
41. ASTM C666 / C666M - 03(2008) Standard Test Method for Resistance of Concrete to Rapid Freezing and Thawing
42. Zalocha, D. and J. Kasperkiewicz, Estimation of the structure of air entrained concrete using a flatbed scanner. Cement and Concrete Research, 2005. 35: p. 5.
43. ASTM C1202 - 10 Standard Test Method for Electrical Indication of Concrete's Ability to Resist Chloride Ion Penetration.

Appendix:Verification of Experimental Program: Testing of Larger ECC Beams

A1.0 Problem Statement: Performance of Approach Slabs

The primary objective of the approach slab is to provide a smooth transition between the roadway and the bridge. Over the past 20 years, approach slab settlement and deterioration has been studied by many researchers. Specifically, researchers have targeted differential settlement in approach slabs to be the root cause of most approach slab failure [1].

When the approach slab is working correctly, a smooth transition between the roadway and the bridge will be felt by the roadway user when entering and exiting the bridge. However, when a failure has occurred, a "bump" will be felt. Differential settlement occurs when one end of the approach slab (typically the roadway end supported by soil) settles while the other end (supported by the bridge abutment) settles a negligible distance. Previous research has determined that several aspects such as consolidation of backfill materials, poor drainage, poor construction methods [1], expansion joint failure, and the type of abutment [2] cause most of the differential settlement problems.

Once the differential settlement reaches a half inch, roadway users are now able to feel the "bump" when entering and leaving a bridge [3]. When differential settlement of 1-inch is reached, it can become a costly problem for the Department of Transportation (DOT) as repair or even replacement of the approach slab is recommended [4]. If differential settlement is allowed to reach two inches, roadway users will experience serious discomfort [5]. Many DOTs have even discovered that a void space will form around the abutment of damaged approach slabs [6]. Jayawickrama *et al.* [7] concluded that this void space was shaped by backfill erosion and loss from water infiltrating though a crack in the approach slab. Once this trench forms, the deterioration of the approach slab is accelerated.

One potential solution to enhance approach slab performance is to prevent water from ever entering a crack; thus, never reaching the soil below. This action ensures that the backfill under the approach slab will not erode and durability will be enhanced. Developed at the University of Michigan, a new type of concrete called engineered cementitious composites (ECC) has been shown to have the ability to deform while keeping crack widths narrower than regular concrete [8-10].

A2.0 Research Objectives

The main objective of this research was to determine the possibility of designing an ECC mix that can rotate to 0.002 radians (the worse-case scenario) at the abutment-approach slab interface. Secondary objectives of the mix design are:

- Minimizing crack width at ultimate failure,
- Providing a high modulus of rupture, toughness, flexural strength, and compressive strength adequate for structural design,
- Creating a mix that is workable for easy use in the field.

The primary objective is to design an ECC/SECC concrete that has ductile strain hardening behavior when loaded under four-point bending. In addition this ECC/SECC concrete should also display high strength and a tight, dense cracking pattern at failure.

A2.1 Preliminary Phase Objective

The preliminary objective of these initial mixes was to obtain an understanding of material behavior and mixing procedure.

A2.2 Trial Mixes Objective

A couple of different objectives exist in this portion of the research. For one, the mix procedure from the preliminary trial mixes was fine-tuned. Also, one of the main components affecting the strength of the concrete is the water to cementitious material ratio (w/cm). The optimum ratio should have good ductility while not sacrificing too much strength. Due to the presence of dry mixes in the previous phase (A2.1), the effects on strength of manipulating the w/cm ratio and, more importantly, the ductility of the ECC must all be considered. Ductility can be measured by the observed cracking pattern, midspan deflection, and load. Once ECC concrete mix can be optimized under these criterions, testing can be scaled up to larger cross sections.

A2.3 Half Scale Objective

In this phase, the mix design from the previous phase (A2.2) was tested under a larger span and cross section. The testing setups were similar to the previous tests but the span and the depth of the beam were increased. Initially, load and midspan deflection were measured, then strain and load were measured later. From the strain calculation, a curvature (also a rotation given as a length) was calculated and compared with rotation demand.

A3.0 Scope of Research

This work investigated the midspan rotation, deflection and load of small-scale beams all the way up to half-scale beams. It was assumed that the midspan rotation would equal the rotation experienced at the end of the approach slab. Parameters such as material proportions, curing time, curing conditions, mixing procedure were optimized to meet the objectives of the project. The testing procedure (the loading rate) was kept constant throughout the duration of the project. The project was limited to the following:

- quasi-static loading
- no cyclic loading
- mixing using a Hobart mixer

Although ASTM procedures were followed as closely as possible, some deviation was necessary. All compression cylinders conform to ASTM C873. All flexural tests followed ASTM C1609 (standard test method for flexural performance of fiber-reinforced concrete) with some modifications as seen below in Table A1.

Table A1. Deviation from ASTM C1609 and Flexural Tests

	ASTM Recommends	UW-Madison Tests	Why different
Size	4 x 4 x 14 in or 6 x 6 x 20 in	1 x 3 x 36 in	Trying to duplicate reference [10] ECC Results
Loading Rate	0.002 in/min	0.039 in/min	It would take 5 hours to run one test. Normal Concrete does not deflect as much as an ECC
Deflection	terminate test at L/150	beam failed at L/80	At L/150, the beam is only at about half the failure deflection

A4.0 Experimental Program

A4.1 Materials

The materials for the ECC mix were as follows: type I ordinary portland cement (Lafarge), ASTM class F fly ash (Headwaters Shufer Station, Illinois), a fine grained sand with an average grain size of 177 μm (US Silica F-80), PVA fiber (Kuraray RECS 15x8 mm), and superplasticizer, SP (Grace Chemical's ADVACAST 575).

Based on the University of Michigan study [10], the volume of fibers was held constant at 2% From the literature review, adding an oiling agent to the fibers leads to increased J_b'; hence the failure mode will shift from modified Griffith cracking to the steady-state cracking. The fibers chosen for this project were pre-coated with an oiling agent by manufacturer at 1.2% of the fiber volume (optimum value from [10]) to account for this factor.

Class F fly ash was used for the majority of this research instead of the more readily available class C fly ash. Initial preliminary trial mixes A and B were the only mix designs to use class C fly ash. Many reference ECC mix designs used class F fly ash; therefore, for mix designs in this research, class F fly ash was selected in favor of class C fly ash.

According to ASTM C618, a few differences exist between class C and class F fly ash. The summation of silicon dioxide (SiO_2), aluminum oxide (Al_2O_3), and iron oxide (Fe_2O_3) chemical percentages must be at least 70% for a class F and at least 50% for a class C. A bituminous coal is generally richer in chemicals such as SiO_2, Al_2O_3, and Fe_2O_3, but has smaller quantities of calcium oxide (CaO) when compared to a lignite coal. Therefore, a class F fly ash is typically produced from burning bituminous coal while a class C is typically produced from burning lignite coal. Because the hydration of cement requires all four chemicals and class C has more CaO, it is generally cementitious, while class F needs excess CaO from the cement to hydrate.

A4.2 Tested Mix Proportions

Table A2: Initial Trial Mixes: PVA-ECC Mix Proportions (1.5 x 3 x 36-in beams)

Mix ID	Fly Ash fa/c	Sand s/c	Water w/c	w/cm	SP SP/c	Fiber, % by volume
Mix A	1.20 (class C)	1.01	0.58	0.26	0.012	2%
Mix B	1.20 (class C)	1.01	0.58	0.26	0.012	2%
Mix C	1.20 (class F)	1.01	0.58	0.26	4 oz/100lbs	2%
Mix D	1.20 (class F)	1.01	0.58	0.26	4 oz/100lbs	2%

Table A3: Trial Mixes: PVA-ECC Mix Proportions (1 x 3 x 15-in beams)

Mix ID	Fly Ash fa/c	Sand s/c	Water w/c	w/cm	SP, oz/100 lb concrete	Fiber, % by volume
Mix 1	1.2	1.01	0.51	0.23	13.77	2%
Mix 2	1.2	1.02	0.54	0.25	4.01	2%
Mix 3	1.2	0.8	0.73	0.33	6.07	2%
Mix 4	1.2	0.8	0.62	0.28	6.14	2%
Mix 5a	1.2	0.8	0.57	0.26	6.22	2%
Mix 5b	1.2	0.8	0.53	0.24	6.3	2%
Mix 6	1.2	0.8	0.62	0.28	6.08	2%
Mix 7	1.2	0.8	0.53	0.24	6.07	2%

Table A4: Half Scale Mixes: PVA-ECC Mix Proportions (5 x 3 x 36-in beams)

Mix ID	Fly Ash fa/c	Sand s/c	Water w/c	w/cm	SP, oz/100lb concrete	Fiber, % by volume
Mix 8, 9	1.2	0.8	0.53	0.23	6.07	2%
Mix 10	1.2	0.7	0.53	0.24	6.07	2%

A4.3 Mixing Procedure

For this initial research, the preliminary trial mixes and were tested. Ultimately, the flexural behavior of the initial trial mixes was unsuccessful, but learning about the workability of ECC and honing in on a mixing procedure was successful. Four initial preliminary trial mixes were run and seven trial mix designs were used. Optimizing the mix design, the mixing procedure was also enhanced.

Initial Trial Mixes

Mix A

1. Ingredients were weighed.
2. Cement, fly ash and sand were mixed together in a concrete mixer for two minutes
3. Water with SP was added slowly and mixed for three minutes
4. Fibers were then slowly added into the concrete mixer until evenly dispersed
5. ECC then cast into molds

Mix B

1. Ingredients were weighed
2. Cement, fly ash and sand were mixed together in a concrete mixer for two minutes
3. Water with SP was added slowly and mixed for three minutes
4. Placed in a large pan
5. Fibers were added slowly into the pan and mixed in by hand until a uniform mix was obtained
6. ECC cast into molds

Mix C and Mix D

1. Ingredients were weighed.
2. Cement, fly ash and sand were mixed together in a large pan by hand until the materials are uniformly distributed.
3. Water with the SP was added slowly. The mix was turned over by hand until well mixed.
4. Fibers were added slowly until even dispersion was apparent
5. ECC cast into molds

Trial Mixes

Mix 1 and Mix 2 (only mixes to include sand correction factor)

Exactly the same as Mix C and D

Mix 3, Mix 4, and Mix 5

1. Ingredients were weighed.
2. Cement, fly ash, and fibers were mixed together in a five gallon bucket by drill operated paint mixer until the materials are uniformly distributed.
3. Water with the SP was added slowly and stirred with the paint mixer.
4. Sand was added until the ECC was just workable; the remaining sand was weighed and not added to the matrix.
5. ECC cast into molds

Mix 6 and any later mixes

1. Ingredients were weighed.
2. Cement, fly ash and sand were mixed together in a large pan by drill operated paint mixer until the materials are uniformity distributed.
3. Water with the SP was added slowly and stirred with the paint mixer.
4. Fibers were added slowly until even dispersion was apparent
5. ECC cast into molds

Since mix 1 and 2 of the trial mixes produced extremely dry ECC, much more effort had to be used to place it into the molds. Therefore, the ECC mix design and mix procedure needed some modifications. The most significant change involved the mixing machinery. With the first two mixes, the ingredients were put into a pan and mixed by hand. For all the mixes thereafter, the ingredients were put into a five gallon bucket and mixed with a paint mixer. This made it much easier to achieve uniform and evenly distributed materials in the matrix. It also did not take as long to mix the ingredients together. The mix was therefore more workable when it was poured into molds.

Figure A1. Typical Consistency of an ECC (Shown is Mix 4)

Another way to account for the low workability of mixes 1 and 2 involved lowering the s/c ratio from 1.0 to 0.8 and modifying the sand added to the mix. In mixes 3, 4, and 5, the fibers were added in step two instead of step four and the sand was added in step four instead of step two. Also in step four, sand was added until the ECC became nearly unworkable. The excess sand was not added to the mix. If the sand was absorbing water in the first two mixes, then less sand would be added to the matrix. It turned out that adding sand all the way up to the 0.8 sand/cement ratio did not affect the workability. If the quantity of sand did have an effect on the workability, this too dry boundary was in between the 0.8 sand/cement ratio and 1.0 sand/cement ratio.

Therefore it was determined to revert to the mixing procedure recommended [10, 11]. In mixes 6 and 7, the sand was again added in step two and the fibers were added in step four. All mixes after these preliminary tests also followed this procedure.

A4.4 Flexural Test Setup

Initial Trial Mixes

A four point bending test was chosen to measure the flexural load and deflection. Each ECC mix design was cast into beams measuring 1.5 x 3 x 36-in with the 1.5-in dimension representing the strong axis. The beams were covered with plastic and cured at room conditions. After 24 hours, beams were demolded and covered with plastic and cured at room a temperature and relative humidity.

Figure A2. Initial Preliminary Test Setup Mold (The Mold is Upside Down and the Top Side of the Beam when it was in the Mold is now the Largest Face Shown in the Picture)

After 7 days of curing, the beams were ready for testing. The span on the each beam was 30 in. The distance between the loading points was 10 in. The loading rate chosen was 0.039 in/min. A SATEC machine was used to measure load and an average deflection under each loading point. For these preliminary trial mixes, learning ECC behavior and mix procedure was critical.

Figure A3. Flexural Test Setup of Preliminary Trial Mixes

Trial Mixes

A four point bending test was used to measure the flexural load. Each batch of ECC was cast into beams measuring 1 x 3 x 15-in with the 1 in dimension representing the strong axis. The beams were covered with plastic and were cured at room temperature and humidity. After 48 hours, the beams were demolded and were covered with plastic and cured under lab conditions.

It is worth noting that the mix design (mostly the water content) between the initial preliminary trial mixes and the trial mixes changed slightly. In this report, the beams were demolded and tested at two different ages, 9 hours and 90 days.

Figure A4. The Molds for the Trial Mixes

After 9 days of curing, the beams were ready for testing in flexure and compression. For flexure, the span on each beam was 11 in. The distance between the top loading points was 3 in. The loading rate chosen was 0.039 in/min. A Sintech machine was used to measure load and an LVDT was used to measure the midspan deflection.

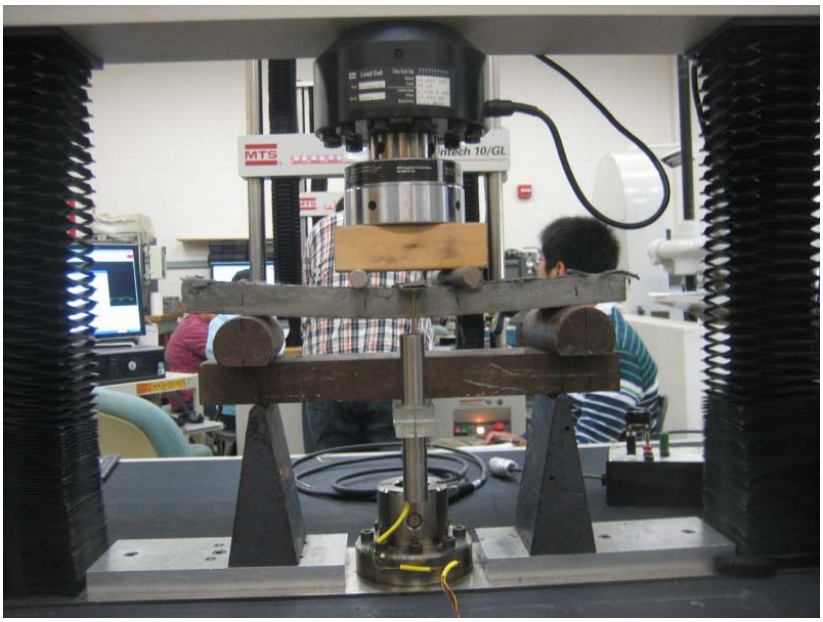

Figure A5. Flexural Test Setup of Trial Mixes

Half Scale Mixes

For this particular beam size, two different test setups were used. One setup involved measuring load and midspan displacement with an LVDT and the other setup involved measuring load and using strain gauges to measure strain on the compression face and the tension face; with the latter test setup described, two LVDTs were mounted on the top and bottom of each beam to verify strain data.

Figure A6. The molds for the half-scale tests

Each beam cast for this test measured 3 x 5 x 36-in with the 5 in dimension representing the strong axis. The beams were covered with plastic and cured at a room temperature and humidity. After 48 hours, the beams were demolded and were again covered with plastic and cured under lab conditions until testing day.

A four point bending test was used to apply load. For flexure, the span on each beam was 30 in and the distance between loading points was 10 in. An LVDT was used to measure the midspan displacement and the loading was controlled by force. Load was manually recorded for a given displacement on the LVDT. Therefore, the density of readings was greater in the elastic range over the inelastic range.

In the next test setup, an Instron machine was used to apply load. The loading on this machine can be displacement controlled and recorded using a data acquisition system, so collected experimental data were more accurate. In addition, strain gauges and LVDTs were mounted at midspan on the top and bottom of each beam. For flexure, the span on each beam was 30 in and the distance between loading points was 10 in. The loading rate was 0.039 in/min.

Figure A7. First Test Setup of Half-Scale Mixes

Figure A8. Second Test Setup of Half-Scale Mixes

A5.0 Test ResultsA5.1 Failure Criterion for Completed Tests

Failure of each beam is defined as the point where the load is reduced by 20% of the peak load. The flexural behavior of each beam cast at different w/cm ratio is scattered. Two different types of cracking patterns were observed, one with dense, multiple cracks (Figure A9a) and another one with larger cracks evenly spaced at about an inch in between the 3 in span (Figure A9b). Results from these flexural tests have shown that a beam with a dense cracking pattern will tend to reach its peak load at higher midspan deflection than a beam with one-inch spaced cracking.

Figure A9. The Two Different Cracking Patterns Observed: Multiple-Cracking Pattern a) and 1-in Spaced Cracking b)

Initially, it was proposed that changing the w/cm ratio would define the cracking scenario. However, it was observed that the w/cm ratio did not have much impact on the cracking pattern. Rather, the distribution of moment had a larger affect. To combat this problem, the use of a bearing pad helped create consistent satisfactory results at the end of the trial mixes phase of the research.

A5.2 Load vs. Deflection of Trial Mixes

Mixtures 1 and 2

Beams based on these mixtures did not demonstrate favorable results. As discussed, these were low workable mixtures. No multiple cracking was seen in these mixes and only Griffith type, one inch spaced cracking. Because the ECC had to be packed into place, it was nearly impossible to distribute the fibers. Voids or regions where fibers were not distributed may have created weak points over the span with maximum moment between the loading points.

Mixtures 3-7

Beams cast with Mix 3 had a w/cm ratio of 0.33 and yielded some success, but with inconsistent results (Figure A10). The beam tested at 48 hours had low strength but did show excellent multiple, steady-state cracking. Some strain hardening occurred with this beam. The beam labeled 2-1 in the following figure showed an increase in ultimate load by a factor of nearly two, but lost nearly 1/10 in of midspan deflection. The other two beams tested in this mix had an increase in strength from the 48 hour test, but did not show much steady-state cracking. Thus the conclusion that steady-state cracking is required for large deflections and increased curvatures at failure. Mixes 4-6 (Figures A11-A14) were not successful as failure occurred at a much lower deflection. Mix 5b displayed a high load capacity, however, failed prior to reaching a high deflection. Other mixtures did not display a high load capacity. Mix 7 (Figure a15) displayed good results as it maintained both high load and deflection capacities. A summary of mechanical response for all tested mixtures is presented in Figures A16-A17.

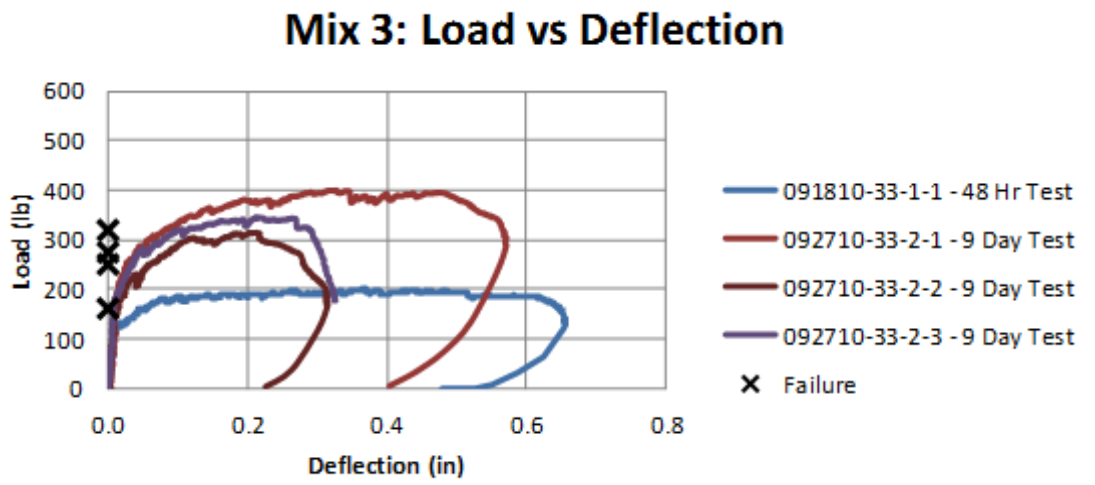

Figure A10. Mix 3 - Load vs. Deflection for ECC with w/cm = 0.33

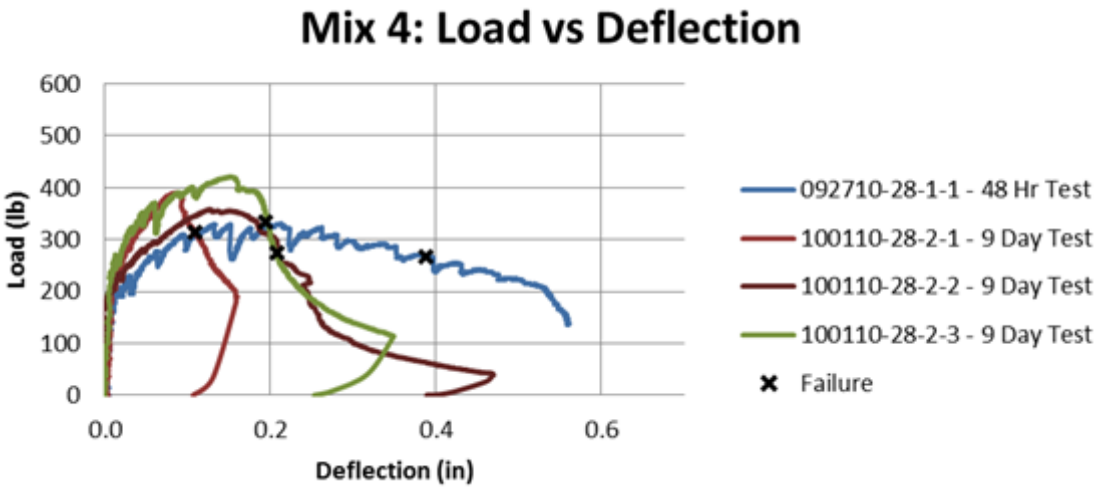

Figure A11. Mix 4 - Load vs. Deflection for ECC with w/cm = 0.28

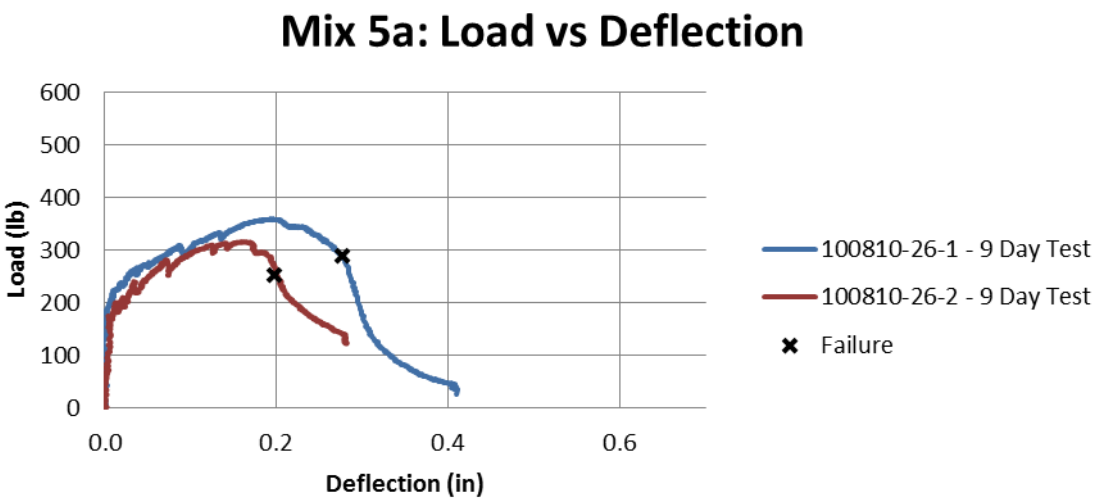

Figure A12. Mix 5a - Load vs. Deflection for ECC with w/cm = 0.26

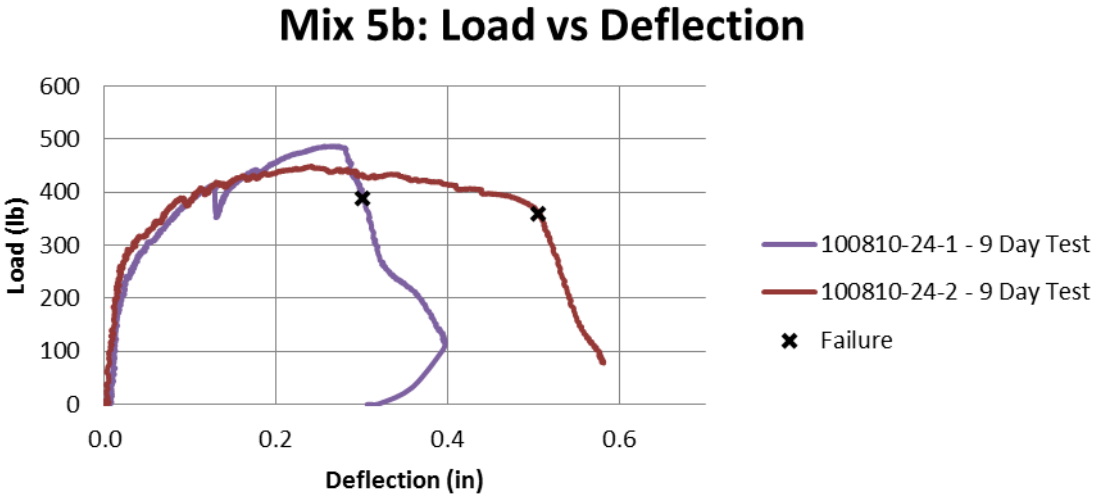

Figure A13. Mix 5b - Load vs. Deflection for ECC with w/cm = 0.24

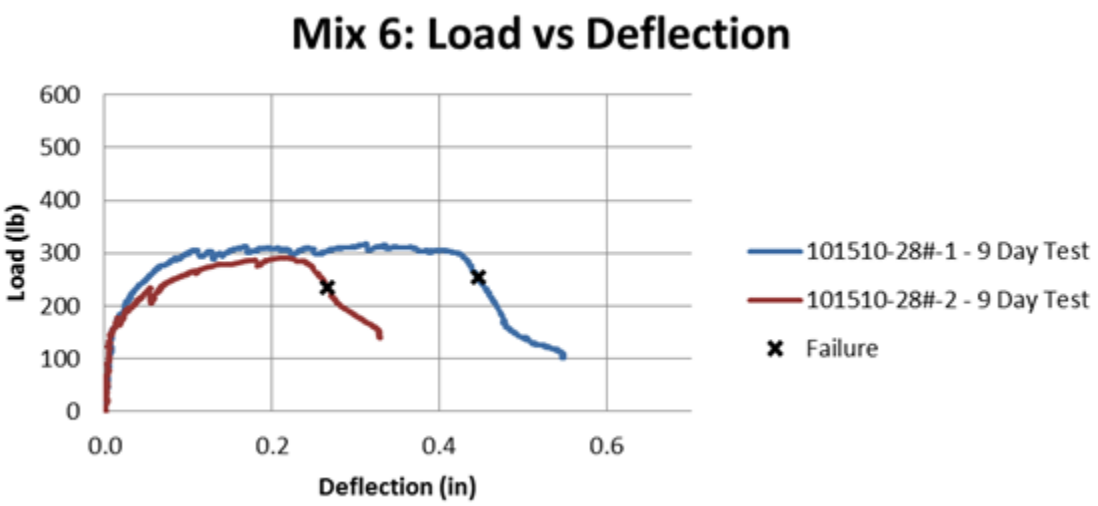

Figure A14. Mix 6 - Load vs. Deflection for ECC with w/cm = 0.28

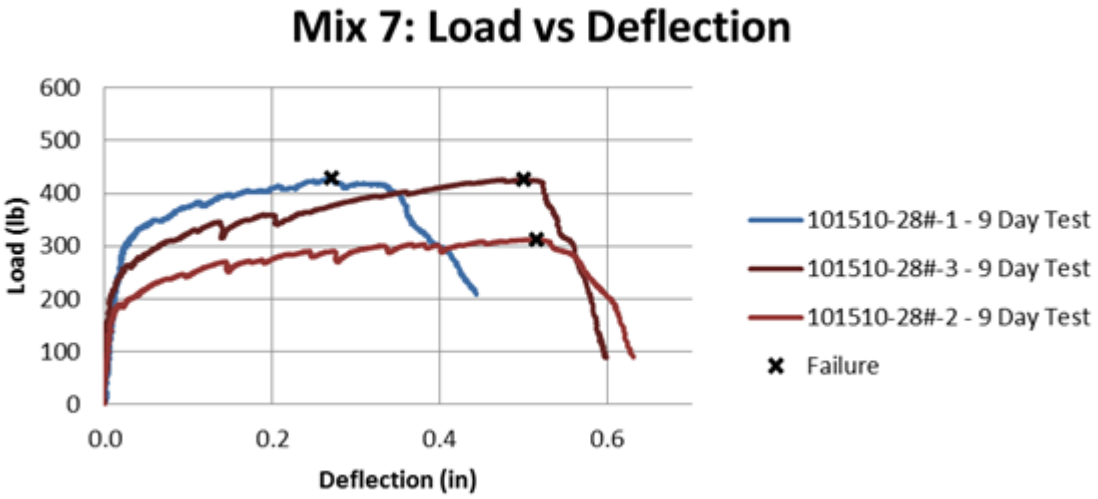

Figure A15. Mix 7 - Load vs. Deflection for ECC with w/cm = 0.24

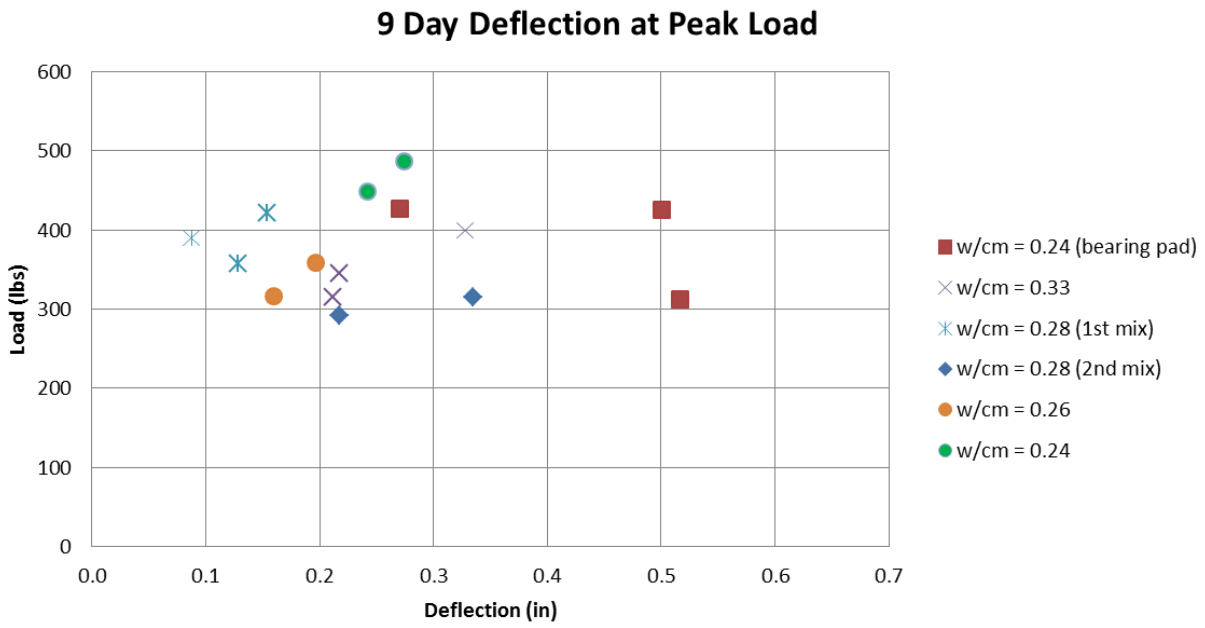

Figure A16. Flexural Test Results at Peak Load

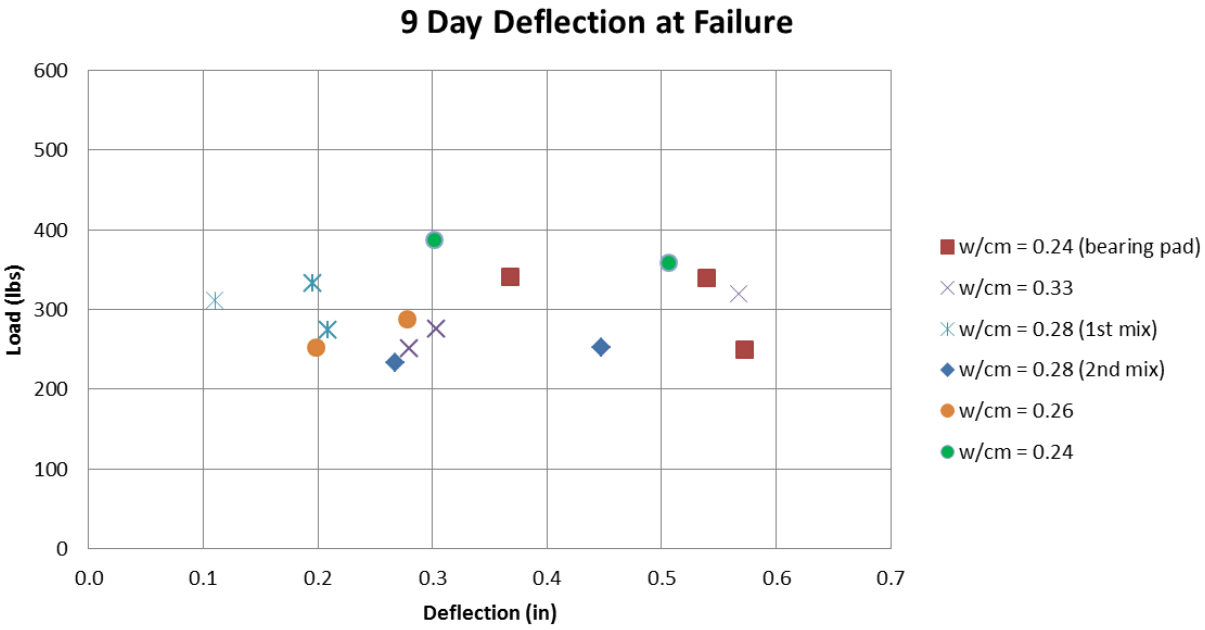

Figure A17. Flexural Test Results at failure (20% of peak load)

A5.3 Half Scale Mixes

Load vs. deflection curves (Figure A18) and moment-curvature (Figure A19) are displayed below. The measured values and the predicted values are displayed. This data represents the initial steps towards half scale and eventually full scale mixtures. It is evident that more work is required for transferring laboratory findings into construction practice.

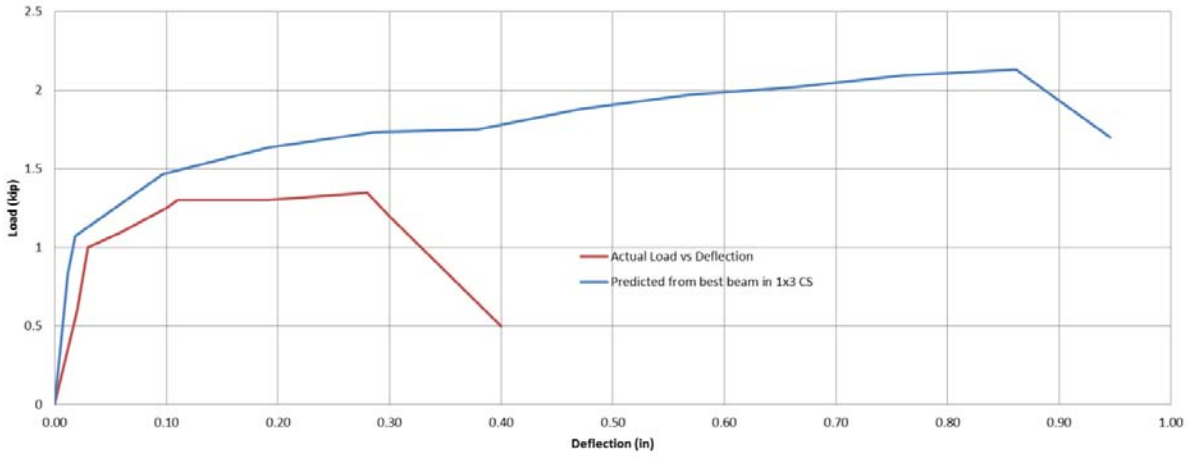

Figure A18. Load vs. Deflection (Mix 8)

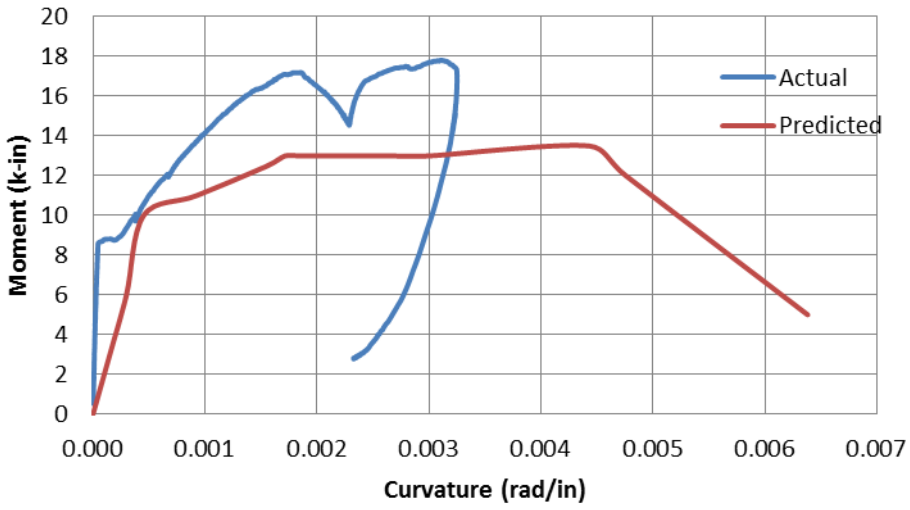

Figure A19. Moment Curvature (Mix 9)

A 6.0 Additional Reading

1. Seo Jeong Bok. The Bump at the End of the Bridge: An Investigation [Report]- College Station: Texas A&M University, 2003.
2. Helwany Sam, Koutnik Therese Ellen and Ghorbanpoor Al. Evaluation of Bridge Approach Settlement Mitigation Methods [Report].- Milwaukee: University of Wisconsin, 2007.
3. Wahls H. E. NCHRP Synthesis of Highway Practices 159: Design and Construction of Bridge Approaches. [Report].- Washington D.C.: Tranportation Research Board, National Research Council, 1990.
4. Zaman M., Gopalasingam A. and Laguros. Consolidation of Settlement of Bridge Approach Foundations Journal of Geotechnical Engineerings, ASCE, 1991.- Vol. 117.
5. Stark T. K., Olson S. M. and Long J. H. Differential Movement at the Embankment/Structure Interface - Mitigation and Rehabilitation Report No. IAB=H1 [Report].- Springfield: Illinois Department of Transportation, 1995.
6. CTC & Associates, LLC Concrete Bridge Approach Pavements: A Survey of State Practices [Report].- Madison: WisDOT Research & Library Unit, 2010.
7. Jayawickrama, P., Nash, P., Leaverton, M. and Mishra, D. (2005). "Water Intrusion in Base/Subgrade Materials at Bridge Ends." *TxDOT Report, FHWA/TX-06/0-5096-1*, Texas Tech University, Lubbock, Texas.
8. Li, V.C., Wang S. PVA fiber reinforced engineered cementitious composites material design and performances
9. Li, V.C. On Engineered Cementitious Composites (ECC) A review of the Material and Its Applications
10. Kanda, T. and Li, V. C., "Practical Design Criteria for Saturated Pseudo Strain Hardening Behavior in ECC", Journal of Advanced Concrete Technology, Vol. 4, No. 1, pp59-72, 2006.
11. Wang, S., "Micromechanics based matrix design for engineered cementitious composites," Ph.D. thesis, University of Michigan, 2005

CFIRE

University of Wisconsin-Madison
Department of Civil and Environmental Engineering
1410 Engineering Drive, Room 270
Madison, WI 53706
Phone: 608-263-3175
Fax: 608-263-2512
cfire.wistrans.org